

LIDAR Notes

R. Todd Lines

15 May 2015

Contents

Preface	vii
Introduction	ix
I Lidar Basics	1
1 Lidar Basic Concept	3
1.1 Basic System Design	4
1.1.1 Range definition and Range measurement	4
1.1.2 Pulse Shapes	5
1.2 Basic Techniques	8
1.2.1 Aerosol Backscatter Measurements	8
1.2.2 Differential Absorption Lidar	9
1.2.3 Raman Lidar	11
1.2.4 Fluorescence Lidar	11
II Fundamental Equations	13
2 Basics of Radiative Transfer	15
2.1 Solutions to the free space wave equation	17
2.1.1 Paraxial Wave Equation	17
2.2 Transmission: Beer's Law	20
3 Derivation of the Basic Lidar Equations	23
3.1 Scattering Form	25
3.1.1 Power Received	26
3.1.2 Basic Scattering Lidar Equation	27
3.1.3 Summary	31
3.2 Topographic Lidar (Ladar) Equation	31
3.2.1 Topographic range finding	34

3.3	Fluorescence Lidar Equation	35
3.4	Raman Lidar Equation	39
4	Differential Absorption Lidar (DIAL) Equation	43
4.1	Aerosol backscatter DIAL	43
4.2	Differential Absorption Using Surface Reflectivity	45
4.2.1	Digression	47
4.2.2	Corrections to the DIAL equation (NEEDS TO BE REWRITEN, DON'T USE)	50
4.2.3	Calculate the minimum detectable concentration for surface reflectance DIAL	52
4.2.4	Calculate the minimum energy required for achieving detection of C_{\min}	54
4.2.5	Surface DIAL Example	55
4.3	Three Line and Multi-Line DIAL	57
III	Laser Topics	59
5	Light/Laser Amplification and Detection	61
6	Laser Beam Propagation	63
6.1	Gaussian beams[1]	63
IV	Practical Application	71
7	General Error Analysis	73
8	Accuracy	75
9	Precision:Concentration length and Propagation of Errors	77
9.1	Formula for propagation of errors	78
10	Pulse Detection	83
11	Background, Clutter, and Noise	85
11.1	Detection Techniques	85
11.1.1	Direct Detection	85
11.1.2	Coherent Detection	85
11.2	Background	87
11.2.1	Solar Illumination	87
11.2.2	Thermal Background	87
11.2.3	Scattered Laser Radiation	89
11.3	Clutter	89
11.4	Speckle	89
11.5	Optical and Electrical Noise	89

11.5.1	Dark Current	90
11.5.2	Johnson Noise	90
11.5.3	Photovoltaic Sensors	91
11.5.4	Photoconductor Sensors	93
11.6	Quantization error	95
11.6.1	Compare to concentration signal	96
11.6.2	SNR	102
11.7	False Alarm Rate Calculation	102
11.7.1	Probability of Detection Theory	102
11.7.2	Example, Gaussian noise	107
11.8	Connection to error analysis	112
11.9	Geometric Form Factor	115
11.9.1	Simple Cases	117
11.10	Surface Reflectivity	119
11.11	Lambertian Surfaces	119
11.11.1	Non-Lambertian Surfaces	120
11.11.2	Cross section of a circular extended target	123
11.11.3	Scattering	123
11.11.4	Light Sources	124
12	Area of Illumination for a Circular Aperture	125
12.1	Effects of the Earth's Curvature.	126
12.2	Spherical Earth Sensor footprint	128
13	Discussion of Solid Angle	131
14	Using Spectral Libraries	133
14.1	Library Units	133
14.2	Calculation of Cross Sections	135
14.2.1	HITRAN[2] Cross Section Calculation	135
14.3	Temperature and Pressure dependence of the Halfwidth	136
14.4	Combined Temperature Dependence	137
14.4.1	Pressure factor $\mathcal{L}_{peak}(p)$	138
14.5	Example: Methane Cross Section	139
14.5.1	Input Data	139
14.5.2	Halfwidth	139
14.5.3	Cross Section	139

14.5.4 Max at ν_p	140
14.5.5 Pressure variation at ν_o	140
14.5.6 PMNNL Cross Section Calculation	141
Appendix A: Conversion from concentration in ppm to molecules/Vol	
A.1 DATA	145
A.2 Calculations	146
A.3 Conversion from ppm to #mol/V	147
Appendix B: Poisson Statistics	
	149
Appendix C: Glossary	
B.1 Basic Suffixes in Radiometry	151
B.2 General Glossary	151

Preface

This document contains my notes on lidar/lidar. It is a compilation of notes I have collected since my grad student days. The drivetrains are based on a book by Raymond Measures[3] that has been the standard lidar text for many years. It is currently back in print. I have not cleaned the notes to be presentable to a general audience, so I hope you will forgive their rough nature. When you find errors, or if you have suggestions, please let me know.

Special thanks to Joe Lippert, and Mike Millard.

Introduction

The basic theory of lidar signal return will be developed. Standard practice involves making many simplifying assumptions that are, for the most part, practical in actual lidar systems. This makes the equations simpler and easier to understand, but also can provide a danger to the engineer who applies them without understanding. Throughout the derivation of the basic lidar equations, assumptions will be called out in an attempt to help the reader be conscious of their use and to judge their appropriateness in individual applications.

A brief review of basic radiative transfer theory will be given. This will build the basic theory necessary to understand the lidar equations. An assumption will be made that the reader will understand the basics of classical electrodynamics and quantum theory. Thus, this will only be a review designed to set the context. For more complete treatments, the beginning student is referred to books by Jackson[4], Liou[5], and Schott[5].

Part I

Lidar Basics

Chapter 1

Lidar Basic Concept

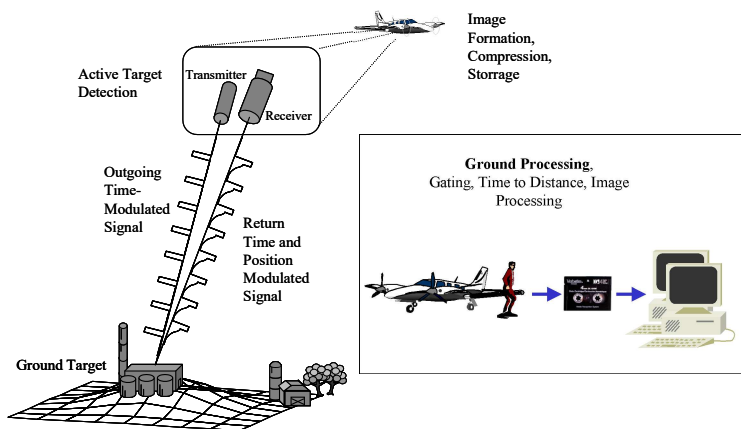


Figure 1.1: Typical Lidar System Including Ground Processing

Anyone who has used a flashlight can understand the concept of a lidar. A lidar is a sensor that provides its own light source. Lidar is similar to radar, so similar that lidar is often referred to as “laser radar.” The word “lidar” stands for *light detection and ranging* just as the word “radar” stands for *radio frequency detection and ranging*. The difference is that radar uses radio frequency radiation to illuminate a target, and lidar uses shorter wavelengths (UV to IR). Many lidar are pulsed systems requiring timing of the pulse from the sensor to the target and back again. This may seem complicated, but it is really not that different from flash photography.

In figure 1.1, a typical lidar system is shown. The transmitter usually consists of a laser source and an optical system (the ‘flash’ part of the lidar). The receiver

usually consists of a telescope and detector system (the ‘camera’ part of the lidar). The lidar in the figure produces many pulses (‘flashes’) that illuminate the target. The pulses are reflected off the target (In figure 1.1 the target is the ground and buildings) and are collected by the receiver optical system and converted into a digital form by the lidar detection and digitization electronics. The basic concepts of the lidar design, operation, and processing will be outlined below. A more mathematical treatment will be given in Chapter 3.

1.1 Basic System Design

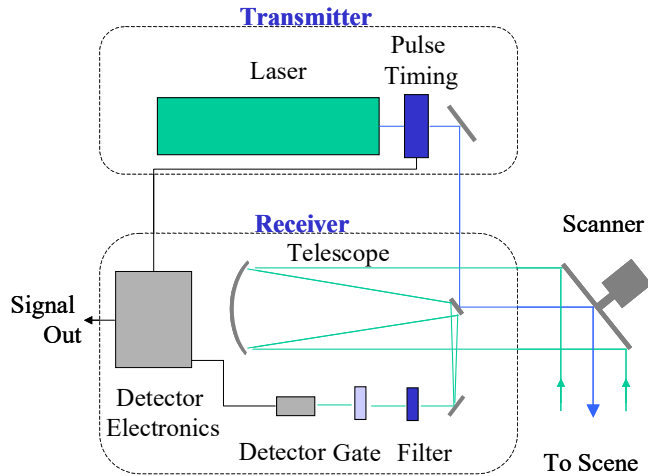


Figure 1.2: Basic Lidar components

Figure 1.2 shows the basic components of a lidar system. The transmitter consists of a laser source and its affiliated optical and electronic components. The receiver consists of the light gathering optics and the detector system. There are many types of lidar and therefore there are many variations on this basic theme. Some lidar systems designed for remote chemical analysis have several lasers generating different wavelengths of light. The detector system shown in Figure 1.2 is very simple. More complex systems might include superheterodyne based coherent detectors used in vibrometry or Doppler wind detection.

1.1.1 Range definition and Range measurement

The range is the distance from the lidar sensor to the object or target that has been detected. An example is shown in figure 1.3. The light from the transmitter travels at a nearly constant speed of $c = 2.998 \times 10^8$ m/s. The light detected at the receiver will have traveled to the target and back, thus it will have traveled

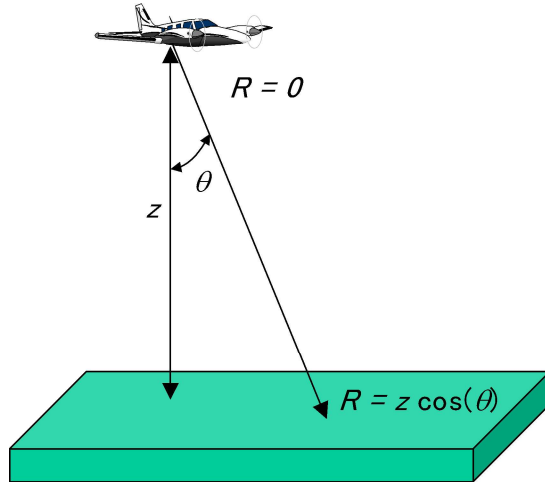


Figure 1.3:

a distance of $2R$. If the light is emitted as discrete pulses, then we can record how long it takes the pulse to travel to the target and back. Knowing that c is constant, we can use the round trip time, t , to find the range

$$R = \frac{ct}{2} \quad (1.1)$$

This is the ranging part of *light detection and ranging*. Range information can be used as in traditional radar to measure distance. Because laser beams have low divergence angles (they have very narrow beams) the lidar can be scanned to build very high resolution maps of range to scatterers or targets (see figure 1.4 below). If the range measurement is from an aircraft to the ground, the result may be a high density digital elevation map. This is the most common commercial use of lidar today. There are also obvious military use of high density digital elevation maps, and in military circles the type of lidar that collects this type of data has been named *ladar*, which stands for *laser detection and ranging*. The distinction is not obvious from the name, since most lidar measurements of atmospheric targets also use lasers.

1.1.2 Pulse Shapes

It would be ideal if the emitted pulse was infinitely narrow in time and had a zero bandwidth, but such a pulse cannot be produced in practice. Real pulses have both temporal shape and spectral shape. A brief description of a simple laser pulse follows.

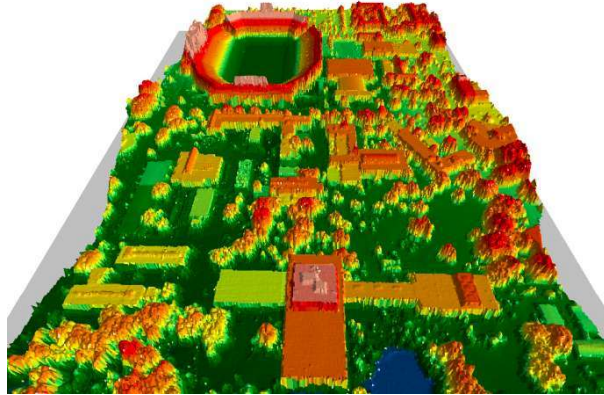


Figure 1.4: Terrain map of the University of Florida taken with the Optek ALTM instrument. <http://www.optech.on.ca/>

Temporal (in range) pulse shape

Equation (1.1) is accurate to within the width of a pulse for a reflective target or a scatterer. To understand the interaction of the light with the target and the limitations this interaction places on ranging, we will need to understand that each emitted pulse has a shape. A typical laser pulse is roughly shaped like a Gaussian, however, much more complex shapes are possible. The pulse is generated as a function of time, but because time and range are related through equation (1.1), the laser pulse can be thought of as having a pulse width in range. The return signal is a convolution of the shape of the objects encountered by the pulse and the pulse shape. For example, if pulse is emitted from the lidar and hits a smooth flat surface, the return pulse has the same shape as the emitted pulse, but if the smooth flat surface is tipped so that the pulse strikes it at an angle, the return pulse is longer than the emitted pulse. In this case the *range resolution* of the lidar is degraded. To see this, consider a photon that travels at the beginning of a pulse. Suppose this photon strikes the top of the surface in figure 1.5.b. Another photon from the trailing edge of the emitted pulse may hit the bottom of the surface in figure 1.5.b. Because it travels a shorter distance than the first photon, it may return at the same time, or even before the first photon, even though it left later. This means we have less ability to determine the range. From this example it is clear that the range resolution depends on the size of the original pulse and on the shape of the surface. The exact form of this dependency is given by a convolution.

Although range resolution is degraded when the lidar beam strikes complex objects, other information may be gained. If the pulse strikes a tree, for example, the shape of the return pulse can be used to classify the structure of the tree and distinguish different types of trees.

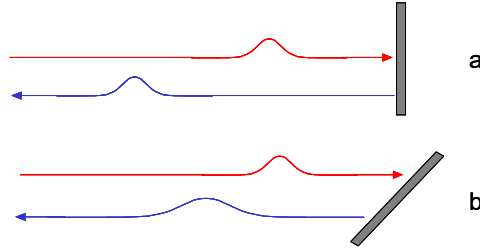


Figure 1.5: The Return Pulses (Blue) are a Convolution of the Emitted Pulse Shape (Red) and the Surface Encountered. In a) the light strikes normal to the surface and the return pulse is the same as the emitted pulse. In b) the light strikes the surface at an angle, stretching the pulse.

Spectral Line Shape

We often represent light as a sine wave of a single frequency. It is very hard to generate a truly single frequency signal. Every laser has some narrow bandwidth of frequencies over which it emits light. Thus, each pulse will have a *spectral* shape as well as its temporal shape. Again the simplest spectral line shape looks like a Gaussian. Laser lines are very narrow, sometimes only tens of nanometers wide. The line is described by its peak wavelength, λ_o , and its width, $\Delta\lambda$.

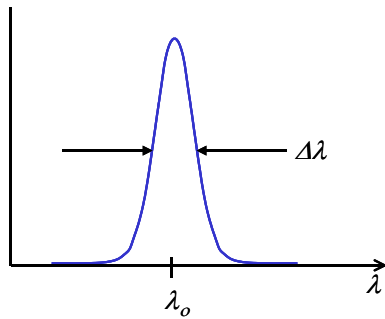


Figure 1.6: The laser line is described by its center frequency, λ_o , and its line width $\Delta\lambda$.

1.2 Basic Techniques

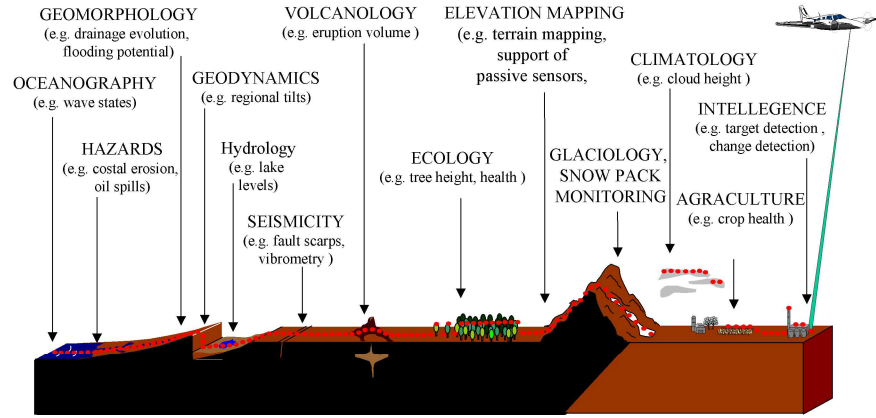


Figure 1.7:

It would be impossible to describe all the uses of lidar in a short section. Most readers will be familiar with the use of lidar in police work and many may have seen 3D tomography imagery taken with lidar in recent disasters . Figure 1.7 lists many of the common uses of lidar. Ranging and tomographic measurements have already been discussed in section 1.1.2. A few additional general use categories will be discussed below.

1.2.1 Aerosol Backscatter Measurements

In order for a lidar measurement to be made, something must stop the laser light in its progress and reverse the direction of the light so it can be collected back at the lidar instrument. In tomographic ranging, a hard surface (like the surface of the Earth, or the top of a building) can certainly do this. But to provide the ability to study the atmosphere, we would like some other reflector or scatterer that will allow us to return light along the lidar path. The atmospheric aerosols, most prevalent in the troposphere (lower atmosphere) provide such a scatterer. An example of lidar measurements of the lower atmosphere taken by the NASA LITE lidar instrument is given in figure 1.8. In the figure, clouds can be seen in two levels, one at about 5 km and another at about 12 km. Lower, a layer of haze can be seen. Soot, dust, pollen, and other small particles make up this layer of aerosols. Particles from the surface are brought up into the atmosphere by convection. Higher in the atmosphere ice crystals form another source of particles. In all these cases, the particles, when illuminated, will scatter light back to the sensor. In lidar terminology we say that the light is *backscattered* by the particles.

If there are many particles, no light can get through, and the lidar beam

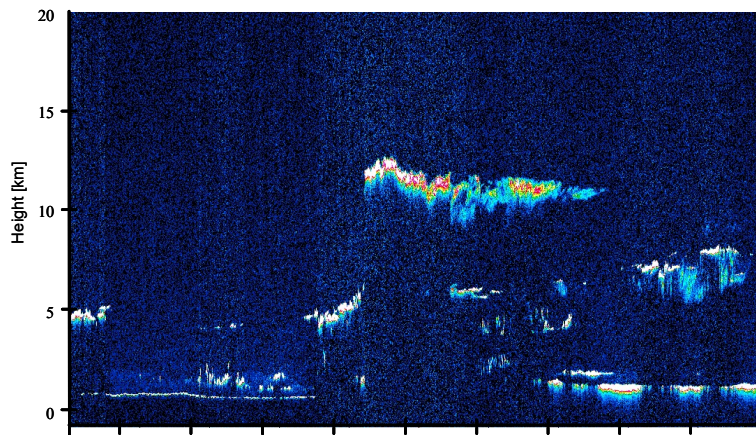


Figure 1.8: Lidar backscatter measurements taken by the NASA LITE instrument. Two levels of clouds are clearly visible as well as a stratiform layer of cloud and haze near the surface. Notice that the LITE beam does not penetrate the thicker storm clouds. Also notice at the left of the image that the ground return is visible (at about 1 km).

is stopped. In the figure we see this happened when the lidar illuminated the 12 km storm clouds. No signal is present below the clouds. But for thinner concentrations of particles, some of the light gets through to illuminate the volumes of air below (see figure 1.9). Particles from the lower volumes will also backscatter light to the lidar receiver. By watching the lidar return as a function of time, we probe different levels of the atmosphere.

The very fact of the backscatter from particles gives a lidar the ability to study clouds and some forms of pollution. Clever lidar systems have been designed that will not only detect the presence of particles, but can give information on the particle size.

The usefulness of backscatter measurements goes beyond particle detection, however, as we will see in the next section.

1.2.2 Differential Absorption Lidar

Differential absorption lidar (DIAL) is covered in detail in section 4. In this section we will introduce the concept. DIAL is a spectroscopic technique. DIAL and its close cousin, differential absorption spectroscopy (DAS) seek to detect and quantify gases in the atmosphere. Examples are the detection of Ozone and or monitoring of CO_2 levels.

These techniques use a common mechanism. The gas targets they seek to detect have absorption features that prevent part of the laser light from traveling through the volume that contains the gas.

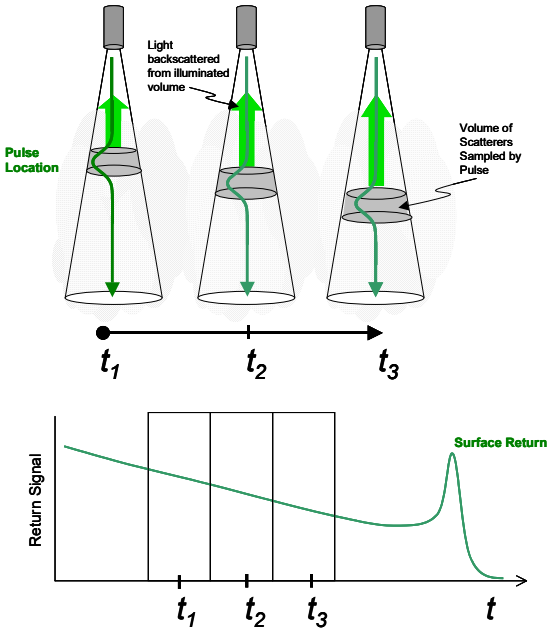


Figure 1.9: Ranging in an Aerosol Return. The pulse illuminates a volume of scatterers at time t_1 . The particles scatter light back to the sensor creating part of the time resolved return signal shown below. The light is not extinguished in the first volume so the pulse travels on to the second volume (t_2) where again the particles scatter light to the sensor. The process is repeated at t_3 and so on until the pulse is reflected by the surface.

DIAL chooses one of these absorption features. Two laser wavelengths are used, one wavelength near the center of the absorption feature, one wavelength off the absorption feature, but not far from its base (see figure 1.11). The light with wavelength on the absorption feature will be absorbed, that is, reduced in brightness. By comparing the signal at the two wavelengths, the amount of absorbing gas present in the volume can be determined.

The concept is simple, but there is one piece that we have not explained. The light must return to the lidar sensor in order for the measurement to take place. The gas only removes light from the signal, it cannot change the direction of travel of the light. This is where our aerosol backscatter becomes useful. If the two wavelengths are not too different, then they will scatter alike from the aerosols. The same amount of light would return from the aerosols from each of the wavelengths if there were no absorbing gas. But with the gas present, the signals will be different, and the gas concentration can be measured. If we use the fact that the pulse illuminates different layers of the atmosphere as a function of time, we can not only detect the gas target, but also give its

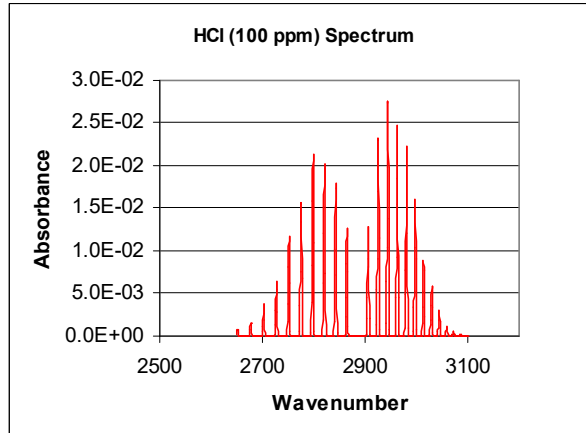


Figure 1.10: Absorbance of HCL as a function of wavenumber (cm^{-1}). Courtesy Joesph Lippert of Kodak Research Laboratory.

range. Using this technique, scanning lidar systems have been developed that can collect data to build three dimensional maps of factory plumes or other chemical effluent releases.

As you can imagine, the backscattered signal from aerosols is only a weak signal. Detection of a gas can be improved by looking at all the light that travels to the surface of the earth (or some other hard solid object) and back for both wavelengths at once. This technique can provide several orders of magnitude better signal-to-noise ratio over aerosol backscatter measurements, but because it integrates the entire signal for each pulse, the technique cannot provide ranging. Because it cannot range, this technique is often called differential absorption spectroscopy, but is also known (somewhat erroneously)as Surface Reflectance DIAL. In section 4.2 we will discuss this technique further

1.2.3 Raman Lidar

Not done yet

1.2.4 Fluorescence Lidar

Not done yet

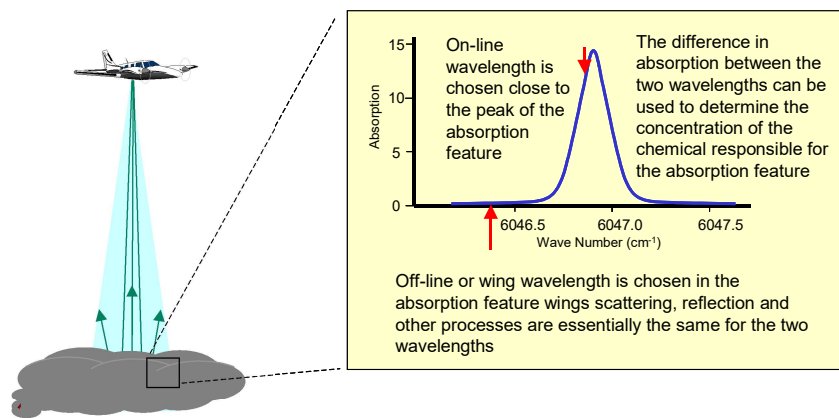


Figure 1.11: Differential Absorption Lidar and Differential Absorption Spectroscopy Concept.

Part II

Fundamental Equations

Chapter 2

Basics of Radiative Transfer

Not done yet

To describe the transfer of radiation through the atmosphere[6][1], we begin with Maxwell's equations in Gaussian units,

$$\nabla \cdot \mathcal{E} = 4\pi\rho \quad (2.1)$$

$$\nabla \cdot \mathcal{B} = 0 \quad (2.2)$$

$$\nabla \times \mathcal{E} = -\frac{1}{c} \frac{\partial \mathcal{B}}{\partial t} \quad (2.3)$$

$$\nabla \times \mathcal{B} = \frac{1}{c} \frac{\partial \mathcal{E}}{\partial t} + \frac{4\pi}{c} \mathbf{j} \quad (2.4)$$

where \mathcal{E} and \mathcal{B} are the electric and magnetic fields, ρ is the charge density, \mathbf{j} is the current density, c is the speed of light and t is time. The operator ∇ is the usual gradient operator.

For material media, we may always write

$$\rho = -\nabla \cdot \mathcal{P}(\mathbf{r}, t) \quad (2.5)$$

$$\mathbf{j} = \frac{\partial \mathbf{P}(\mathbf{r}, t)}{\partial t} + c \nabla \times \mathcal{M}(\mathbf{r}, t) \quad (2.6)$$

where $\mathcal{P}(\mathbf{r}, t)$ is the polarization and $\mathcal{M}(\mathbf{r}, t)$ is the magnetization. We will take the usual time dependence for all electromagnetic fields. For example

$$\mathcal{E}(\mathbf{r}, t) = \mathcal{E}(\mathbf{r}) \exp(-i\omega t) + c.c. \quad (2.7)$$

where $\mathcal{E}(\mathbf{r})$ stands for the complex valued field amplitude vector, a function of position \mathbf{r} , and where ω is the angular frequency. The notation *c.c.* refers to the complex conjugate of the preceding term. The wave number k is given by

$$k = \frac{\omega}{c} = \frac{2\pi}{\lambda} \quad (2.8)$$

where λ is the wavelength. Only linear, static, nonmagnetic media will be considered, so that the complex amplitudes $[\mathcal{P}(\mathbf{r}), \mathcal{M}(\mathbf{r})]$ may be written as

$$\mathcal{P} = \chi \mathcal{E} \quad (2.9)$$

$$\mathcal{M} = \mathbf{0} \quad (2.10)$$

where the explicit dependence on position has not been written, and χ is the complex electric susceptibility.

The complex permittivity is given in terms of the complex susceptibility by

$$\epsilon(\mathbf{r}) = 1 + 4\pi\chi(\mathbf{r}) \equiv m^2(\mathbf{r}) \quad (2.11)$$

where the last equality defines the complex refractive index $m(\mathbf{r})$. Using this last equation, the displacement field \mathcal{D} may be written as

$$\mathcal{D} = \mathcal{E} + 4\pi\mathcal{P} = \epsilon\mathcal{E} \quad (2.12)$$

which yields

$$\nabla \cdot \mathcal{D} = 0 \quad (2.13)$$

$$\nabla \cdot \mathcal{B} = 0 \quad (2.14)$$

$$\nabla \times \mathcal{E} = -\frac{1}{c} \frac{\partial \mathcal{B}}{\partial t} \quad (2.15)$$

$$\nabla \times \mathcal{B} = \frac{1}{c} \frac{\partial \mathcal{D}}{\partial t} \quad (2.16)$$

Starting with the curl of equation (2.15) we obtain

$$\nabla \times (\nabla \times \mathcal{E}) = -\frac{1}{c} \left(\nabla \times \frac{\partial \mathcal{B}}{\partial t} \right) \quad (2.17)$$

$$\nabla \times (\nabla \times \mathcal{E}) = -\frac{1}{c} \frac{\partial}{\partial t} (\nabla \times \mathcal{B}) \quad (2.18)$$

we use the vector calculus general identity

$$\nabla \times (\nabla \times \mathcal{E}) = \nabla (\nabla \cdot \mathcal{E}) - \nabla^2 \mathcal{E} \quad (2.19)$$

to arrive at the form

$$\nabla (\nabla \cdot \mathcal{E}) - \nabla^2 \mathcal{E} = -\frac{1}{c^2} \frac{\partial^2 \mathcal{D}}{\partial t^2} \quad (2.20)$$

finally we use the definition of \mathcal{D} to write

$$\nabla (\nabla \cdot \mathcal{E}) - \nabla^2 \mathcal{E} = -\frac{1}{c^2} \left(\frac{\partial^2 \mathcal{E}}{\partial t^2} + 4\pi \frac{\partial^2 \mathcal{P}}{\partial t^2} \right) \quad (2.21)$$

For laser remote sensing, we are generally interested in solutions to this equation that lead to transverse fields. For such fields

$$\nabla \cdot \mathcal{E} = 0 \quad (2.22)$$

Therefore we have the wave equation

$$\nabla^2 \mathcal{E} - \frac{1}{c^2} \frac{\partial^2 \mathcal{E}}{\partial t^2} = +\frac{4\pi}{c^2} \frac{\partial^2 \mathcal{P}}{\partial t^2} \quad (2.23)$$

For a free space propagation the polarization density vanishes (there is no material media)

$$\nabla^2 \mathcal{E} - \frac{1}{c^2} \frac{\partial^2 \mathcal{E}}{\partial t^2} = 0 \quad (2.24)$$

2.1 Solutions to the free space wave equation

For our purposes, we may start with the propagation of monochromatic fields (equation 2.7).

$$\mathcal{E}(\mathbf{r}, t) = \mathcal{E}(\mathbf{r}) \exp(-i\omega t) + c.c. \quad (2.25)$$

Then the free space wave equation may be written as

$$\nabla^2 \mathcal{E}(\mathbf{r}) + k^2 \mathcal{E}(\mathbf{r}) = 0 \quad (2.26)$$

A simple solution to this equation is

$$\mathcal{E}(\mathbf{r}) = \mathcal{E}_o e^{i\mathbf{k} \cdot \mathbf{r}} \quad (2.27)$$

a plane wave, where \mathcal{E}_o is a constant \mathbf{k} is a vector whose squared magnitude is the wave number squared, k^2 .

Another solution is

$$\mathcal{E}(\mathbf{r}) = \frac{A}{r} e^{ikr} \quad (2.28)$$

for $r \neq 0$. This is a spherical wave. For this solution the intensity of the wave will decrease with r^2 .

2.1.1 Paraxial Wave Equation

First let's define a Euclidian coordinate system. We have

$$r = \sqrt{x^2 + y^2 + z^2} \quad (2.29)$$

If we use the spherical wave solution to the wave equation and concentrate on a small area of observation near the point $x = 0, y = 0, z = R$, we have

$$r = \sqrt{x^2 + y^2 + R^2} \quad (2.30)$$

$$= R \sqrt{1 + \frac{x^2 + y^2}{R^2}} \quad (2.31)$$

Now let's say that $x^2 + y^2$ is much smaller than R^2 then, using the binomial expansion,

$$\sqrt{\left(1 + \frac{x^2 + y^2}{R^2}\right)} \simeq 1 + \frac{x^2 + y^2}{2R^2} + \dots \quad (2.32)$$

and

$$kr \approx kR + \frac{k(x^2 + y^2)}{2R} \quad (2.33)$$

then in this *peraxial approximation* the field is given by

$$\mathcal{E}(\mathbf{r}) = \frac{A}{R} e^{ikR} e^{ik\frac{(x^2 + y^2)}{2R}} \quad (2.34)$$

Note that we replaced r by R in the denominator, but in the numerator more accuracy is needed and there for both terms from equation (2.33). For this to be a good approximation

$$\frac{x^2 + y^2}{\lambda R} \ll \left(\frac{R}{\sqrt{x^2 + y^2}} \right)^2 \quad (2.35)$$

This condition comes from the need of the next term in the expansion in equation (2.33) being small compared to the second term.

To construct a beam-like behavior from solutions to the free space wave equation we change the form of the solution to have not constnat coefficients, for example

$$\mathcal{E}(\mathbf{r}) = \mathcal{E}_o(\mathbf{r}) e^{i\mathbf{k}\cdot\mathbf{r}} \quad (2.36)$$

for the plane wave. We seek a solution to the wave equatoin which has nearly the unidirectionality of a plane wave, but with finite beam cross section. We will make the restrictions that $\mathcal{E}_o(\mathbf{r})$ and $\partial\mathcal{E}_o(\mathbf{r})/\partial z$ do not vary much within a distance on the order of a wavelength in the z direction.

$$\begin{aligned} \lambda \left| \frac{\partial \mathcal{E}_o(\mathbf{r})}{\partial z} \right| &\ll |\mathcal{E}_o(\mathbf{r})| \\ \lambda \left| \frac{\partial^2 \mathcal{E}_o(\mathbf{r})}{\partial z^2} \right| &\ll \left| \frac{\partial \mathcal{E}_o(\mathbf{r})}{\partial z} \right| \end{aligned} \quad (2.37)$$

This means that over distances in z on the order of several wavelengths $\mathcal{E}(\mathbf{r})$ varies like e^{ikz} .

Our new solution must satisfy the wave equation, we have

$$\nabla^2 \mathcal{E}_o(\mathbf{r}) e^{i\mathbf{k}\cdot\mathbf{r}} - \frac{1}{c^2} \frac{\partial^2 \mathcal{E}_o(\mathbf{r}) e^{i\mathbf{k}\cdot\mathbf{r}}}{\partial t^2} = 0 \quad (2.38)$$

To start our solution we observe $\partial^2 \mathcal{E}(\mathbf{r}) / \partial z^2$

$$\begin{aligned}
\frac{\partial^2}{\partial z^2} \mathcal{E}_o(\mathbf{r}) e^{ikz} &= \frac{\partial}{\partial z} \left(e^{ikz} \frac{\partial}{\partial z} \mathcal{E}_o(\mathbf{r}) + \mathcal{E}_o(\mathbf{r}) \frac{\partial}{\partial z} e^{ik\mathbf{k}\cdot\mathbf{r}} \right) \\
&= \left(e^{ikz} \frac{\partial}{\partial z} \mathcal{E}_o(\mathbf{r}) + ik \mathcal{E}_o(\mathbf{r}) e^{ikz} \right) \\
&= \frac{\partial}{\partial z} \left(e^{ikz} \frac{\partial}{\partial z} \mathcal{E}_o(\mathbf{r}) \right) + \frac{\partial}{\partial z} (ik \mathcal{E}_o(\mathbf{r}) e^{ikz}) \\
&= e^{ikz} \frac{\partial}{\partial z} \frac{\partial}{\partial z} \mathcal{E}_o(\mathbf{r}) + \frac{\partial}{\partial z} \mathcal{E}_o(\mathbf{r}) ike^{ikz} + ik \mathcal{E}_o(\mathbf{r}) ike^{ikz} + ike^{ikz} \frac{\partial}{\partial z} \mathcal{E}_o(\mathbf{r}) \\
&= +2ike^{ikz} \frac{\partial \mathcal{E}_o(\mathbf{r})}{\partial z} + e^{ikz} \frac{\partial^2 \mathcal{E}_o(\mathbf{r})}{\partial z^2} - k^2 \mathcal{E}_o(\mathbf{r}) e^{ikz}
\end{aligned}$$

If we use the conditions in equation (2.37) then

$$\frac{\partial^2}{\partial z^2} \mathcal{E}_o(\mathbf{r}) e^{ikz} = e^{ikz} \left(2ik \frac{\partial \mathcal{E}_o(\mathbf{r})}{\partial z} - k^2 \mathcal{E}_o(\mathbf{r}) \right) \quad (2.39)$$

and the wave equation is

$$\left(\frac{\partial^2}{\partial x^2} + \frac{\partial^2}{\partial y^2} + \frac{\partial^2}{\partial z^2} \right) \mathcal{E}_o(\mathbf{r}) e^{i\mathbf{k}\cdot\mathbf{r}} + k^2 \mathcal{E}_o(\mathbf{r}) e^{ikz\mathbf{r}} \quad (2.40)$$

$$\left(\frac{\partial^2}{\partial x^2} + \frac{\partial^2}{\partial y^2} \right) \mathcal{E}_o(\mathbf{r}) e^{i\mathbf{k}\cdot\mathbf{r}} + e^{ikz} \left(2ik \frac{\partial \mathcal{E}_o(\mathbf{r})}{\partial z} - k^2 \mathcal{E}_o(\mathbf{r}) \right) + k^2 \mathcal{E}_o(\mathbf{r}) e^{ikz\mathbf{r}} \quad (2.41)$$

$$\left(\frac{\partial^2}{\partial x^2} + \frac{\partial^2}{\partial y^2} + 2ik \frac{\partial}{\partial z} \right) \mathcal{E}_o(\mathbf{r}) e^{i\mathbf{k}\cdot\mathbf{r}} \quad (2.42)$$

We define an operator

$$\nabla_T^2 = \left(\frac{\partial^2}{\partial x^2} + \frac{\partial^2}{\partial y^2} \right) \quad (2.43)$$

which allows us to write the *paraxial wave equation* as

$$\nabla_T^2 \mathcal{E}_o(\mathbf{r}) + 2ik \frac{\partial \mathcal{E}_o(\mathbf{r})}{\partial z} = 0 \quad (2.44)$$

with the solution

$$\mathcal{E}(\mathbf{r}) = \mathcal{E}_o(\mathbf{r}) e^{i\mathbf{k}\cdot\mathbf{r}} \quad (2.45)$$

This elementary solution does not describe the details of most laser radar beams, however, because most laser systems have more complex beam profiles. In Section 6.1 we will return to this topic for the most fundamental laser beam the TEM₀₀ Gaussian beam.

Not done yet Need to get to radiance

2.2 Transmission: Beer's Law

We will define the transmission function as the function that maps the initial radiance, I_o into the final radiance I after a distance z .

$$I(\lambda) = I_o(\lambda) T(\lambda, z)$$

where $T(\lambda, z)$ is the transmission.

We write the transmission as an integral over the path length

$$T(\lambda, z) = \exp \left(- \int_{l=0}^z n(l) \sigma(\lambda, l) dl \right)$$

In the case of a plume the concentration may vary along the path, thus n , the concentration, is a function of l . The temperature and pressure may also vary through the plume. the cross section $\sigma(\lambda, l)$ would also vary with temperature and pressure as well as concentration. These variations seem weak (change the value of the cross section by less than a factor of two), so for now we will ignore them.

Transmission is a spectral quantity, so we need to understand its spectral nature. The cross section varies with the wavelength of the illumination. The cross section is given by

$$\sigma(\lambda, l) = S(\lambda, l) \frac{1}{\pi} \frac{\alpha(\lambda, l)}{\alpha(\lambda, l)^2 + (\nu - \nu_o - \delta(\lambda, l) p(l))^2}$$

where $S(\lambda, l)$ is the line strength and $\alpha(\lambda, l)$ is the line width. The quantity $\delta(\lambda, l)$ is a pressure dependent line shift and p is the pressure in the plume at path location l .

The shape of the line is empirical, but we will use a standard line shape from first principals to approximate the true form. This will give the good results for isolated lines, but where two or more lines overlap, the separate lines should be summed. We will assume the line shape

$$f = \frac{1}{\pi} \frac{\alpha}{\alpha^2 + (\nu - \nu_o - \delta p)^2}$$

We really should integrate over wavelength, but the laser spectral line width is so much smaller than the absorption line width that the laser is essentially a delta function. From the spec we have $\Delta\tilde{\nu}_{laser} < 250$ MHz

Then

$$\Delta\tilde{\nu} = \frac{c}{\lambda^2} \Delta\lambda$$

$$\begin{aligned}
\Delta\tilde{\nu}\frac{\lambda^2}{c} &= 250 \text{ MHz} \frac{(3.429 \times 10^{-4} \text{ cm})^2}{3 \times 10^8 \frac{\text{m}}{\text{s}}} \\
&= 9.7984 \times 10^{-14} (\text{MHz}) \frac{\text{cm}^2}{\text{m}} \text{ s} \\
&= 9.7984 \times 10^{-12} \text{ m} \\
&= 9.7984 \times 10^{-3} \text{ nm}
\end{aligned}$$

for the laser line width

For the absorption line

$$\alpha = \Delta\nu \approx \frac{4.2702 \times 10^{-2}}{\text{cm}}$$

$$\Delta\nu = \frac{1}{\lambda^2} \Delta\lambda$$

$$\begin{aligned}
\Delta\lambda &= \lambda^2 \Delta\nu \\
&= (3.429 \times 10^{-4} \text{ cm})^2 \frac{4.2702 \times 10^{-2}}{\text{cm}} \\
&= 5.0209 \times 10^{-9} \text{ cm}
\end{aligned}$$

thus the laser line is three orders of magnitude smaller than the absorption line. We are justified it treating it like a delta function in the calculations.

For now we can assume that $n(l)$ is constant in the plume and zero outside the plume.

$$T(\lambda, z) = \exp(-n\sigma(\lambda)z)$$

Chapter 3

Derivation of the Basic Lidar Equations

We will start by assuming a monostatic lidar system looking toward a target as depicted in figure 3.1. Occasionally we will relax the monostatic assumption, and consider a bistatic system, but unless stated otherwise the following assumption will hold.

Assumption 3-1: a pulsed monostatic lidar

We wish to calculate the increment of signal power $\Delta P(\lambda, R)$ received by the detector in the wavelength interval $(\lambda, \lambda + \Delta\lambda)$ from the range element $(R, R + \Delta R)$.¹ The range element is the shaded volume depicted in figure 3.1.

$$\Delta P(\lambda, R) = \int J(\lambda, R, \mathbf{r}) p(\lambda, R, \mathbf{r}) \Delta\lambda \Delta R dA(R, \mathbf{r}) \quad (3.1)$$

The quantity $J(\lambda, R, \mathbf{r})$ represents the laser-induced spectral radiance at wavelength λ , at position \mathbf{r} in the target plane located at range R , per unit range interval and has units of *power per length⁴ per solid angle* (e.g. $\text{W m}^{-2} \text{cm}^{-2} \text{sr}^{-1}$).

The range, R , is measured from the lidar sensor, thus, $R = 0$ is at the receiver entrance aperture. The quantity $dA(R, \mathbf{r})$ is the element of target area at position \mathbf{r} at range R , and $p(\lambda, R, \mathbf{r})$ is the probability that a photon of wavelength λ emanating from position \mathbf{r} at range R will hit the detector. We may write this last term as

$$p(\lambda, R, \mathbf{r}) = \frac{A_o}{R^2} T(\lambda, R) \xi(\lambda) \xi(R, \mathbf{r}) \quad (3.2)$$

where A_o/R^2 is the acceptance solid angle of the receiver optics in steradians, $T(\lambda, R)$ is the atmospheric transmission factor at wavelength λ and position R ,

¹Following Measures (1984) and using his notation[3]

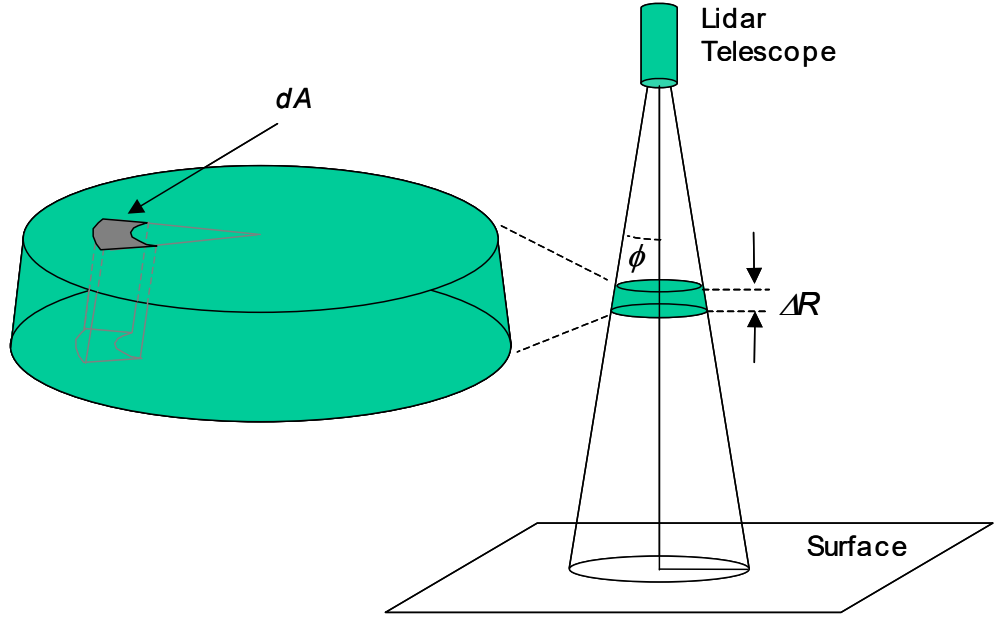


Figure 3.1: Simple Lidar Geometry

$\xi(\lambda)$ is the system spectral transmission factor, and $\xi(R, \mathbf{r})$ is the probability of a photon from position \mathbf{r} in the target plane at range R hitting the detector based on geometry factors alone.

Assumption 3-2: $\xi(R, \mathbf{r})$ depends only on the overlap region

We will assume that $\xi(R, \mathbf{r})$ depends only on the overlap of the area of laser irradiation with the field of view of the receiver optics. This term is commonly called the *overlap factor* or, in its more complete form, the *geometric form factor* (discussed in section 11.9).

The total signal power received by the detector at time, $t = 2R/c$ corresponding to the round trip time of the leading edge of the pulse to range R can be written

$$P(\lambda, t) = \int_0^{R=ct/2} dR \int_{\Delta\lambda} d\lambda \int J(\lambda, R, \mathbf{r}) p(\lambda, R, \mathbf{r}) dA(R, \mathbf{r}) \quad (3.3)$$

The range integral originates from the fact that the received signal is made up from light that is scattered backward along the entire transmit path. At first glance this may seem unnecessary because for low order scattering cases most of the return will come from ΔR , but in the case of multiple scattering it is easy

to see that scattered photons may come from different locations and in different times. In the atmosphere there is Rayleigh scatter from the air molecules, which indeed gives a small return along the entire transmit path.

3.1 Scattering Form

Assumption 3.1-1: $J(\lambda, R, \mathbf{r})$ is due to elastic scattering

If the above assumption is taken, then the interaction term can be written as

$$J(\lambda, R, \mathbf{r}) = \beta_T(\lambda_L, \lambda, R, \mathbf{r}) I(R, \mathbf{r}) \quad (3.4)$$

where $I(R, \mathbf{r})$ is the laser irradiance at position \mathbf{r} and range R , and β_T is the total volume backscatter coefficient given by

$$\beta_T(\lambda_L, \lambda, R, \mathbf{r}) = \sum_i N_i(R, \mathbf{r}) \left(\frac{d\sigma(\lambda_L)}{d\Omega} \right)_i^s \mathcal{L}_i(\lambda) \quad (3.5)$$

$$= \sum_i \beta(\lambda_L, \lambda, R, \mathbf{r}) \mathcal{L}_i(\lambda) \quad (3.6)$$

where $N_i(R, \mathbf{r})$ is the number density of scatter species i , $(d\sigma(\lambda_L)/d\Omega)_i^s$ is the *differential scattering cross section* under irradiation at wavelength λ_L , and $\mathcal{L}_i(\lambda) \Delta\lambda$ is the fraction of the scattered radiation that falls into the receiver wavelength interval $(\lambda, \lambda + \Delta\lambda)$. This form of the total backscatter coefficient has units of inverse length squared (wavelength dependence) multiplied by inverse steradians (e.g. $\text{cm}^{-2} \text{sr}^{-1}$). This differs from the normal (angular dependence) units of inverse length per inverse steradian, (e.g. $\text{cm}^{-1} \text{sr}^{-1}$). This is because the factor $\mathcal{L}_i(\lambda)$ has been included. Since the irradiance is in units of power per area (e.g. W/m^2) we have units of power per volume per steradian (e.g. $\text{W}/(\text{sr m}^3)$) for $J(\lambda, R, \mathbf{r})$.

The quantity $\mathcal{L}_i(\lambda)$ is a line shape for the scattering. It differs from the normal lineshapes due to atomic or molecular extinction (see Chapter 14), but is similar in its definition, thus

$$\int \mathcal{L}_i(\lambda) d\lambda = 1$$

Figure 3.2 shows two different scenarios in which a natural scattering feature is being measured by a lidar receiver system. Figure 3.2a shows a case where the filter function is narrower than the scattering response. In this case signal returning to the sensor may be lost and therefore the factor $\mathcal{L}_i(\lambda) \Delta\lambda < 1$. Figure 3.2b shows a case where the filter band pass is significantly wider than the transition line. Because scattered light from all frequencies in the line shape is passed through the filter, $\mathcal{L}_i(\lambda) \Delta\lambda = 1$. In this case, $\mathcal{L}_i(\lambda)$ is narrow enough that as we integrate across the filter bandpass it behaves like a Dirac delta function

$$\int f(\lambda) \mathcal{L}_i(\lambda - \lambda_o) d\lambda = f(\lambda_o) \quad (3.7)$$

In the sections that follow we will generally assume that our filter is wide enough so that $\mathcal{L}_i(\lambda) \Delta\lambda = 1$. The quantity $\mathcal{L}_i(\lambda)$ must have units of inverse length (e.g. cm^{-1}). so that $\mathcal{L}_i(\lambda) \Delta\lambda$ is unitless.

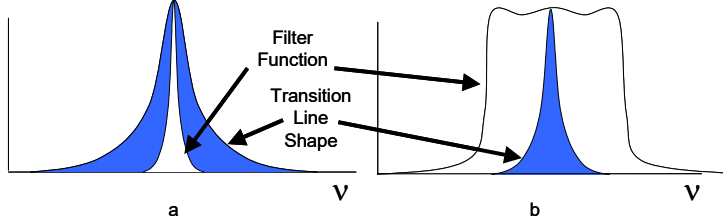


Figure 3.2:

3.1.1 Power Received

The received power can be found using equation (3.3) and (3.2) using assumption 3.1-1 as represented by equation (3.4).

$$\begin{aligned} P(\lambda, t) &= A_o \int_0^{R=ct/2} \frac{1}{R^2} \int_{\Delta\lambda} \xi(\lambda) d\lambda \\ &\times \int \beta(\lambda_L, \lambda, R, \mathbf{r}) I(R, \mathbf{r}) T(\lambda, R) \xi(R, \mathbf{r}) dA(R, \mathbf{r}) dR \end{aligned} \quad (3.8)$$

Remember that $t = 2R/c$ is the round trip time of the leading edge of the pulse from the transmitter to range R . Thus, $P(\lambda, t)$ will be the return from a volume of the atmosphere at range R which has been illuminated by the traveling pulse and is therefore about $\Delta R = ct_L$ long, where t_L is the pulse length, with a cross sectional area of about $A_L(R)$. To predict the detected signal, $P(\lambda, t)$ will be integrated over the detector integration time.

We will make a few assumptions that will lead to the form of the lidar equation that is found in most texts.[7][8][3]

Assumption 3.1-2: Transmitter radiation is narrow band
Assumption 3.1-3: Received radiation is equally narrow band
Assumption 3.1-4: Both are narrower than the receiver's spectral window $\Delta\lambda_o$
Assumption 3.1-5: The target medium is homogeneous

The first three assumptions (3.1-2 –3.1-4) allow us to apply the reasoning that lead to equation (3.7). We will assume that the fractional scattered radiation $\mathcal{L}_i(\lambda) d\lambda$ and therefore the backscattering coefficient can be treated as a delta function. Thus, the equation for the power received is reduced to

$$P(\lambda, t) = A_o \xi(\lambda) \int_0^{R=ct/2} \frac{1}{R^2} \beta(\lambda_L, \lambda, R) T(\lambda, R) \int \xi(R, \mathbf{r}) I(R, \mathbf{r}) dA(R, \mathbf{r}) dR \quad (3.9)$$

Note that the delta function leaves behind a length unit from the integration over wavelength.

3.1.2 Basic Scattering Lidar Equation

Assumption 3.1.2-1: $\xi(R, \mathbf{r}) = 1$ in overlap region and is zero elsewhere

Assumption 3.1.2-2: laser pulse is spatially uniform over area $A_L(R)$

Assumption 3.1.2-3: Laser pulse is square, $\text{rect}(c(t - \tau_{LL})/2, c(t + \tau_L)/2)$

Assumption 3.1.2-4: Range of interest is much greater than pulse length

The first assumption (3.1.2-1) tells us that

$$\int \xi(R, \mathbf{r}) I(R, \mathbf{r}) dA(R, \mathbf{r}) = \xi(R) I(R) A_L(R) \quad (3.10)$$

We will relax these assumptions later treating more realistic pulse shapes and obscurations, etc. For now, we find that the return power is given by

$$P(\lambda, t) = A_o \xi(\lambda) \int_0^{R=ct/2} \beta(\lambda_L, \lambda, R) T(\lambda, R) \xi(R) I(R) A_L(R) \frac{dR}{R^2} \quad (3.11)$$

The last assumption (3.1.2-4) allows us to treat the range-dependent parameters as constants over the small interval of range integration, then

$$\begin{aligned} P(\lambda, t) &= A_o \xi(\lambda) \beta(\lambda_L, \lambda, R) T(\lambda, R) \xi(R) I(R) A_L(R) \\ &\times \frac{c\tau_L}{2R(R - \frac{c\tau_L}{2})} \\ &\simeq A_o \xi(\lambda) \beta(\lambda_L, \lambda, R) T(\lambda, R) \xi(R) I(R) A_L(R) \frac{c\tau_L}{2R^2} \end{aligned} \quad (3.12)$$

Finally we use assumptions (3.1.2-2) and (3.1.2-3) to describe the irradiance as

$$I(R) = \frac{E_L T(\lambda_L, R)}{\tau_L A_L(R)} \quad (3.13)$$

where E_L is the output energy of the laser pulse and $T(\lambda_L, R)$ is the atmospheric transmission factor at the laser wavelength to range R . Because we know that energy divided by time is power, ($P_L = E_L/\tau_L$), we can write the illumination term as

$$I(R) = \frac{P_L T(\lambda_L, R)}{A_L(R)} \quad (3.14)$$

Recall that the units of $I(R)$ are power per unit area (W/m^2).

The transmission is given by

$$T(\lambda_L, R) = \exp \left(- \int_0^R \kappa(\lambda_L, R) dR \right) \quad (3.15)$$

where $\kappa(\lambda_L, R)$ is the atmospheric attenuation coefficient at the laser wavelength. The for the receive wavelength we have

$$T(\lambda, R) = \exp \left(- \int_0^R \kappa(\lambda, R) dR \right) \quad (3.16)$$

and the combined transmission is given by

$$T(R) = T(\lambda_L, R) T(\lambda, R) = \exp \left(- \int_0^R (\kappa(\lambda_L, R) + \kappa(\lambda, R)) dR \right) \quad (3.17)$$

For elastic scattering the receive and transmit wavelengths are the same, thus

$$T(\lambda_L, \lambda, R) = T(\lambda_L, R) T(\lambda, R) = \exp \left(-2 \int_0^R (\kappa(\lambda, R) dR) \right) \quad (3.18)$$

The transmission is a unitless quantity.

The amount of radiative energy at wavelength λ received by the detector during the interval $(t, t + \tau_d)$ where τ_d is the detector's response time is given by

$$E(\lambda, R) = \int_{\frac{2R}{c}}^{\frac{2R}{c} + \tau_d} P(\lambda, t) dt \quad (3.19)$$

Assumption 3.1.2-5: $\tau_d \ll \frac{2R}{c}$

This last assumption allows us to write

$$E(\lambda, R) = E_L \frac{A_o}{R^2} \xi(\lambda) \beta(\lambda_L, \lambda, R) T(\lambda_L, \lambda, R) \xi(R) \frac{c \tau_d}{2} \quad (3.20)$$

This is the basic scattering lidar equation

Range resolution

The effective range resolution is limited by the pulse length τ_L , and the detector integration time τ_{int}

In figure 3.3 a) the first photon reaches range R and returns. The forward edge of the pulse continues to travel in range. When the last photon reaches range R (figure 3.3 b), there is light that has reached the detector from the entire shaded area in figure 3.3 c). The projection of this area on the range axis gives

$$\text{resolution} = \frac{c(\tau_{int} + \tau_L)}{2} \quad (3.21)$$

which is the range resolution.

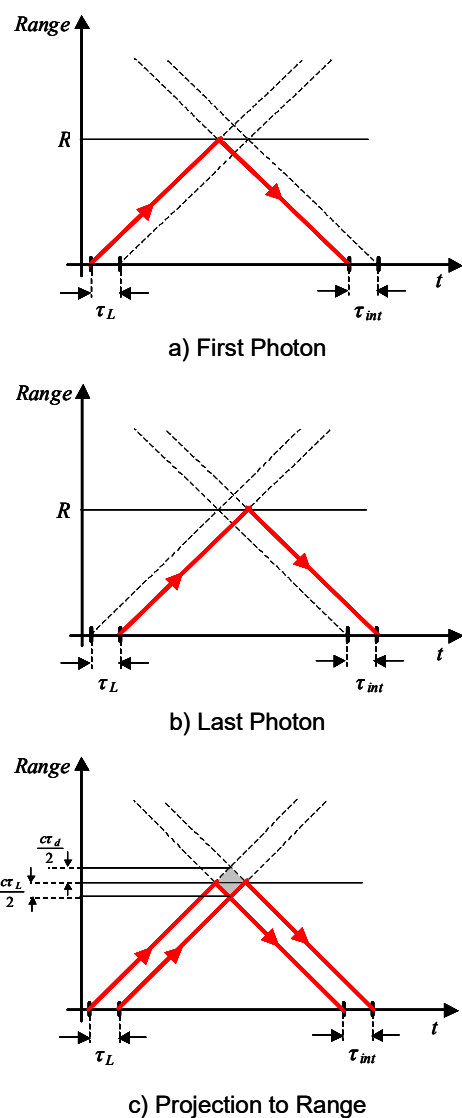


Figure 3.3: Description of the Range Resolution as a Function of the Temporal Pulse Length and the Detector Integration Time. (Patterned after Measures Figure 7.1.[3])

Effects of pulse shape

If we relax the assumption of a square pulse (assumption 3.1.2-3) and choose a more general form for the pulse shape, $\Phi(t')$ we may write the illumination as

$$I(R') = \frac{E_L T(\lambda_L, R')}{A_L(R')} \Phi(t') \quad (3.22)$$

where t' is time measured from a frame fixed to the leading edge of the laser pulse

$$t' = \frac{2(R - R')}{c} \quad (3.23)$$

and R' is the range corresponding to time t' .

The pulse shape must be normalized such that

$$\int_0^\infty \Phi(t') dt' = 1 \quad (3.24)$$

Using this definition of the pulse shape, we can rewrite equation (3.11)

$$P(\lambda, R) = A_o \xi(\lambda) E_L \int_0^{R=ct/2} \beta(\lambda_L, \lambda, R') T(\lambda_L, \lambda, R') \xi(R') \Phi(R') \frac{dR'}{R'^2} \quad (3.25)$$

where $\Phi(R')$ is the pulse shape in terms of R' . From assumption (3-3.1.2.4) we can say that the factor

$$\beta(\lambda_L, \lambda, R') T(\lambda_L, \lambda, R') \xi(R') \quad (3.26)$$

is constant over the small interval of range for which $\Phi(R')$ is non zero. Then

$$\begin{aligned} P(\lambda, R) &= \frac{A_o}{R^2} \xi(\lambda) E_L \beta(\lambda_L, \lambda, R) T(\lambda_L, \lambda, R) \xi(R) \\ &\times \int_0^{R=ct/2} \Phi(t') \frac{cdt'}{2} \end{aligned} \quad (3.27)$$

The upper limit of this integration corresponds to the time that the scattered radiation from the leading edge of the laser pulse reaches the lidar system. Thus from equation (3.24) we see that

$$\frac{c}{2} \int_0^{R=ct/2} \Phi(t') dt' \approx \frac{c\tau_L}{2} \quad (3.28)$$

thus

$$\begin{aligned} P(\lambda, R) &\simeq \frac{A_o}{R^2} \xi(\lambda_L) P_L \beta(\lambda_L, R) \xi(R) \frac{c\tau_L}{2} \\ &\times \exp \left(-2 \int_0^R (\kappa(\lambda_L, R) dR) \right) \end{aligned} \quad (3.29)$$

Writing this in terms of energy returned yields

$$\begin{aligned} E(\lambda, R) &\simeq \frac{A_o}{R^2} \xi(\lambda_L) P_L \beta(\lambda_L, R) \xi(R) \frac{c\tau_d}{2} \\ &\quad \times \exp \left(-2 \int_0^R (\kappa(\lambda_L, R) dR) \right) \end{aligned} \quad (3.30)$$

which is the same as equation (3.20). For many systems, the pulse shape is not important for the measurement. This is not true for topographic lidar or where ranging is also important.

3.1.3 Summary

To summarize, equations (3.20) and (3.30) are the standard forms of the scattering lidar equation found in the literature.[3][7][8] Both equations assume a pulsed monostatic lidar (assumption 3-1), that $\xi(R, \mathbf{r})$ depends only on the overlap region (assumption 3-2), that $J(\lambda, R, \mathbf{r})$ is due to elastic scattering only (assumption 3.1-1), that the transmitted radiation (assumption 3.1-2) and received radiation (assumption 3.1-3) are narrow band, and that both are narrower than the receiver's spectral bandwidth (assumption 3.1-4), that the target medium is homogeneous (assumption 3.1-5), that $\xi(R, \mathbf{r}) = 1$ in overlap region and is zero elsewhere (assumption 3.1.2-1), that the laser pulse is uniform over area $A_L(R)$ (assumption 3.1.2-3), that the range of interest is much greater than pulse length (assumption 3.1.2-4), and finally that $\tau_d \ll \frac{2R}{c}$ (assumption 3.1.2-5).

It is important to recall that the energy calculated in equations (3.20) or (3.30) come from a small volume of the atmosphere (range cell) defined by the beam cone at R and the range resolution $c(\tau_d + \tau_L)/2$. Each range cell along the path gives a return power that depends on the number of scatterers in the cell and the power of the beam at the range, R . Ground based lidar are often used to measure such returns from particulates as high as 20 km above the surface or more with range resolution of less than a meter.

3.2 Topographic Lidar (Ladar) Equation

Today, many lidar systems measure only the signal reflected from a surface. For example, digital elevation map production using time of flight requires only the surface reflected return. We can derive a special form of the lidar equation for this important special case. First we make the assumption that there is no significant ground penetration.

Assumption 3.2-1: Surface penetration depth is essentially zero

We can find an expression for the surface portion of the return signal by using the scattering cross section for an extended Lambertian surface (see Chapter 11.11.2).

$$\sigma_{scat}(\lambda_L, R) = \int \rho(\lambda_L, \mathbf{r}) dA_L(R, \mathbf{r})$$

where $\rho(\mathbf{r})$ is the surface reflectivity. As we would expect, the cross section has units of area.

The factor $J(\lambda, R, \mathbf{r})$ is the laser induced spectral radiance at wavelength λ at position \mathbf{r} in the target plane located at range R per unit range interval. For each piece of the illuminated target plane, the return is equal to the illumination multiplied by the reflectivity.

$$J(\lambda, R, \mathbf{r}) = I(R, \mathbf{r}) \frac{\rho(\mathbf{r})}{\pi} \mathcal{L}_i(\lambda) \quad (3.31)$$

The factor of π comes from the fact that the laser induced radiation is assumed to be distributed over a complete 180° field of view and the surface is Lambertian.[9]

Assumption 3.2-2: Lambertian Surface

The Lambertian assumption would certainly not be good for a mirrored surface, but for many natural surfaces it is not too bad.

If we take assumption 3.1.2-2 we can again write the illumination factor as

$$I(R) = \frac{P_L T(\lambda_L, R, \mathbf{r})}{A_L(R)} \quad (3.32)$$

then

$$J(\lambda, R, \mathbf{r}) = \frac{P_L T(\lambda_L, R, \mathbf{r})}{A_L(R)} \frac{\rho(\mathbf{r})}{\pi} \mathcal{L}_i(\lambda) \quad (3.33)$$

where the dependence on \mathbf{r} man not be trivial.

Assumption 3.2-3: Sensor apertures are circular and look is nadir

In this simple case the form for $A_L(R, \mathbf{r})$ is simple (see chapter 12)

$$J(\lambda, R, \mathbf{r}) = \frac{P_L T(\lambda_L, R, \mathbf{r}) \rho(\mathbf{r})}{\pi R^2 \phi^2} \frac{\rho(\mathbf{r})}{\pi} \mathcal{L}_i(\lambda) \quad (3.34)$$

where ϕ is the laser beam half divergence angel. Note that we have written both the reflectivity and the atmospheric transmission as functions of \mathbf{r} . For dial measurements, variation in these quantities can be important. By applying assumption 3.1-5 we will ignore background contributions and atmospheric discontinuities. Consider for example pollution monitoring of a smoke stack. The plume is of limited extent. Pollutants are not evenly distributed in the plume

and scatterers are equally inhomogeneous. Areas of buildings, parking lots with or without vehicles, grass, trees, and many other surface types are possible in any combination. These effects are minimized by the dial technique as long as both wavelengths see the same conditions. We will invoke assumption 3.1-5 for both the atmosphere and the surface to yield

$$J(\lambda, R, \mathbf{r}) = \frac{P_L T(\lambda_L, R)}{\pi R^2 \phi^2} \frac{\rho}{\pi} \mathcal{L}_i(\lambda) \quad (3.35)$$

Further, using assumption 3.1.2-1, we can express the probability of return as independent of \mathbf{r} (equation (3.2))

$$p(\lambda, R) = \frac{A_o}{R^2} T(\lambda, R) \xi(\lambda) \xi(R) \quad (3.36)$$

We again use equation (3.3) and substitute in our expression for $J(\lambda, R, \phi)$ and $p(\lambda, R)$

$$\begin{aligned} P(\lambda, t) &= \int_0^{R=ct/2} dR \int_{\Delta\lambda} d\lambda \int \frac{P_L T(\lambda_L, R)}{\pi R^2 \phi^2} \frac{\rho}{\pi} \mathcal{L}_i(\lambda) \frac{A_o}{R^2} T(\lambda, R) \xi(\lambda) \xi(R) dA(R, \mathbf{r}) \quad (3.37) \\ &= \frac{A_o P_L \rho}{\pi} \int_0^{R=ct/2} \frac{T(\lambda_L, R)}{R^2} \xi(R) dR \int_{\Delta\lambda} T(\lambda, R) \xi(\lambda) \mathcal{L}_i(\lambda) d\lambda \int \frac{1}{\pi R^2 \phi^2} dA(R, \mathbf{r}) \\ &= \frac{A_o P_L \rho}{\pi} \int_0^{R=ct/2} \frac{T(\lambda_L, R)}{R^2} \xi(R) dR \int_{\Delta\lambda} T(\lambda, R) \xi(\lambda) \mathcal{L}_i(\lambda) d\lambda \end{aligned}$$

We use assumptions (3.1-2 –3.1-4) to claim that the integration over wavelength is trivial

$$\int_{\Delta\lambda} \mathcal{L}_i(\lambda) T(\lambda, R) \xi(\lambda) d\lambda = T(\lambda, R) \xi(\lambda) \quad (3.38)$$

and therefore,

$$P(\lambda, t) = \frac{A_o P_L \rho}{\pi} \int_0^{R=ct/2} \frac{T(\lambda_L, R) T(\lambda, R)}{R^2} \xi(R) \xi(\lambda) dR \quad (3.39)$$

We can simplify the notation by observing that assumption 3.1-1 is still in effect, thus, $\lambda_L = \lambda$

$$P(\lambda, t) = \frac{A_o P_L \rho \xi(\lambda)}{\pi} \int_0^{R=ct/2} \frac{T^2(\lambda, R)}{R^2} \xi(R) dR \quad (3.40)$$

By assuming that the radiation will elastically reflect from the surface, (assumption 3.1-1) and by using a Lambertian surface (assumption 3.2-2) we can approximate the geometric form factor $\xi(R) \simeq \xi(R_T) \delta(R_T)$ then

$$P(\lambda, t) = \frac{A_o P_L \rho}{\pi} \frac{T^2(\lambda, R_T)}{R_T^2} \xi(\lambda) \xi(R_T) \quad (3.41)$$

Finally, using our assumption of circular apertures, we can write A_o as $\pi D^2/4$. This gives the common form of the *topographic lidar equation*.[3][7][8]

$$\begin{aligned} P(\lambda, t) &= \frac{P_L \rho D^2}{4R_T^2} \xi(\lambda) \xi(R_T) T(\lambda_L, R_T)^2 \\ &= \frac{E_L \rho D^2}{4R_T^2 \tau_L} \xi(\lambda) \xi(R_T) T(\lambda, R_T)^2 \end{aligned} \quad (3.42)$$

or, writing out the transmission,

$$P(\lambda, t) = \frac{P_L \rho D^2}{4R_T^2} \xi(\lambda) \xi(R_T) \exp \left(-2 \int_0^{R_T} \kappa(\lambda, R) dR \right) \quad (3.43)$$

Again we can write this as the return energy per sample

$$E(\lambda, R) = \int_{\frac{2R}{c}}^{\frac{2R}{c} + \tau_d} \frac{P_L \rho D^2}{4R_T^2} \xi(\lambda) \xi(R_T) \exp \left(-2 \int_0^{R_T} \kappa(\lambda, R) dR \right) dt \quad (3.44)$$

$$E(\lambda, t) = \frac{P_L \tau_d \rho D^2}{4R_T^2} \xi(\lambda) \xi(R_T) \exp \left(-2 \int_0^{R_T} \kappa(\lambda, R) dR \right) \quad (3.45)$$

In the tomographic equation, the ground leaving pulse shape is a convolution of the pulse shape and the surface shape. For a flat surface with no features, the return pulse looks very much like the incident pulse. If the laser beam strikes the flat surface at an angle, the return pulse will be lengthened. but for complicated surfaces (e.g. a forest) the return pulse shape may be complicated.

3.2.1 Topographic range finding

We can determine the range to a topographic surface to better than the resolution described in equation (3.21).[10][11][12][13] By assuming the target is a hard surface, like the ground, we can assume that the pulse will be elastically reflected. Thus the leading edge of the transmitted pulse will be the leading edge of the receive pulse. By subsampling the pulse ($\tau_L > \tau_{int}$) we can watch for the rise of the return pulse. A threshold value can be used based on the slope of the return pulse and knowledge of the transmit pulse (see figure 3.4).

In section (3.1.2) we found that the minimum spatial resolution was given by

$$\text{resolution} = \frac{c(\tau_{int} + \tau_L)}{2}$$

But now we know we would prefer to subsample with $\tau_{int} < \tau_L$ so the system can do better than the minimum spatial case. Suppose we choose a detector that can respond quickly, within a few nanoseconds. Then we might have an integration time of about 20 ns. This gives about a three meter minimum spatial

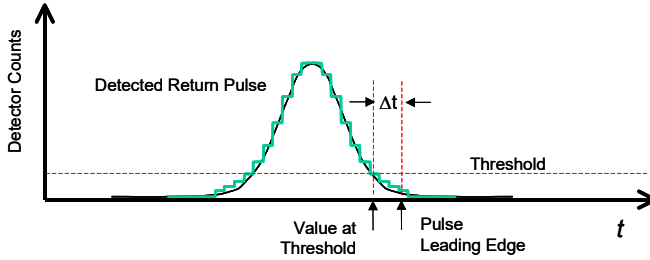


Figure 3.4: Topographic range resolution can be smaller than the pulse length if the detection system can subsample the pulse.

resolution just due to the integration time. We want the laser pulse duration to be larger than this. Suppose

$$\tau_L = 10\tau_{int}$$

then

$$\begin{aligned} \text{resolution} &= \frac{c(\tau_{int} + 10\tau_{int})}{2} \\ &= \frac{c\tau_{int}(11)}{2} \\ &= (2.99792458 \times 10^8 \text{ m s}^{-1}) \frac{(20 \text{ ns})(11)}{2} \\ &= 32.977 \text{ m} \end{aligned}$$

Of course the idea is that with a suitable pulse finding strategy, we can do much better than the 33 m resolution. We will take up this topic later when we discuss pulselengthfinding routines.

The electronics sampling rate must support τ_{int} . For our example, the system would require a sampling rate of f_s

$$f_s = \frac{1}{\tau_{int}} = \frac{1}{20 \text{ ns}} = 50.0 \text{ MHz}$$

Of course a higher sample rate would be nice, but a faster detector would be needed. This might become especially important if matched filter detection is used to find low power return pulses in the presence of noise.

3.3 Fluorescence Lidar Equation

Not done yet

Let us take the case where the laser illumination excites fluorescence in the target material. The relaxation time of the material must be accounted for in

the equation for received power. Beginning again with equation (3.3) we seek an expression for $J(\lambda, R, \mathbf{r})$. for the case where there are multiple species within the target volume.

$$J(\lambda, R, \mathbf{r}) = \sum_i \frac{N_{u_i}(R, \mathbf{r}) hc \mathcal{L}_{F_i}(\lambda)}{4\pi \lambda \tau_{rad_i}} \quad (3.46)$$

where $N_{u_i}(R, \mathbf{r})$ represents the number density of laser-excited molecules or atoms of species i , capable of undergoing fluorescence; $\mathcal{L}_{F_i}(\lambda) \Delta\lambda$ represents the fraction of fluorescence emitted by species i into the wavelength interval $(\lambda, \lambda + \Delta\lambda)$; τ_{rad_i} is the radiative lifetime for the excited molecules or atoms of species i ; and h and c are Planck's constant and the speed of light respectively.

For simplicity we will assume that only one molecular species will be excited by the laser and that the return to the ground state emits radiation at some wavelength, λ , which is longer than the laser wavelength, λ_L .

Assumption 3.3-1: Only one molecular species is excited

If the laser power is too high stimulated emission will cause saturation, thus there is an upper bound on the fluorescence excitation level. Because of this we will assume that the incident beam is weak.

Assumption 3.3-2: Weak excitation

The temporal variation of the excited-state number density $N_u(R, t)$ can be expressed by the form

$$\frac{dN_u(R, t)}{dt} = \frac{\lambda_L \sigma_A(\lambda_L)}{hc} N_l(R, t) I(R, t) - \frac{N_u(R, t)}{\tau} \quad (3.47)$$

where $\sigma_A(\lambda_L)$ represents the absorption cross section per molecule, $N_l(R, t)$ represents the ground-state number density in the target plane, τ is the observed lifetime of the excited state given by

$$\frac{1}{\tau} = \frac{1}{\tau_{rad}} + C_Q \quad (3.48)$$

where τ_{rad} is the radiative lifetime of the excited state and C_Q is the collision quenching rate for the excited state. We have assumed a homogeneous target medium to remove the dependence on \mathbf{r} .

Assumption 3.3-3: Homogeneous target medium

It should be noted that equation (3.48) is an approximation and fails in the case of a three or more level transition structure.

We will further assume that the excitation is weak enough that no nonlinear effects are observed and depletion of the ground state is negligible. If the ground-state population prior to irradiation is $N_o(R)$ and we assume that the original population of the excited state is zero ($N_u(R, 0) = 0$), then

$$N_u(R, t) = \frac{\lambda_L N_o(R) \sigma_A(\lambda_L)}{hc} \exp\left(\frac{-t}{\tau}\right) \int_0^t I(R, x) e^{\frac{x}{\tau}} dx \quad (3.49)$$

where $I(R, x)$ is the irradiance at some time, x after the leading edge of the laser pulse reaches this location.

The pulse excites fluorescence as it travels. To understand this, we will observe two points in the target medium, R , and R' where $R > R'$. Let the laser pulse length be L , then if $R - R' < L$ we find when the leading edge of the laser pulse reaches the range R , the target medium at R' will have been exposed to laser radiation for a period

$$t' = \frac{(R - R')}{c} \quad (3.50)$$

Thus, fluorescence induced by the leading edge of the laser pulse in the detector direction will be enhanced by fluorescence from the target medium at range R' . Material at R' having been exposed for a period $2t'$.

To find the radiance to place in our equation(3.3) we combine equations (3.46) and (3.49).

$$J(\lambda, R, \mathbf{r}) = \frac{N_o(R) \sigma_A(\lambda_L) \lambda_L \mathcal{L}_F(\lambda)}{4\pi\lambda\tau_{rad}} \exp\left(\frac{-t}{\tau}\right) \int_0^t I(R, x) e^{\frac{x}{\tau}} dx \quad (3.51)$$

Here we introduce the concept of a spectrally integrated fluorescence cross section

$$\sigma_F(\lambda_L) \equiv \sigma_A(\lambda_L) \left(\frac{\tau}{\tau_{rad}} \right) \quad (3.52)$$

Given this definition, we can define the power arriving at the detector.

$$\begin{aligned} P(\lambda, t) &= \frac{A_o \sigma_A(\lambda_L) \lambda_L}{4\pi\tau} \\ &\times \int_0^R \xi(R') A_L(R') N_o(R') \exp\left(\frac{-t}{\tau}\right) \frac{1}{R'^2} \\ &\times \int_0^t I(R, x) e^{\frac{x}{\tau}} dx \int_{\Delta\lambda} \mathcal{L}_F(\lambda) \xi(\lambda) T(\lambda, R) \frac{d\lambda}{\lambda} dR' \end{aligned} \quad (3.53)$$

Note that Measures somehow took out the factor of $1/\lambda$. It is not clear how he justified that action.

Assumption 3.3-4: Receiver spectral window \ll fluorescence spectral width

Usually the spectral window of the receiver is small compared to the spectral width of the fluorescence. If this is the case we can approximate the integral over wavelength.

$$\int_{\Delta\lambda} \mathcal{L}_F(\lambda) \xi(\lambda) T(\lambda, R) \frac{d\lambda}{\lambda} = \frac{1}{\lambda} T(\lambda_c, R) \mathcal{L}_F(\lambda_c) \int_{\Delta\lambda} \xi(\lambda) \frac{1}{\lambda} T(\lambda_c, R) \mathcal{L}_F(\lambda_c) K_o(\lambda_c) d\lambda \quad (3.54)$$

where $K_o(\lambda)$ is the *filter function*,

$$K_o(\lambda) \equiv \int_{\Delta\lambda} \xi(\lambda') d\lambda' \quad (3.55)$$

and were the wavelength, λ_c , on the right hand side indicates the band center of the receiver. Measures describes $K_o(\lambda)$ as “the effective bandwidth which would transmit, with unit transmission efficiency, the same fraction of the fluorescence as achieved by the real system.” We again use equation (3.22) for the illumination term.

$$I(R') = \frac{E_L T(\lambda_L, R')}{A_L(R')} \Phi(t') \quad (3.56)$$

Another assumption allows us to write the received energy.

- | |
|---|
| Assumption 3.3-5: The target total attenuation coefficient is constant |
| Assumption 3.3-6: Overlap factor is weakly dependent upon range $\xi(R) \approx \xi(R_o)$ |
| Assumption 3.3-7: The physical extent of the target is small |

The boundary of the target medium is labeled R_o . Then, the energy received by the detector in the time interval $(t, t + \tau_d)$ is

$$E(\lambda, R) = E_L T(R_o) K_o(R_o) \xi(R_o) \frac{A_o N_o \sigma_F(\lambda_L) \mathcal{L}_F(\lambda)}{4\pi R^2 \tau} \times \int_t^{t+\tau_d} \int_{R_o}^R dR' \exp(-\kappa_T(R' - R_o)) \exp\left(-\frac{t'}{\tau}\right) \quad (3.57)$$

$$\times \int_0^{t'} \Phi(x) e^{\frac{x}{\tau}} dx dt' \quad (3.58)$$

where

$$T(R_o) = T(\lambda, R') T(\lambda_L, R') \quad (3.59)$$

and where

$$T(R_o) = \exp\left(-\int_0^{R_o} \kappa(R) dR\right) \quad (3.60)$$

and where by assumption 3.3-6 $\xi(R)$ has been replaced by $\xi(R_o)$ and where by assumption 3.3-7 a factor of $1/R^2$ has been taken out of the range integration and λ_L/λ is considered close to unity.

It would be nice to write this equation in a form more like the scattering equation (equation 3.20). Toward this goal, we write

$$E(\lambda, R) = E_L K_o(R_o) T(R_o) \xi(R_o) \frac{A_o}{R^2} N_o \frac{\sigma_F(\lambda_L, \lambda)}{4\pi} \frac{c\tau_d}{2} \gamma(R) e^{-\kappa_T(R-R_o)} \quad (3.61)$$

where

$$\sigma_F(\lambda_L, \lambda) \equiv \sigma_F(\lambda_L) \mathcal{L}_F(\lambda) \quad (3.62)$$

is the *fluorescence cross section* and

$$\begin{aligned} \gamma(R) &= \frac{2}{c\tau_d} e^{\kappa_T(R'-R_o)} \int_t^{t+\tau_d} dt' \int_{R_o}^R dR' \exp(-\kappa_T(R' - R_o)) \exp\left(-\frac{t'}{\tau}\right) \\ &\times \int_0^{t'} \Phi(x) e^{\frac{x}{\tau}} dx \end{aligned} \quad (3.63)$$

is the *fluorescence lifetime correction factor*.

Note that the filter function, $K_o(\lambda)$ is used in place of $\xi(\lambda)$. The medium only exists in a region bounded by R_o , thus the transmission has been separated into two terms, $T(R_o)$ and $\exp(-\kappa_T(R - R_o))$. If the optical depth of the medium is large, then the exponential factor in equation(3.61) is often combined with the fluorescence lifetime correction factor

$$\bar{\gamma}(z) = \gamma(z) e^{-\kappa_T L z} \quad (3.64)$$

where L is the target depth, and therefore $\kappa_T L$ is the target optical depth. The value z is the penetration depth or the depth of the lidar beam into the target medium.

3.4 Raman Lidar Equation

Raman scattering is an inelastic process. We can write the lidar equation for Raman scattering by relaxing assumption 3.1-, but otherwise following the same procedure as for elastic scattering. We begin with equation (3.3)

$$P(\lambda, t) = \int_0^{R=ct/2} dR \int_{\Delta\lambda} d\lambda \int J(\lambda, R, \mathbf{r}) p(\lambda, R, \mathbf{r}) dA(R, \mathbf{r}) \quad (3.65)$$

We again use equations (3.4), (3.5) and (3.2).

$$\begin{aligned} P(\lambda, t) &= A_o \int_0^{R=ct/2} \frac{1}{R^2} \int_{\Delta\lambda} T(\lambda, R) \xi(\lambda) d\lambda \\ &\times \int \sum_i N_i(R, \mathbf{r}) \left(\frac{d\sigma(\lambda_L)}{d\Omega} \right)_i^s \mathcal{L}_i(\lambda) \\ &\times I(R, \mathbf{r}) \xi(R, \mathbf{r}) dA(R, \mathbf{r}) dR \end{aligned} \quad (3.66)$$

We can write this equation as a sum over all the various target components

$$P(\lambda, t) = \sum_i P_i(\lambda, t) \quad (3.67)$$

where

$$\begin{aligned} P_i(\lambda, t) &= A_o \int_0^{R=ct/2} \frac{1}{R^2} \int_{\Delta\lambda} \xi(\lambda) T(\lambda, R) \left(\frac{d\sigma(\lambda_L)}{d\Omega} \right)_i^s \mathcal{L}_i(\lambda) d\lambda dR \\ &\times \int I(R, \mathbf{r}) \xi(R, \mathbf{r}) N_i(R, \mathbf{r}) dA(R, \mathbf{r}) dR \end{aligned} \quad (3.68)$$

If the target is homogeneous (assumption 3.1-5), this equation may be simplified

$$\begin{aligned} P_i(\lambda, t) &= A_o \int_0^{R=ct/2} I(R) \xi(R) N_i(R) \frac{A_L(R)}{R^2} \\ &\times \int_{\Delta\lambda} \xi(\lambda) T(\lambda, R) \left(\frac{d\sigma(\lambda_L)}{d\Omega} \right)_i^s \mathcal{L}_i(\lambda) d\lambda dR \end{aligned} \quad (3.69)$$

Raman scattering is not elastic, but it does have very short time constants, thus we can take approximation 3.1.2-4. Following the same logic that lead to equation (3.12) we arrive at the form.

$$\begin{aligned} P_i(\lambda, t) &= A_o I(R) \xi(R) N_i(R) A_L(R) \frac{c\tau_L}{2R^2} \\ &\times \int_{\Delta\lambda} \xi(\lambda) T(\lambda, R) \left(\frac{d\sigma(\lambda_L)}{d\Omega} \right)_i^s \mathcal{L}_i(\lambda) d\lambda \end{aligned} \quad (3.70)$$

or rearranging the terms, we can write

$$\begin{aligned} P_i(\lambda, t) &= \frac{A_o c \tau_L}{2R^2} I(R) \xi(R) N_i(R) A_L(R) \\ &\times \int_{\Delta\lambda} \xi(\lambda) T(\lambda, R) \left(\frac{d\sigma(\lambda_L)}{d\Omega} \right)_i^s \mathcal{L}_i(\lambda) d\lambda \end{aligned} \quad (3.71)$$

If we assume a square pulse (assumption 3.1.2-3) the we can again write the illumination simply as in equation (3.14)

$$I(R) = \frac{P_L T(\lambda_L, R)}{A_L(R)} \quad (3.72)$$

$$\begin{aligned} P_i(\lambda, t) &= \frac{P_L \pi D^2 c \tau_L}{8R^2} \xi(R) N_i(R) T(\lambda_L, R) \\ &\times \int_{\Delta\lambda} \xi(\lambda) T(\lambda, R) \left(\frac{d\sigma(\lambda_L)}{d\Omega} \right)_i^s \mathcal{L}_i(\lambda) d\lambda \end{aligned} \quad (3.73)$$

In summary, though not specifically called out in every case, this equation is a result of assumptions 3-2, 3.1-2 3.1-5, 3.1.2-1, 3.1.2-2, 3.1.2-3 3.1.2-4, and 3.1.2-5. The most serious are probably 3.1-5 and 3.1.2-2, because many targets of interest will not be homogeneous and may not fill the beam.

If one species dominates, we can write

$$\begin{aligned} P(\lambda, t) &= \frac{P_L \pi D^2 c \tau_L}{8R^2} \xi(R) N_i(R) T(\lambda_L, R) \\ &\times \int_{\Delta\lambda} \xi(\lambda) T(\lambda, R) \left(\frac{d\sigma(\lambda_L)}{d\Omega} \right)_1^s \mathcal{L}_1(\lambda) d\lambda \\ &+ \sum_{i=2}^N P_i(\lambda, t) \end{aligned} \quad (3.74)$$

where the last term will be small. Whether or not this is true may depend on the target species and the target environment. If the receiver band width is wider than the feature of interest, we again use approximations 3.1-2 –3.1-4

$$\begin{aligned} E_L(\lambda, t) &= \frac{E_L D^2 c \tau_d}{8R^2} \xi(R) N_i(R) T(\lambda_L, R) \\ &\times \xi(\lambda) T(\lambda, R) \left(\frac{d\sigma(\lambda_L)}{d\Omega} \right)_1^s \\ &+ \sum_{i=2}^N P_i(\lambda, t) \end{aligned} \quad (3.75)$$

The Raman cross section is described by many authors.[1][3] For Nitrogen, Measures gives a value of

$$\frac{d\sigma}{d\Omega} \approx (4.3 \pm 0.2) \times 10^{-31} \text{ cm}^2 \text{ sr}^{-1} \quad (3.76)$$

This is the 2331 vibrational A-branch of nitrogen excited by light of wavelength 514.5 nm. The cross section has a $1/\lambda^4$ wavelength dependence, thus for an excitation wavelength of 337.1 nm the cross section value is $2.8 \times 10^{-30} \text{ cm}^2 \text{ sr}^{-1}$. Other species cross sections are usually measured relative to Nitrogen.

The power P_L which is used in these equations is the average transmit laser power . Often it is useful to define the power per pulse

$$P_p = P_L \frac{\tau_L}{\tau_c}$$

where here τ_c is the collection time or the time over which light from pulses is gathered by the receiver. The power per pulse is often very large compared to the average power.

Chapter 4

Differential Absorption Lidar (DIAL) Equation

The concept of differential absorption is simple. It requires two laser wavelengths, one on an absorption feature of a gas or liquid, and one off the feature. Concentrations of the absorber are determined by observing the ratio between the two wavelength's return signals. A derivation of the DIAL algorithm follows.[3][14][15][16][17][18][19]

4.1 Aerosol backscatter DIAL

Aerosol backscatter DIAL is the first of two differential absorption techniques we will describe. This technique uses the backscattered signal from atmospheric aerosols as the principal return mechanism. Two wavelengths, λ_{on} and $\lambda_{off} = \lambda_{on} \pm \delta\lambda$ are selected such that λ_{on} is near line center for the absorption feature of interest, and λ_{off} lies in the wing of the absorption feature. Because the principle return is from scattering we use equation (3.20).

$$\begin{aligned} P(\lambda, R) &= \frac{A_o}{R^2} \xi(\lambda_L) P_L \beta(\lambda_L, R) \xi(R) \frac{c\tau_L}{2} \\ &\times \exp \left(-2 \int_0^R (\kappa(\lambda_L, R) dR) \right) \end{aligned} \quad (4.1)$$

Assumption 4.1-1: The two transmit pulses are the same except for wavelength

If the assumption (4.1-1) is made, then the ratio of the received powers is given by

$$\frac{P(\lambda_{on}, R)}{P(\lambda_{off}, R)} = \frac{\xi(\lambda_{on}) \beta(\lambda_{on}, R)}{\xi(\lambda_{off}) \beta(\lambda_{off}, R)} \exp \left(-2 \int_0^R (\kappa(\lambda_{on}, R) - \kappa(\lambda_{off}, R)) dR \right) \quad (4.2)$$

Of particular importance is the fact that we have assumed that the pulses have equal output power. The absorption coefficient for the species i is given by

$$\kappa_i(\lambda, R) = N_i(R) \sigma_{a_i}(\lambda) \quad (4.3)$$

where $\sigma_{a_i}(\lambda)$ is the absorption cross section for the species i . If we then define $\bar{\kappa}(\lambda, R)$ as the absorption coefficient for all species except the species of interest, we may write equation (4.2) as

$$\begin{aligned} & \int_0^R N_i(R) (\sigma_a(\lambda_{on}) - \sigma_a(\lambda_{off})) dR \\ &= \frac{1}{2} \ln \left(\frac{P(\lambda_{off}, R) \xi(\lambda_{on}) \beta(\lambda_{on}, R)}{P(\lambda_{on}, R) \xi(\lambda_{off}) \beta(\lambda_{off}, R)} \right) \\ & \quad - \int_0^R (\bar{\kappa}(\lambda_{on}, R) - \bar{\kappa}(\lambda_{off}, R)) dR \end{aligned} \quad (4.4)$$

We write this in differential form

$$\begin{aligned} N_i(R) &= \frac{1}{(\sigma_a(\lambda_{on}) - \sigma_a(\lambda_{off}))} \\ & \times \left[\frac{1}{2} \frac{d}{dR} \left(\ln \left(\frac{P(\lambda_{off}, R) \xi(\lambda_{on}) \beta(\lambda_{on}, R)}{P(\lambda_{on}, R) \xi(\lambda_{off}) \beta(\lambda_{off}, R)} \right) \right) \right. \\ & \quad \left. - (\bar{\kappa}(\lambda_{on}, R) - \bar{\kappa}(\lambda_{off}, R)) \right] \end{aligned} \quad (4.5)$$

We can simplify this equation if we assume the transmit and receive optics have the same (spectral) response at $(\lambda_{on}, \lambda_{off})$.

$\boxed{\text{Assumption 4.1-2: } \xi(\lambda_{on}) = \xi(\lambda_{off})}$

This assumption is usually fairly good, (if not, the difference can be measured and corrected)

$$\begin{aligned} N_i(R) &= \frac{1}{(\sigma_a(\lambda_{on}) - \sigma_a(\lambda_{off}))} \\ & \times \left[\frac{1}{2} \frac{d}{dR} \left(\ln \left(\frac{P(\lambda_{off}, R)}{P(\lambda_{on}, R)} \right) - \ln \left(\frac{\beta(\lambda_{off}, R)}{\beta(\lambda_{on}, R)} \right) \right) \right. \\ & \quad \left. - (\bar{\kappa}(\lambda_{on}, R) - \bar{\kappa}(\lambda_{off}, R)) \right] \end{aligned} \quad (4.6)$$

The fact that the wavelengths are so close allows us to further assume that $\beta(\lambda_{on}) = \beta(\lambda_{off})$ and $E(\lambda_{on}, R) = E(\lambda_{off}, R)$

$\boxed{\text{Assumption 4.1-3: } \beta(\lambda, R), \bar{\kappa}(\lambda, R) \text{ independent of wavelength over } \delta\lambda}$

This assumption simplifies the equation a great deal. Within the bounds of our assumptions, the concentration is proportional to the differential of the

log ratio of the receive powers from the range element δR and the constant of proportionality is twice the difference in the cross sections.

$$N_i(R) = \frac{1}{2(\sigma_a(\lambda_{on}) - \sigma_a(\lambda_{off}))} \frac{d}{dR} \left(\ln \left(\frac{P(\lambda_{off}, R)}{P(\lambda_{on}, R)} \right) \right) \quad (4.7)$$

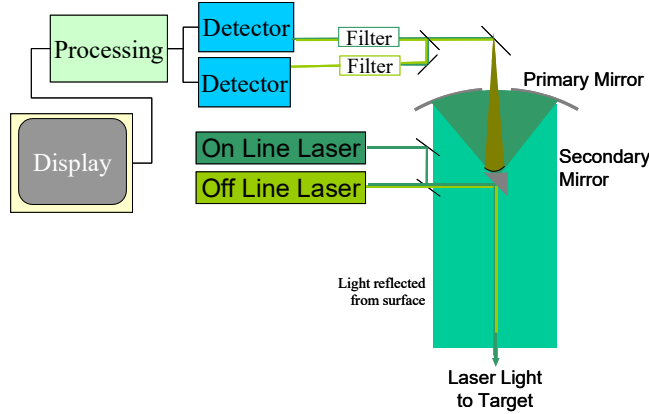


Figure 4.1:

4.2 Differential Absorption Using Surface Reflectivity

If a columnar measurement of a species is sufficient, the DIAL technique can be modified to provide several orders of magnitude improvement in signal to noise[7][8][25][33][34][35][37]. We begin with equation (3.43).

$$P(\lambda, t) = \frac{P_L \rho D^2}{4R_T^2} \xi(\lambda) \xi(R_T) \exp \left(-2 \int_0^{R_T} \kappa(\lambda, R) dR \right) \quad (4.8)$$

Like in DIAL we measure on line and off line wavelength. The algorithm is similar to DIAL, we begin with the ratio of the return powers

$$\begin{aligned} \frac{P(\lambda_{on}, t)}{P(\lambda_{off}, t)} &= \frac{\xi(\lambda_{on}) \xi(R_T)}{\xi(\lambda_{off}) \xi(R_T)} \\ &\times \exp \left(-2 \int_0^{R_T} (\kappa(\lambda_{on}, R) - \kappa(\lambda_{off}, R)) dR \right) \end{aligned} \quad (4.9)$$

46 CHAPTER 4. DIFFERENTIAL ABSORPTION LIDAR (DIAL) EQUATION

taking the log of both sides and rearranging yields

$$\begin{aligned} \frac{1}{2} \ln \left(\frac{P(\lambda_{off}, t)}{P(\lambda_{on}, t)} \right) &= \int_o^{R_T} (\bar{\kappa}(\lambda_{on}, R) - \bar{\kappa}(\lambda_{off}, R)) dR \\ &\quad + \int_o^{R_T} N(R) (\sigma_a(\lambda_{on}) - \sigma_a(\lambda_{off})) dR \end{aligned} \quad (4.10)$$

Using the same definitions and approximations as in the DIAL case we see that

$$\begin{aligned} \int_0^{R_T} N(R) dR &= \frac{1}{(\sigma_a(\lambda_{on}) - \sigma_a(\lambda_{off}))} \left[\frac{1}{2} \ln \left(\frac{P(\lambda_{off}, t)}{P(\lambda_{on}, t)} \right) \right. \\ &\quad \left. - \int_o^{R_T} (\bar{\kappa}(\lambda_{on}, R_T) - \bar{\kappa}(\lambda_{off}, R_T)) dR \right] \end{aligned} \quad (4.11)$$

where again we have assumed $\xi(\lambda_{on}) = \xi(\lambda_{off})$.

In some cases, we will wish to measure a gas that is naturally present in the atmosphere. In such cases, the background concentration must be measured and subtracted from the value calculated from equation (4.11).

$$\int_0^{R_T} N(R) dR = \int_0^{R_{\text{plume top}}} N(R) dR + \int_{R_{\text{plume top}}}^{R_{\text{plume bottom}}} N(R) dR$$

What we have calculated before, in the absence of a background is the part now written as

$$\int_{R_{\text{plume top}}}^{R_{\text{plume bottom}}} N(R) dR$$

The remaining part is the background concentration length. For a well mixed gas (constant concentration along the path length R)

$$\int_0^{R_{\text{plume top}}} N(R) dR = N_b R_T$$

Thus in the presence of a background concentration

$$\begin{aligned} \int_0^{R_T} N(R) dR &= \left[\frac{1}{(\sigma_a(\lambda_{on}) - \sigma_a(\lambda_{off}))} \left(\frac{1}{2} \ln \frac{P(\lambda_{off}, t)}{P(\lambda_{on}, t)} \right) \right. \\ &\quad \left. - \int_o^{R_T} (\bar{\kappa}(\lambda_{on}, R_T) - \bar{\kappa}(\lambda_{off}, R_T)) dR \right] + N_b R_T \end{aligned} \quad (4.12)$$

In such cases, the on line laser illumination (λ_{on}) may be attenuated to the point where insufficient return is generated. The solution to this problem is to detune off the peak of the absorption line until the columnar absorption no longer extinguishes the beam. Exact choice of λ_{on} may therefore be difficult. Tunable laser systems can alleviate the need for a single design point for λ_{on} .

4.2.1 Digression

Suppose the reflectivity and the target gas are not uniform over the laser beam. Then J is still a function of \mathbf{r} , and we may not take assumption 3.1.2-2. Then,

$$J(\lambda, R, \mathbf{r}) = \frac{P_L T(\lambda_L, R, \mathbf{r}) \rho(\mathbf{r})}{A_L(R)} \mathcal{L}_i(\lambda) \quad (4.13)$$

and

$$p(\lambda, R, \mathbf{r}) = \frac{A_o}{R^2} T(\lambda, R, \mathbf{r}) \xi(\lambda) \xi(R, \mathbf{r}) \quad (4.14)$$

The signal power is given by

$$\begin{aligned} P(\lambda, t) &= \frac{P_L A_o}{\pi} \int_0^{R=ct/2} \frac{1}{A_L(R) R^2} \int_{\Delta\lambda} \xi(\lambda) \mathcal{L}_i(\lambda) \\ &\times \int T(\lambda_L, R, \mathbf{r}) T(\lambda, R, \mathbf{r}) \rho(\mathbf{r}) dA(R, \mathbf{r}) \xi(R, \mathbf{r}) d\lambda dR \end{aligned} \quad (4.15)$$

We follow the same stream of logic as we did in section 3.2. As before we can integrate over wavelength using assumptions 3.1-2 – 3.1-4.

$$\begin{aligned} P(\lambda, t) &= \frac{P_L A_o}{\pi} \int_0^{R=ct/2} \frac{1}{A_L(R) R^2} \xi(\lambda) \\ &\times \int T(\lambda_L, R, \mathbf{r}) T(\lambda, R, \mathbf{r}) \rho(\mathbf{r}) \xi(R, \mathbf{r}) dA(R, \mathbf{r}) dR \end{aligned} \quad (4.16)$$

We integrate over range, again assuming the surface acts like a delta function (assumption 3.2-3).

$$\begin{aligned} P(\lambda, t) &= \frac{P_L A_o}{\pi} \frac{\xi(\lambda)}{A_L(R_T) R_T^2} \\ &\times \int T(\lambda_L, R_T, \mathbf{r}) T(\lambda, R_T, \mathbf{r}) \rho(\mathbf{r}) \xi(R_T, \mathbf{r}) dA(R_T, \mathbf{r}) \end{aligned} \quad (4.17)$$

Finally, we can use Appendix 12 to write out the laser spot area

$$\begin{aligned} P(\lambda, t) &= \frac{P_L A_o}{\pi} \frac{\xi(\lambda)}{\pi R_T^2 \phi^2} \\ &\times \int T(\lambda_L, R_T, \phi, \theta) T(\lambda, R_T, \phi, \theta) \rho(\phi, \theta) \xi(R_T, \phi, \theta) \phi d\phi d\theta \end{aligned} \quad (4.18)$$

Thus, this equation could be used for a case where we wish to look at a nonuniform concentration of a particular gas, say natural gas leaking from a pipe in a residential area, with a bistatic system. If we assume the atmosphere to have no dependence on θ and ϕ , then we can separate the absorption form the target and atmosphere simply as

$$T(\lambda_L, R_T, \phi, \theta) = T_T(\lambda_L, R_T, \phi, \theta) T(\lambda_L, R_T) \quad (4.19)$$

48 CHAPTER 4. DIFFERENTIAL ABSORPTION LIDAR (DIAL) EQUATION

there will be some scattering due to aerosols at visible and IR wavelengths, If we assume we can ignore multiple scattering, then

$$T(\lambda_L, R_T) = T_{\text{absorption}}(\lambda_L, R_T) T_{\text{scattering}}(\lambda_L, R_T) \quad (4.20)$$

but unless the aerosol is the desired target, its only effect is to increase the extinction of both the on and off line signals. Thus we may write

$$\begin{aligned} P(\lambda, t) &= \frac{P_L D^2}{4\pi R_T^2 \phi^2} \xi(\lambda_L) T(\lambda_L, R_T) \\ &\times \int \rho(\phi, \theta) T_A(\lambda_L, R_T, \phi, \theta) \xi(R_T, \phi, \theta) \phi d\phi d\theta \end{aligned} \quad (4.21)$$

because the online and wing wavelengths are close together, and because they have been chosen to be carefully to measure only one line, we can assume reasonably that the atmosphere and scattering will not be significantly different between $P(\lambda_{on}, t)$ and $P(\lambda_{off}, t)$.

$$\frac{P(\lambda_{on}, t)}{P(\lambda_{off}, t)} = \frac{\int \rho(\phi, \theta) T_A(\lambda_{on}, R_T, \phi, \theta) \xi(R, \phi, \theta) \phi d\phi d\theta}{\int \rho(\phi, \theta) T_A(\lambda_{off}, R_T, \phi, \theta) \xi(R, \phi, \theta) \phi d\phi d\theta} \quad (4.22)$$

Again we have assumed that $\xi(\lambda_{on}) = \xi(\lambda_{off})$. The implication is that we still must know much about the surface and the distribution of the absorbing gas before we can determine the concentration of the absorber. Let us further assume $\xi(R)$ is simple and does not depend on (ϕ, θ) and that we have a uniform reflective surface $\rho(\phi, \theta) = \rho$. Then

$$\frac{P(\lambda_{on}, t)}{P(\lambda_{off}, t)} = \frac{\int T_A(\lambda_{on}, R_T, \phi, \theta) \phi d\phi d\theta}{\int T_A(\lambda_{off}, R_T, \phi, \theta) \phi d\phi d\theta} \quad (4.23)$$

For λ_{off} there may be little difference in absorption due to the inhomogeneity of the plume. thus

$$\int T_A(\lambda_{off}, R_T, \phi, \theta) \phi d\phi d\theta \approx T_A(\lambda_{off}, R_T) A_L \quad (4.24)$$

and

$$\frac{P(\lambda_{on}, t)}{P(\lambda_{off}, t)} = \frac{\int T(\lambda_{on}, R_T, \phi, \theta) \phi d\phi d\theta}{T(\lambda_{off}, R_T) A_L} \quad (4.25)$$

Example: Target half fills the illumination patch

In the (unrealistically) simple case of a plume that half fills the laser illumination patch, this would reduce to

$$\frac{P(\lambda_{on}, t)}{P(\lambda_{off}, t)} = \frac{\frac{1}{2} T(\lambda_{on}, R_T) + \frac{1}{2} T(\lambda_{off}, R_T)}{T(\lambda_{off}, R_T)} \quad (4.26)$$

where again we have used the assumption that in the absence of absorber $T(\lambda_{on}, R_T) = T(\lambda_{off}, R_T)$.

$$2 \frac{P(\lambda_{on}, t)}{P(\lambda_{off}, t)} = \frac{T(\lambda_{on}, R_T) + T(\lambda_{off}, R_T)}{T(\lambda_{off}, R_T)} \quad (4.27)$$

Following the same reasoning that lead to equation (4.9)

$$\ln \left(2 \frac{P(\lambda_{on}, t)}{P(\lambda_{off}, t)} - 1 \right) = -2 \int_0^{R_T} (\kappa(\lambda_{on}, R) - \kappa(\lambda_{off}, R)) dR \quad (4.28)$$

which yields, for this special case

$$\begin{aligned} \int_0^{R_T} N_i(R) dR &= \frac{1}{2(\sigma(\lambda_{on}) - \sigma(\lambda_{off}))} \\ &\times \left[-\ln \left(2 \frac{P(\lambda_{on}, t)}{P(\lambda_{off}, t)} - 1 \right) \right] \\ &- (\bar{\kappa}(\lambda_{on}, R_T) - \bar{\kappa}(\lambda_{off}, R_T)) \end{aligned} \quad (4.29)$$

We may compare this with the case of a uniform plume given in equation (4.11). The factor

$$\left(\ln \frac{P(\lambda_{off}, t)}{P(\lambda_{on}, t)} \right) \quad (4.30)$$

has been replaced by

$$\left[-\ln \left(2 \frac{P(\lambda_{on}, t)}{P(\lambda_{off}, t)} - 1 \right) \right] \quad (4.31)$$

thus ignoring the absorption due to other components for a moment, we can see that given the same return, in the partial plume case we would need to be a much higher concentration of target absorber.

Example: Inhomogeneous. surface reflectivity in illumination patch

Now assume the plume is uniform and large, but the reflectivity changes.

$$\frac{P(\lambda_{on}, t)}{P(\lambda_{off}, t)} = \frac{T(\lambda_{on}, R_T) \int \rho(\phi, \theta) \phi d\phi d\theta}{T(\lambda_{off}, R_T) \int \rho(\phi, \theta) \phi d\phi d\theta} \quad (4.32)$$

If we assume the reflectivity has two different values and each occupies half of A_L (e.g. the plume is over an area half occupied by a reflective roof and half by a grass field), then

$$\frac{P(\lambda_{on}, t)}{P(\lambda_{off}, t)} = \frac{T(\lambda_{on}, R_T) \left(\rho_1 \frac{A_L}{2} + \rho_2 \frac{A_L}{2} \right)}{T(\lambda_{off}, R_T) \left(\rho_1 \frac{A_L}{2} + \rho_2 \frac{A_L}{2} \right)} \quad (4.33)$$

or simply

$$\frac{P(\lambda_{on}, t)}{P(\lambda_{off}, t)} = \frac{T(\lambda_{on}, R_T)}{T(\lambda_{off}, R_T)} \quad (4.34)$$

which shows the power of the DIAL technique for clutter reduction. Still, we should not lose sight of the fact that both $P(\lambda_{on}, t)$, and $P(\lambda_{off}, t)$ will be smaller by the factor

$$\frac{(\rho_1 + \rho_2)}{2\rho_1} \quad (4.35)$$

where we have chosen $\rho_2 < \rho_1$. Recall that this is not a general formula, but rather results from a (somewhat contrived) special case. In general, the signal at both λ_{on} and λ_{off} will be smaller than if we had a uniform area of reflectance ρ_1 . Thus other signal to noise considerations will apply.

4.2.2 Corrections to the DIAL equation (NEEDS TO BE REWRITTEN, DON'T USE)

In the derivation of the DIAL equation we assumed that many terms canceled in the ratio of the powers. If these terms do not cancel, we may be able to use support data or statistics to correct the concentration or concentration length calculations. Using the surface reflectance dial case, we start with the topographic equation (3.2).

$$P(\lambda, t) = \frac{P_L \rho D^2}{4R_T^2} \xi(\lambda) \xi(R_T) \exp\left(-2 \int_0^{R_T} \kappa(\lambda, R) dR\right) \quad (4.36)$$

As before we form the ratio of the powers to derive the surface DIAL equation.

$$\frac{P(\lambda_{on}, t)}{P(\lambda_{off}, t)} = \frac{\frac{P_{L_{on}} \rho_{on} D^2}{4R_T^2} \xi(\lambda_{on}) \xi_{on}(R_T) \exp\left(-2 \int_0^{R_T} \kappa(\lambda_{on}, R) dR\right)}{\frac{P_{L_{off}} \rho_{off} D^2}{4R_T^2} \xi(\lambda_{off}) \xi_{off}(R_T) \exp\left(-2 \int_0^{R_T} \kappa(\lambda_{off}, R) dR\right)} \quad (4.37)$$

by rearranging terms and splitting the target gas absorption and the atmospheric absorption we have

$$\begin{aligned} & -\frac{1}{2} \ln \left(\frac{P(\lambda_{on}, t) P_{L_{off}} \rho_{off} D^2 \xi(\lambda_{off}) \xi_{off}(R_T)}{P(\lambda_{off}, t) P_{L_{on}} \rho_{on} D^2 \xi(\lambda_{on}) \xi_{on}(R_T)} \right) \\ &= \int_0^{R_T} N(\sigma_a(\lambda_{on}, R) - \sigma_a(\lambda_{off}, R)) dR + \int_0^{R_T} \bar{\kappa}(\lambda_{on}, R) - \bar{\kappa}(\lambda_{off}, R) dR \end{aligned} \quad (4.38)$$

As before we define

$$C_\sigma = (\sigma_a(\lambda_{on}, R) - \sigma_a(\lambda_{off}, R)) \quad (4.40)$$

and

$$C_k = 2 \int_0^{R_T} \bar{\kappa}(\lambda_{on}, R) - \bar{\kappa}(\lambda_{off}, R) dR \quad (4.41)$$

to yield

$$\int_0^{R_T} NdR = -\frac{1}{2C_\sigma} \left(\ln \left(\frac{P(\lambda_{on}, t) P_{L_{off}} \rho_{off} D^2 \xi(\lambda_{off}) \xi_{off}(R_T)}{P(\lambda_{off}, t) P_{L_{on}} \rho_{on} D^2 \xi(\lambda_{on}) \xi_{on}(R_T)} \right) + C_k \right) \quad (4.42)$$

The terms D and R_T still cancel and if we express the transmit powers as $P_{L_{off}} = bP_L$ and $P_{L_{on}} = aP_L$, then

$$\int_0^{R_T} NdR = -\frac{1}{2C_\sigma} \left(\ln \left(\frac{P(\lambda_{on}, t) b \rho_{off} \xi(\lambda_{off}) \xi_{off}(R_T)}{P(\lambda_{off}, t) a \rho_{on} \xi(\lambda_{on}) \xi_{on}(R_T)} \right) + C_K \right) \quad (4.43)$$

Changing units, we may define the corrections

$$\int_0^{R_T} NdR = \frac{C_{sys}}{2(N_a C_{N_a}) C_s(t, p) C_\sigma} \left(\ln \left(\frac{a P(\lambda_{off}, t)}{b P(\lambda_{on}, t)} C_\rho C_\lambda C_{GFF} \right) + C'_K \right) \quad (4.44)$$

where

Correction Term	Correction Issue Addressed
$C_\rho = \frac{\rho_{on}}{\rho_{off}}$	Reflectivity
$C_\lambda = \frac{\xi(\lambda_{on})}{\xi(\lambda_{off})}$	Spectral optics
$C_{GFF} = \frac{\xi_{on}(R_T)}{\xi_{off}(R_T)}$	Geometric form factors
$C_{sys} = (1 \times 10^6) \times (\text{other})$	Units factor and system constants
$C'_K = C_K + (\text{other})$	Transmission plus additive error
$N_a C_{N_a}$	Units factor (air density)
$C_s(t, p)$	X-section temp and pressure correction

and where the minus sign has been incorporated into the logarithm. The factors C_{sys} and C'_K are both theoretical correction factors and serve as fit parameters that can be modified using measurements from the system. We note that many of the corrections are *multiplicative*. Thus, proper correction or proper design to minimize these errors is critical to quantification in gas measurements.

$$\int_0^{R_T} NdR = -\frac{1}{2C_\sigma} \ln \left(\frac{P(\lambda_{on}, t) b}{P(\lambda_{off}, t) a} \right) - \frac{1}{2C_\sigma} \ln \left(\frac{\xi(\lambda_{off}) \xi_{off}(R_T)}{\xi(\lambda_{on}) \xi_{on}(R_T)} \right) - \frac{1}{2C_\sigma} \ln \left(\frac{\rho_{off}}{\rho_{on}} + C_K \right) \quad (4.45)$$

The first term on the right hand side of the equation contains the dependency on the return signal. The second term contains only factors that are static or at least very slowly varying quantities as the instrument operates. The third term contains factors that fluctuate as the sensor operates. The fluctuations may be slowly varying or may be rapidly varying fluctuations depending on the operational conditions of the sensor. For example, ρ_{off}/ρ_{on} may vary pulse-to-pulse on an airborne platform depending on the PRF of the laser radar system.

$$\int_0^{R_T} NdR = -\frac{1}{2C_\sigma} \ln \left(\frac{P(\lambda_{on}, t) b}{P(\lambda_{off}, t) a} \right) - C_{fixed} - C_{fluctuating} \quad (4.46)$$

Effective Cross Section Correction

The term $(\sigma(\lambda_{on}) - \sigma(\lambda_{off}))$ in the surface dial concentration length equation deserves some attention. Errors in this term directly affect the concentration length measurement. Unfortunately, there are usually many uncertainties in our knowledge of the on line cross section due to our knowledge of atmospheric parameters in the target gas region. Ismail and Browell[19] give the following systematic effects on the cross section value used in the DIAL measurements.

1. Modification of the laser spectral profile by molecular absorption
2. Doppler broadening of the elastically backscattered signal and other atmospherics spectral broadening effects
3. Pressure shifts of absorption lines
4. Temperature sensitivity of absorption lines
5. Laser spectral purity
6. laser wavelength uncertainty
7. Knowledge of laser spectral output

The first four error sources are atmospheric, the last three are effects of the laser and optical systems. If the laser spectral width is not negligible in comparison to the line width, then it is necessary to replace the target gas cross section with an effective cross section σ_{eff} which is the convolution of the lidar spectrum with the absorption line. Usually the off line or wing cross section is negligible as compared to the on line cross section. Given this assumption, the effective cross section is given by[19]

$$\sigma_{eff}(R) = \frac{\int G(\nu, R) \sigma_a(\nu_{on}) d\nu}{\int G(\nu, R) d\nu} \quad (4.47)$$

where $G(\nu, R)$ is the altitude dependent on-line lidar spectral intensity profile and $\sigma_a(\nu_{on})$ is the target on-line cross section expressed in terms of the wavenumber, ν . Ismail and Browell suggest that for tropospheric cases Doppler broadening dominates and they consistently utilize the Voigt absorption cross section line shape.

Equation (4.47) is non-linear and is best solved numerically.

4.2.3 Calculate the minimum detectable concentration for surface reflectance DIAL

We can find a theoretical minimum detectable concentration for DIAL techniques. We start by looking for the minimum detectable difference between the on-line and wing return energy. This difference must be greater than the noise

equivalent energy. We choose to form our expression in terms of a minimum signal to noise ratio.

The difference in energy collected is

$$\Delta E = \Delta E_o - \Delta E_w \quad (4.48)$$

where E_o is the energy collected at the on-resonance wavelength, λ_{on} , and E_w is the energy collected at the wing wavelength, λ_{off} . Because surface enhanced DIAL is not range resolved, we have

$$\Delta E = E_w(\lambda_{off}, t) - E_o(\lambda_{on}, t) \quad (4.49)$$

we wish the change in energy to be greater than $E_o(\lambda_{on}, t) / SNR$ so

$$E_w(\lambda_{off}, t) - E_o(\lambda_{on}, t) \geq \frac{E_o(\lambda_{on}, t)}{SNR} \quad (4.50)$$

Using the tomographic lidar equation,

$$\begin{aligned} & E_L \frac{A_o}{R_T^2} \xi(\lambda_{off}) \xi(R_T) \frac{\rho(\lambda_{off}) \tau_d}{\pi \tau_L} T^2(\lambda_{off}, R_T) \\ & - E_L \frac{A_o}{R_T^2} \xi(\lambda_{on}) \xi(R_T) \frac{\rho(\lambda_{on}) \tau_d}{\pi \tau_L} T^2(\lambda_{on}, R_T) \\ & \geq E_L \frac{A_o}{R_T^2} \xi(\lambda_{on}) \xi(R_T) \frac{\rho(\lambda_{on}) \tau_d}{\pi \tau_L} T^2(\lambda_{on}, R_T) \frac{1}{SNR} \end{aligned} \quad (4.51)$$

We assume the optics are the same (e.g. A_o , $p(\lambda)$ are the same for both wavelengths) and the laser power is the same, The geometric form factor is set to 1, and the system spectral response $\xi(\lambda_{on}) \simeq \xi(\lambda_{off})$. We are left with

$$T^2(\lambda_{off}, R_T) - T^2(\lambda_{on}, R_T) \geq T^2(\lambda_{on}, R_T) \frac{1}{SNR}$$

We take the case where the two sides are just equal and rearrange

$$\left(\frac{1}{SNR} + 1 \right) T^2(\lambda_{on}, R_T) = T^2(\lambda_{off}, R_T)$$

writing out the exponentials yields

$$\begin{aligned} & \left(\frac{1}{SNR} + 1 \right) \exp \left(-2 \int_0^{R_T} (\bar{\kappa} + N(R) \sigma(\lambda_{on})) dR \right) \\ & = \exp \left(-2 \int_0^{R_T} (\bar{\kappa} + N(R) \sigma(\lambda_{off})) dR \right) \end{aligned} \quad (4.52)$$

Dividing to combine exponentials yields

$$\left(\frac{1}{SNR} + 1 \right) = \exp \left(-2 \int_0^{R_T} (\bar{\kappa} + N(R) \sigma(\lambda_{off})) dR + 2 \int_0^{R_T} (\bar{\kappa} + N(R) \sigma(\lambda_{on})) dR \right)$$

Now we assume that the cross section for the wing wavelength is very small and can be neglected $\sigma(\lambda_{off}) \ll \sigma(\lambda_{on})$. Then

$$\begin{aligned} \left(\frac{1}{SNR} + 1 \right) &= \exp \left(-2 \int_0^{R_T} \bar{\kappa} dR + 2 \int_0^{R_T} (\bar{\kappa} + N(R) \sigma(\lambda_{on})) dR \right) \\ &= \exp \left(2 \int_0^{R_T} (N(R) \sigma(\lambda_{on})) dR \right) \end{aligned} \quad (4.53)$$

we can take the logarithm of both sides and rearrange to yield

$$\int_0^{R_T} (N(R)) dR = \frac{1}{2\sigma(\lambda_{on})} \ln \left(\frac{1}{SNR} + 1 \right) \quad (4.54)$$

where the left hand side is the minimal detectable columnar number density, N_{min} . We can use the formula

$$C_{min} = \frac{N_{min} \times 10^6}{N_{atm}} \quad (4.55)$$

to find the concentration in ppm·m.

4.2.4 Calculate the minimum energy required for achieving detection of C_{min}

The form of the minimum detectable concentration is surprisingly simple. Unfortunately it gives us no insight into what laser power is required to achieve the minimum. We therefore seek to derive a minimum required laser energy?? such that the minimum detectable concentration can be observed.

Suppose, as Measures does, that we are dark current limited. Then

$$E(\lambda_{on}, R_T) \geq \frac{1}{D^*} \left\{ \frac{F_G A_d}{4B\xi_e} \right\}^{\frac{1}{2}} SNR_{min} \quad (4.56)$$

Assume that $F_G/\xi_e = 1$ Then

$$E_L \frac{A_o}{R_T^2} \xi(\lambda_{on}) \xi(R_T) \frac{\rho(\lambda_{on}) \tau_d}{\pi \tau_L} T^2(\lambda_{on}, R_T) \geq \frac{1}{D^*} \left\{ \frac{A_d}{4B} \right\}^{\frac{1}{2}} SNR_{min} \quad (4.57)$$

Rearranging yields and solving for minimum laser power

$$E_{L min} = \frac{R_T^2 \pi \tau_L}{\rho(\lambda_{on}) \tau_d A_o \xi(\lambda_{on}) \xi(R_T) D^*} \left\{ \frac{A_d}{4B} \right\}^{\frac{1}{2}} SNR_{min} T^{-2}(\lambda_{on}, R_T) \quad (4.58)$$

Define U^* just because Measures does

$$U^*(\lambda_{on}) = A_o \xi(\lambda_{on}) c \tau_d D^* \left\{ \frac{A_d}{4B} \right\}^{-\frac{1}{2}} \quad (4.59)$$

then, assuming the geometric form factor $\xi(R_T) = 1$

$$E_{L_{\min}} = \left(\frac{\pi c \tau_L SNR_{\min}}{\rho(\lambda_{on}) U^*(\lambda_{on})} \right) R_T^2 \exp \left(2 \int_0^{R_T} \kappa(\lambda_{on}, R) dR \right) \quad (4.60)$$

We can split the transmission into two factors

$$E_{L_{\min}} = \left(\frac{\pi c \tau_L SNR_{\min}}{\rho(\lambda_{on}) U^*(\lambda_{on})} \right) R_T^2 \exp(2\bar{\kappa}R_T) \exp \left(2 \int_0^{R_T} N(R) \sigma(\lambda_{on}) dR \right) \quad (4.61)$$

This is the form for the minimum laser energy needed to achieve detection of the minimum detectable concentration.

4.2.5 Surface DIAL Example

Methane (CH_4) has an absorption line at $3.391 \mu\text{m}$. The cross section for this line has been measured to be (See Measures page 118[3])

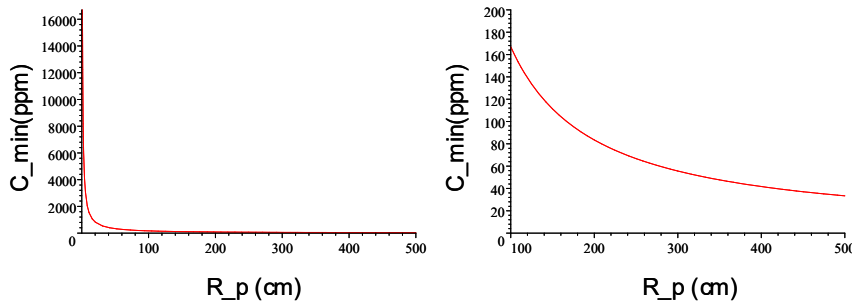
$$\sigma = 0.6 \times 10^{-18} \text{ cm}^2$$

Then if $SNR = 1.5$, and $N_{atm} = 2.55 \times 10^{19} \text{ cm}^{-3}$ and we assume a constant density plume of $R_p = 2 \text{ m}$ height

$$\begin{aligned} \int N_{\min} dR &= N_{\min} R_p = \frac{1}{2\sigma} \ln \left(\frac{1}{SNR} + 1 \right) \\ &= \frac{1}{2\sigma R_p} \ln \left(\frac{1}{SNR} + 1 \right) \\ N_{\min} &= 2.1284 \times 10^{15} \frac{1}{\text{cm}^3} \end{aligned} \quad (4.62)$$

$$\begin{aligned} C_{\min} &= \frac{N_{\min} \times 10^6}{N_{atm}} \\ &= 83.467 \text{ ppm} \end{aligned} \quad (4.63)$$

Because N_{\min} varies as $1/R_p$, the minimum concentration will also vary as $1/R_p$.



56 CHAPTER 4. DIFFERENTIAL ABSORPTION LIDAR (DIAL) EQUATION

to make the expression for minimum concentration independent of the plume height, we can multiply by the plume height

$$\begin{aligned} C_{\min} (\text{ppm-m}) &= R_p C_{\min} (\text{ppm}) \\ &= R_p \left[\frac{1}{2\sigma R_p} \ln \left(\frac{1}{SNR} + 1 \right) \frac{10^6}{N_a} \right] \\ &= \frac{1}{2\sigma} \ln \left(\frac{1}{SNR} + 1 \right) \frac{10^6}{N_{atm}} \end{aligned}$$

This value does not depend on the plume dimension in any way. For our example

$$C_{\min} (\text{ppm-m}) = 166.94 \text{ ppm-m}$$

To find the minimum laser power needed to detect this concentration, we will choose values for the following parameters

$$\begin{aligned} \tau_L &= 1 \times 10^{-8} \text{ s} \\ \tau_d &= 1 \times 10^{-8} \text{ s} \\ A_o &= \pi(0.1 \text{ m})^2 \\ c &= 3 \times 10^8 \frac{\text{m}}{\text{s}} \\ \rho &= 0.1 \\ D &= 10^{10} \text{ cm Hz}^{\frac{1}{2}} \text{ W}^{-1} \\ A_d &= (1 \times 10^{-4} \text{ m})^2 \\ B &= \frac{1}{2\tau_d} \\ U &= A_o c \tau_d D \left\{ \frac{A_d}{4B} \right\}^{-\frac{1}{2}} \end{aligned}$$

Then, from equation (4.61)

$$E_{L_{\min}} = \left(\frac{\pi c \tau_L S}{\rho U} \right) R_T^2 \exp(2\kappa R_T) \exp(2\sigma N R_p) \quad (4.64)$$

or

$$E_{L_{\min}} = 6.1823 \times 10^{-13} R_t^2 \exp(0.0001 R_t) \text{ J} \quad (4.65)$$

where R_T is in meters.

We may choose a nominal flight level for a small plane of $R_T = 1500 \text{ ft}$. Then

$$E_{L_{\min}} = 0.13527 \mu\text{J}$$

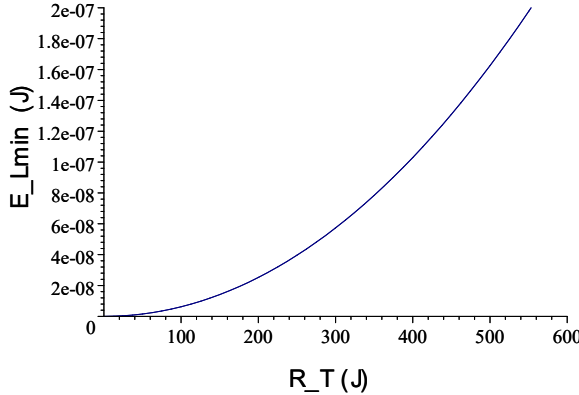


Figure 4.2:

4.3 Three Line and Multi-Line DIAL

Sometimes, the absorption line we wish to measure is on the wings of another absorption or is contaminated by continuum absorption. In these situations, more accuracy can be obtained in DIAL measurements if three or more laser lines are employed in the algorithm. Figure 4.3 shows the concept. Laser lines are matched to frequencies ν_o , ν_{w_1} , and ν_{w_2} . The two wing measurements are used to estimate the return value of the background spectra at ν_o in the absence of the target gas. We may call this return power $P_{est}(\lambda_{on}, t)$. Then the DIAL algorithm proceeds as in equations (4.7) or (4.11) with $P(\lambda_{off}, t)$ replaced by $P_{est}(\lambda_{on}, t)$, except that $(\bar{\kappa}(\lambda_{on}, R_T) - \bar{\kappa}(\lambda_{off}, R_T)) \rightarrow (\bar{\kappa}(\lambda_{on}, R_T) - \bar{\kappa}_{est}(\lambda_{on}, R_T)) = 0$ and $(\sigma_a(\lambda_{on}) - \sigma_a(\lambda_{on})) \rightarrow \sigma_a(\lambda_{on})$ where $\bar{\kappa}_{est}(\lambda_{on}, R_T)$ is the estimated absorption coefficient of the atmosphere in the absence of the target gas. Then the DIAL equation becomes

$$\int_0^{R_T} N(R) dR = \frac{1}{2\sigma_a(\lambda_{on})} \left(\ln \frac{P_{est}(\lambda_{on}, t)}{P(\lambda_{on}, t)} \right)$$

and we see that error due to the background atmospheric absorption has been eliminated. More laser lines could help define the shape of the absorption feature or background absorption, but producing many laser lines may be impractical.

Another algorithm for three line dial involves *a priori* understanding of the background absorption. This *Basian* technique requires measurement of three different wavelengths, but all three are measured on one side of the absorption feature of interest. This new technique has not yet been validated.

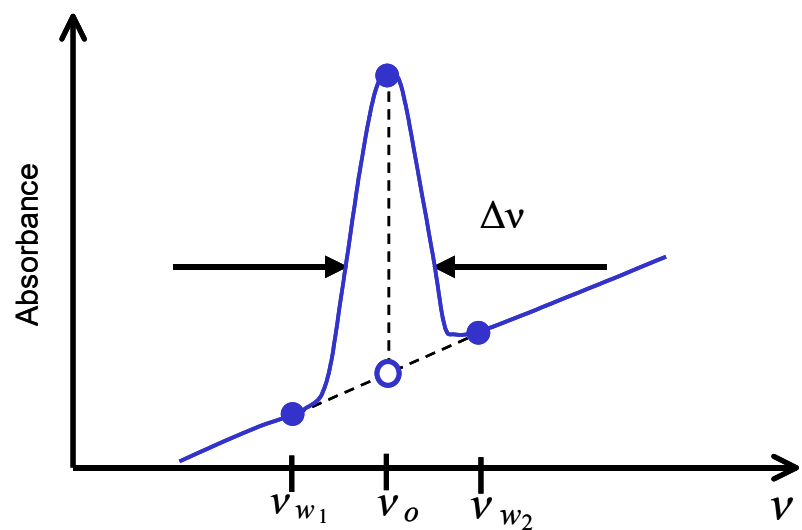


Figure 4.3:

Part III

Laser Topics

Chapter 5

Light/Laser Amplification and Detection

Description of how lasers work

Not done yet

Chapter 6

Laser Beam Propagation

Not done yet

6.1 Gaussian beams[1]

Not done yet

In section 2.1.1 we defined the paraxial wave equation (2.44).

$$\nabla_T^2 \mathcal{E}_o(\mathbf{r}) + 2ik \frac{\partial \mathcal{E}_o(\mathbf{r})}{\partial z} = 0 \quad (6.1)$$

In real laser beams, the intensity of a beam profile propagating in the z -direction is negligible at points sufficiently far from the z -axis. The simplest achievable beam profile is a Gaussian beam.

We define a Gaussian beam intensity profile with the form

$$I(x, y, z) = |\mathcal{E}_o(\mathbf{r})|^2 \exp\left(-\frac{2(x^2 + y^2)}{w^2}\right) \quad (6.2)$$

in a plane perpendicular to the direction of travel (z -direction as defined in Section 2.1.1). This form for the intensity profile follows the form of the well known Gaussian function

$$\mathbb{G}(x) = \frac{1}{\sqrt{2\pi}w} \exp\left(-\frac{x^2}{2w^2}\right) \quad (6.3)$$

We seek a solution to the free space wave equation (equation 2.24) that has a form like equation (6.2).

The field takes the form

$$\mathcal{E}_o(\mathbf{r}) = A e^{ik \frac{x^2 + y^2}{2q(z)}} e^{ip(z)} \quad (6.4)$$

where A is a constant and $q(z)$ and $p(z)$ must be determined. We start with $q(z)$ by noting that if we allow

$$q(z) = \frac{2i}{kw^2} = \frac{i\lambda}{\pi w^2} \quad (6.5)$$

we recover the desired Gaussian intensity profile. A result of allowing this for $q(z)$ is that the spot size, w , may grow with z , which is what happens in real beams.

We need to solve

$$\nabla_T^2 \left(A e^{ik\frac{x^2+y^2}{2q(z)}} e^{ip(z)} \right) + 2ik \frac{\partial}{\partial z} \left(A e^{ik\frac{x^2+y^2}{2q(z)}} e^{ip(z)} \right) = 0 \quad (6.6)$$

$$A \nabla_T^2 \left(e^{ik\frac{x^2+y^2}{2q(z)}} e^{ip(z)} \right) + 2ikA \frac{\partial}{\partial z} \left(e^{ik\frac{x^2+y^2}{2q(z)}} e^{ip(z)} \right) = 0 \quad (6.7)$$

Begin by computing

$$\frac{\partial}{\partial z} \left(A e^{ik\frac{x^2+y^2}{2q(z)}} e^{ip(z)} \right) = A \left(e^{ik\frac{x^2+y^2}{2q(z)}} \frac{\partial}{\partial z} (e^{ip(z)}) + e^{ip(z)} \frac{\partial}{\partial z} \left(e^{ik\frac{x^2+y^2}{2q(z)}} \right) \right) \quad (6.8)$$

$$= A \left(e^{ik\frac{x^2+y^2}{2q(z)}} i \frac{\partial p(z)}{\partial z} (e^{ip(z)}) + i k e^{ip(z)} e^{ik\frac{x^2+y^2}{2q(z)}} \frac{\partial}{\partial z} \left(\frac{x^2+y^2}{2q(z)} \right) \right) \quad (6.9)$$

$$= i A e^{ik\frac{x^2+y^2}{2q(z)}} e^{ip(z)} \left(\frac{\partial p(z)}{\partial z} - k \frac{(x^2+y^2)}{2q^2(z)} \frac{\partial q(z)}{\partial z} \right) \quad (6.10)$$

We also need

$$A \nabla_T^2 \left(e^{ik\frac{x^2+y^2}{2q(z)}} e^{ip(z)} \right) = A \left(\frac{\partial^2}{\partial x^2} + \frac{\partial^2}{\partial y^2} \right) \left(e^{ik\frac{x^2+y^2}{2q(z)}} \right) \quad (6.11)$$

$$= A e^{ip(z)} e^{ik\frac{x^2+y^2}{2q}} \frac{1}{q^2} ((ikq - k^2 x^2) + (ikq - k^2 y^2)) \quad (6.12)$$

$$= A e^{ip(z)} e^{ik\frac{x^2+y^2}{2q}} \left(\frac{2ik}{q} - k^2 \frac{x^2+y^2}{q^2} \right) \quad (6.13)$$

Then our wave equation becomes

$$A e^{ip(z)} e^{ik\frac{x^2+y^2}{2q(z)}} \left(\frac{2ik}{q} - k^2 \frac{x^2+y^2}{q^2} \right) + (2ik) i A e^{ik\frac{x^2+y^2}{2q(z)}} e^{ip(z)} \left(\frac{\partial p(z)}{\partial z} - k \frac{(x^2+y^2)}{2q^2(z)} \frac{\partial q(z)}{\partial z} \right) \quad (6.14)$$

$$\frac{2ik}{q} - k^2 \frac{x^2+y^2}{q^2} - 2k \frac{\partial p(z)}{\partial z} + 2k^2 \frac{(x^2+y^2)}{2q^2(z)} \frac{\partial q(z)}{\partial z} \quad (6.15)$$

$$2k \left(\frac{i}{q} - \frac{\partial p(z)}{\partial z} \right) + \frac{k^2}{q^2(z)} (x^2+y^2) \left(\frac{\partial q(z)}{\partial z} - 1 \right) \quad (6.16)$$

If we require

$$\frac{\partial q(z)}{\partial z} = 1 \quad (6.17)$$

and

$$\frac{\partial p(z)}{\partial z} = \frac{i}{q} \quad (6.18)$$

then we have a solution. These equation yield

$$q(z) = q_o + z \quad (6.19)$$

$$p(z) = i \ln \left(\frac{q_o + z}{q_o} \right) \quad (6.20)$$

where the boundary conditions give are $q_o = q(0)$, and we assume $p(0) = 0$.

Unfortunately q may be complex. Then

$$\frac{1}{q(z)} = \frac{1}{R(z)} + \frac{i\lambda}{\pi w^2(z)} \quad (6.21)$$

with $R(z)$ and $w(z)$ real. This gives us the desired form from equation (6.5) when $R(z) \rightarrow \infty$. Our field equation becomes

$$\mathcal{E}_o(\mathbf{r}) = A e^{ik \frac{x^2+y^2}{2R(z)}} e^{-\frac{x^2+y^2}{w^2(z)}} e^{ip(z)} \quad (6.22)$$

The last term may be written as

$$e^{ip(z)} = \exp \left(-\ln \left(\frac{q_o + z}{q_o} \right) \right) \quad (6.23)$$

$$= \frac{1}{1 + \frac{z}{q_o}} \quad (6.24)$$

$$= \frac{1}{1 + \frac{z}{R_o} + \frac{i\lambda z}{\pi w_o^2}} \quad (6.25)$$

where $R_o = R(z=0)$ and $w_o = w(z=0)$. We wish to choose values for R_o and w_o . Once these are determined we know $R(z)$ and $w(z)$ for all z . Let us choose $z=0$ as the point where $R_o = \infty$ and

$$\frac{1}{q_o} = \frac{i\lambda}{\pi w_o^2} \quad (6.26)$$

then

$$\frac{1}{q(z)} = \frac{1}{q_o + z} \quad (6.27)$$

$$= \frac{\frac{1}{q_o}}{1 + \frac{z}{q_o}} \quad (6.28)$$

$$= \frac{\frac{i\lambda}{\pi w_o^2}}{1 + z \frac{i\lambda}{\pi w_o^2}} \quad (6.29)$$

$$= \frac{\left(\frac{i\lambda}{\pi w_o^2} + z \left(\frac{\lambda}{\pi w_o^2} \right)^2 \right)}{\left(1 + \left(z \frac{i\lambda}{\pi w_o^2} \right)^2 \right)} \quad (6.30)$$

$$= \frac{\frac{i\lambda}{\pi w_o^2}}{1 + \left(z \frac{i\lambda}{\pi w_o^2} \right)^2} + \frac{\frac{1}{z} \left(\frac{\lambda z}{\pi w_o^2} \right)^2}{1 + \left(z \frac{i\lambda}{\pi w_o^2} \right)^2} \quad (6.31)$$

We set this equal to $1/q(z)$

$$\frac{1}{q(z)} = \frac{1}{R(z)} + \frac{i\lambda}{\pi w^2(z)} \quad (6.32)$$

$$= \frac{\frac{i\lambda}{\pi w_o^2}}{1 + \left(z \frac{i\lambda}{\pi w_o^2} \right)^2} + \frac{\frac{1}{z} \left(\frac{\lambda z}{\pi w_o^2} \right)^2}{1 + \left(z \frac{i\lambda}{\pi w_o^2} \right)^2} \quad (6.33)$$

then

$$R(z) = \frac{1 + \left(z \frac{i\lambda}{\pi w_o^2} \right)^2}{\frac{1}{z} \left(\frac{\lambda z}{\pi w_o^2} \right)^2} \quad (6.34)$$

$$= \frac{1 + z^2 \left(\frac{i\lambda}{\pi w_o^2} \right)^2}{z \left(\frac{\lambda}{\pi w_o^2} \right)^2} \quad (6.35)$$

$$= \frac{1}{z \left(\frac{\lambda}{\pi w_o^2} \right)^2} + z \quad (6.36)$$

We define a new parameter, z_o and give it the name *Rayleigh range*.

$$z_o = \frac{\pi w_o^2}{\lambda} \quad (6.37)$$

then

$$R(z) = \frac{z_o^2}{z} + z \quad (6.38)$$

Using this parameter we can write the other term in $1/q(z)$

$$\frac{i\lambda}{\pi w^2(z)} = \frac{\frac{i\lambda}{\pi w_o^2}}{1 + \left(z \frac{i\lambda}{\pi w_o^2}\right)^2} \quad (6.39)$$

$$\frac{1}{w^2(z)} = \frac{1}{w_o^2} \frac{1}{1 + \left(z \frac{i\lambda}{\pi w_o^2}\right)^2} \quad (6.40)$$

$$w^2(z) = w_o^2 \left(1 - \left(\frac{z}{z_o}\right)^2\right) \quad (6.41)$$

With $R_o = \infty$ we may also write

$$e^{ip(z)} = \frac{1}{1 + i \frac{z}{z_o}} = \frac{\left(1 - i \frac{z}{z_o}\right)}{\left(1 + i \frac{z}{z_o}\right) \left(1 - i \frac{z}{z_o}\right)} \quad (6.42)$$

$$= \frac{\left(1 - i \frac{z}{z_o}\right)}{\left(1 + \left(\frac{z}{z_o}\right)^2\right)} \quad (6.43)$$

$$= \frac{1}{\sqrt{1 + \left(\frac{z}{z_o}\right)^2}} e^{-i\phi(z)} \quad (6.44)$$

where $\phi(z) = \tan^{-1}(z/z_o)$. The field equation is then

$$\mathcal{E}_o(\mathbf{r}) = \frac{A e^{-i\phi(z)}}{\sqrt{1 + \left(\frac{z}{z_o}\right)^2}} e^{ik \frac{x^2 + y^2}{2R(z)}} e^{-\frac{x^2 + y^2}{w^2(z)}} e^{ikz} \quad (6.45)$$

This solution is a beam like equation that is a solution within the paraxial approximation which has a Gaussian intensity profile in a plane $z = \text{constant}$. The spot size $w(z)$ has a minimum, w_o at a location $z = 0$ and grows with distance from this location. The minimum spot is called the *beam waist*. The distance z_o is defined such that

$$w(z_o) = w_o \sqrt{2} \quad (6.46)$$

This means that the Rayleigh range is a measure of the waist region where the spot size is smallest. The smaller the spot size w_o the smaller the Rayleigh range and the greater the rate of growth with z of the spot size away from the waist.

The far field divergence angle for the beam is defined as

$$\theta = 1.22 \frac{\lambda}{D} \quad (6.47)$$

where λ is the wavelength of the light and D is the diameter of the aperture of an optical system. For our Gaussian beam we may define

$$\theta \approx \frac{w(z)}{z} \approx \frac{w_o}{z_o} = \frac{\lambda}{\pi w_o} \quad z \gg z_o \quad (6.48)$$

So the divergence angle of a Gaussian beam is of the same order as that associated with the diffraction of a plane wave by an aperture of diameter $D \simeq w_o$.

For completeness the intensity becomes

$$I(x, y, z) = \left| \frac{A e^{-i\phi(z)}}{\sqrt{1 + \left(\frac{z}{z_o}\right)^2}} e^{ik\frac{x^2+y^2}{2R(z)}} e^{\frac{x^2+y^2}{w^2(z)}} e^{ikz} \right|^2 \quad (6.49)$$

$$= \frac{|A|^2}{1 + \left(\frac{z}{z_o}\right)^2} e^{-\frac{x^2+y^2}{w^2(z)}} \quad (6.50)$$

For $z \gg z_o$ the beam has an inverse square dependency on z from the waste

$$I(x, y, z) = \frac{|A|^2 z_o^2}{z^2} e^{-\frac{x^2+y^2}{w^2(z)}} \quad z \gg z_o \quad (6.51)$$

We may define

$$I_o = |A|^2 \quad (6.52)$$

then

$$I(x, y, z) = \frac{I_o z_o^2}{z^2} e^{-\frac{x^2+y^2}{w^2(z)}} \quad z \gg z_o \quad (6.53)$$

At large distances the beam waste is

$$w(z) = \sqrt{w_o^2 \left(1 - \left(\frac{z}{z_o}\right)^2\right)} \quad (6.54)$$

$$= w_o \left(\frac{z}{z_o}\right) = \frac{\lambda z}{\pi w_o} \quad (6.55)$$

The field at large distances is given by

$$\mathcal{E}_o(\mathbf{r}) = \frac{A z_o^2 e^{i(kz - \frac{\pi}{2})}}{z^2} e^{ik\frac{x^2+y^2}{2R(z)}} e^{-\frac{x^2+y^2}{w^2(z)}} \quad (6.56)$$

In this limit

$$R(z) = \frac{z_o^2}{z} + z \quad (6.57)$$

$$\approx z \quad (6.58)$$

giving

$$\mathcal{E}_o(\mathbf{r}) = -iA z_o \left[\frac{e^{ikz}}{z} e^{ik\frac{x^2+y^2}{2z}} \right] e^{-\frac{x^2+y^2}{w^2(z)}} \quad (6.59)$$

where we recognize the bracketed term as a spherical wave centered at $z = 0$. Thus far from the beam waist we have a Gaussian spherical wave (but remember this is true not too far from the z -axis).

Beam quality M^2

The propagation of a Gaussian beam is completely described by its waist and its divergence. For an ideal TEM₀₀ beam, the product of the beam waste, ω_o , and the divergence angle, θ_o , is given by the wavelength divided by π .

$$\omega_o \theta_o = \frac{\lambda}{\pi} \quad (6.60)$$

Achievable beams do not follow the ideal diffraction limited performance. When a beam deviates from the ideal Gaussian, the product of the beam waist and the divergence angle increases by the *beam quality factor*, M^2 .

$$\omega \theta = M^2 \frac{\lambda}{\pi} \quad (6.61)$$

The factor M^2 represents how many times wider the focused spot is than the theoretical minimum. An M^2 of 2, for example, means that the focused beam will be twice the ideal minimum spot size. High quality beams may achieve $M^2 < 1.1$. Multimode lasers produce poorer beam qualities. A typical value may be $M^2 = 4$.

Part IV

Practical Application

Chapter 7

General Error Analysis

We wish to determine the predicted uncertainty in an ensemble of measurements of surface reflectance DIAL lidar systems. We wish to include both receiver error and interfearing uncertainties that come from the affect of the environmental variability. For gases naturally occurring in the atmosphere, the natural background level must be considered. Of course, there will be both systematic and random error in this system. The systematic error will be treated as an accuracy error while the random component will be treated with standard error propagation. For the random errors uncertainties are treated as Gaussian distributed random variables.

Chapter 8

Accuracy

The words “accuracy of the measurement” will be used to describe how different the mean of the ensemble of measurements is from the mean of the truth values for the ensemble. Thus the accuracy describes any bias to the system. The equation that describes the concentration length measurement is given as

$$L_C[\text{ppm} \cdot \text{m}] = \frac{1 \times 10^6}{N_a C_\sigma} \left(\frac{1}{2} \ln \left(\frac{E_f}{E_n} \frac{E_n^{(T)}}{E_f^{(T)}} \right) - C_K \right) \quad (8.1)$$

This equation is the overall concentration length. It can be used directly for the ethane measurement, but the methane measurement must account for the atmospheric methane background. In this case, we have

$$L_{C\text{plume}}[\text{ppm} \cdot \text{m}] = \frac{1 \times 10^6}{N_a C_\sigma} \left(\frac{1}{2} \ln \left(\frac{E_f}{E_n} \frac{E_n^{(T)}}{E_f^{(T)}} \right) - C_K \right) - L_{C\text{background}} \quad (8.2)$$

The background cannot be separated from the plume in the measurement, itself. We can estimate the background by using measurements in the near vicinity of those containing a plume. For the background measurement we have

$$L_{C\text{background}}[\text{ppm} \cdot \text{m}] = \frac{1 \times 10^6}{N_a C_\sigma (\text{m}^2)} \left(\frac{1}{2} \ln \left(\frac{E_f}{E_n} \frac{E_n^{(T)}}{E_f^{(T)}} \right) - C_K \right) \quad \text{no plume} \quad (8.3)$$

with an error

$$\sigma_{L_{C\text{background}}} \quad (8.4)$$

that will be determined by the analysis of the random error. Thus there is the potential for a bias of the order

$$\text{bias} = 1 \times 10^6 \frac{C_K}{N_a C_\sigma} + L_{C\text{background}} \quad (8.5)$$

In theory, the nearest neighbor (no plume) measurements can also be used to determine the bias term

$$1 \times 10^6 \frac{C_K}{N_a C_\sigma} \quad (8.6)$$

Using the sensor to measure the background and knowing the atmospheric conditions will allow us to model the bias. Uncertainty in the measurements will leave a residual bias that can be modeled as a Gaussian random variable and will be included in the precision measurement.

Chapter 9

Precision:Concentration length and Propagation of Errors

The signal we wish to measure is concentration length. This is given in terms of the measured laser return power as

$$L_C[\text{ppm} \cdot \text{m}] = \frac{1 \times 10^6}{N_a C_\sigma} \left(\frac{1}{2} \ln \left(\frac{E_f}{E_n} \frac{E_n^{(T)}}{E_f^{(T)}} \right) - C_K \right) \quad (9.1)$$

Where:

Parameter	Description	Units
$C_\sigma = (\sigma(\lambda_{on}) - \sigma(\lambda_{off}))$	Difference in target gas absorption x-sections	m^2
$C_K = \int_0^{R_T} (\kappa(\lambda_{on}, R) - \kappa(\lambda_{off}, R)) dr$	Difference in atmospheric concentration length	unitless
E_f	Off line pulse return power	J
E_n	On line pulse return power	J
$E_f^{(T)}$	Off line pulse transmitt power	J
$E_n^{(T)}$	On line pulse transmitt power	J
N_a	Density of air in molecules per m^{-3} (held constant)	m^{-3}

This equation includes the conversion from the concentration length in m^{-2} to $\text{ppm} \cdot \text{m}$

$$L_C[\text{ppm} \cdot \text{m}] = L_C [\text{m}^{-2}] \frac{1 \times 10^6}{N_a} \quad (9.2)$$

We wish to find the error on the concentration length measurement. We will simplify by defining

$$C_\sigma = C_\sigma (\text{ppm}) = \frac{N_a C_\sigma (\text{m}^2)}{1 \times 10^6}$$

9.1 Formula for propagation of errors

$$\sigma_u^2 = \left(\frac{\partial f}{\partial x} \right)^2 \sigma_x^2 + \left(\frac{\partial f}{\partial y} \right)^2 \sigma_y^2 + 2\text{cov}(x, y) \frac{\partial f}{\partial x} \frac{\partial f}{\partial y} \quad (9.3)$$

The units of our signal are [ppm·m] so we expect the variance σ_u^2 to have units of [ppm·m]². We will need to make assumptions about the variation of the parameters in our signal equation. The standard formula gives the following variance for concentration length

$$\begin{aligned} \sigma_L^2 &= \left(\frac{\partial L_C}{\partial E_f} \right)^2 \sigma_{P_f}^2 + \left(\frac{\partial L_C}{\partial E_n} \right)^2 \sigma_{E_n}^2 + \left(\frac{\partial L_C}{\partial E_f^{(T)}} \right)^2 \sigma_{E_f^{(T)}}^2 + \left(\frac{\partial L_C}{\partial E_n^{(T)}} \right)^2 \sigma_{E_n^{(T)}}^2 \\ &\quad + \left(\frac{\partial L_C}{\partial C_\sigma} \right)^2 \sigma_{C_\sigma}^2 + \left(\frac{\partial L_C}{\partial C_K} \right)^2 \sigma_{C_K}^2 \\ &\quad + 2\text{cov}(E_n, E_f) \frac{\partial L_C}{\partial E_f} \frac{\partial L_C}{\partial E_n} + 2\text{cov}(E_f^{(T)}, E_n^{(T)}) \frac{\partial L_C}{\partial E_f^{(T)}} \frac{\partial L_C}{\partial E_n^{(T)}} \\ &\quad + 2\text{cov}(E_n, E_f^{(T)}) \frac{\partial L_C}{\partial E_f^{(T)}} \frac{\partial L_C}{\partial E_n} + 2\text{cov}(E_n, E_n^{(T)}) \frac{\partial L_C}{\partial E_n^{(T)}} \frac{\partial L_C}{\partial E_n} \\ &\quad + 2\text{cov}(E_f, E_f^{(T)}) \frac{\partial L_C}{\partial E_f^{(T)}} \frac{\partial L_C}{\partial E_f} + 2\text{cov}(E_f, E_n^{(T)}) \frac{\partial L_C}{\partial E_n^{(T)}} \frac{\partial L_C}{\partial E_f} \\ &\quad + 2\text{cov}(E_n, C_\sigma) \frac{\partial L_C}{\partial C_\sigma} \frac{\partial L_C}{\partial E_n} + 2\text{cov}(C_\sigma, E_f) \frac{\partial L_C}{\partial C_\sigma} \frac{\partial L_C}{\partial E_f} \\ &\quad + 2\text{cov}(E_n^{(T)}, C_\sigma) \frac{\partial L_C}{\partial C_\sigma} \frac{\partial L_C}{\partial E_n^{(T)}} + 2\text{cov}(C_\sigma, E_f^{(T)}) \frac{\partial L_C}{\partial C_\sigma} \frac{\partial L_C}{\partial E_f^{(T)}} \\ &\quad + 2\text{cov}(C_\sigma, C_K) \frac{\partial L_C}{\partial C_\sigma} \frac{\partial L_C}{\partial C_K} + 2\text{cov}(E_n, C_K) \frac{\partial L_C}{\partial C_K} \frac{\partial L_C}{\partial E_n} \\ &\quad + 2\text{cov}(C_K, E_f) \frac{\partial L_C}{\partial C_K} \frac{\partial L_C}{\partial E_f} + 2\text{cov}(E_n^{(T)}, C_K) \frac{\partial L_C}{\partial C_K} \frac{\partial L_C}{\partial E_n^{(T)}} \\ &\quad + 2\text{cov}(C_K, E_f^{(T)}) \frac{\partial L_C}{\partial C_K} \frac{\partial L_C}{\partial E_f^{(T)}} \end{aligned}$$

some of the cross correlation terms are zero because there is no dependency

between the terms.

$$\begin{aligned}
\sigma_L^2 &= \left(\frac{\partial L_C}{\partial E_f} \right)^2 \sigma_{E_f}^2 + \left(\frac{\partial L_C}{\partial E_n} \right)^2 \sigma_{E_n}^2 + \left(\frac{\partial L_C}{\partial E_f^{(T)}} \right)^2 \sigma_{E_f^{(T)}}^2 + \left(\frac{\partial L_C}{\partial E_n^{(T)}} \right)^2 \sigma_{E_n^{(T)}}^2 \\
&\quad + \left(\frac{\partial L_C}{\partial C_\sigma} \right)^2 \sigma_{C_\sigma}^2 + \left(\frac{\partial L_C}{\partial C_K} \right)^2 \sigma_{C_K}^2 \\
&\quad + 2\text{cov}(E_n, E_f) \frac{\partial L_C}{\partial E_f} \frac{\partial L_C}{\partial E_n} + 2\text{cov}(E_f^{(T)}, E_n^{(T)}) \frac{\partial L_C}{\partial E_f^{(T)}} \frac{\partial L_C}{\partial E_n^{(T)}} \\
&\quad + 2\text{cov}(E_n, E_f^{(T)}) \frac{\partial L_C}{\partial E_f^{(T)}} \frac{\partial L_C}{\partial E_n} + 2\text{cov}(E_n, E_n^{(T)}) \frac{\partial L_C}{\partial E_n^{(T)}} \frac{\partial L_C}{\partial E_n} \\
&\quad + 2\text{cov}(E_f, E_f^{(T)}) \frac{\partial L_C}{\partial E_f^{(T)}} \frac{\partial L_C}{\partial E_f} + 2\text{cov}(E_f, E_n^{(T)}) \frac{\partial L_C}{\partial E_n^{(T)}} \frac{\partial L_C}{\partial E_f} \\
&\quad + 2\text{cov}(E_n, C_\sigma) \frac{\partial L_C}{\partial C_\sigma} \frac{\partial L_C}{\partial E_n} + 2\text{cov}(C_\sigma, E_f) \frac{\partial L_C}{\partial C_\sigma} \frac{\partial L_C}{\partial E_f} \\
&\quad + 2\text{cov}(E_n^{(T)}, C_\sigma) \frac{\partial L_C}{\partial C_\sigma} \frac{\partial L_C}{\partial E_n^{(T)}} + 2\text{cov}(C_\sigma, E_f^{(T)}) \frac{\partial L_C}{\partial C_\sigma} \frac{\partial L_C}{\partial E_f^{(T)}} \\
&\quad + 2\text{cov}(E_n, C_K) \frac{\partial L_C}{\partial C_K} \frac{\partial L_C}{\partial E_n} + 2\text{cov}(C_K, E_f) \frac{\partial L_C}{\partial C_K} \frac{\partial L_C}{\partial E_f}
\end{aligned}$$

The partial derivatives are as follows:

$$\frac{\partial}{\partial E_f} \left(\frac{1}{C_\sigma} \left(\frac{1}{2} \ln \left(\frac{E_f}{E_n} \frac{E_n^{(T)}}{E_f^{(T)}} \right) - C_K \right) \right) = \frac{1}{2C_\sigma} \frac{1}{E_f} \quad (9.6)$$

$$\frac{\partial}{\partial E_n} \left(\frac{1}{C_\sigma} \left(\frac{1}{2} \ln \left(\frac{E_f}{E_n} \frac{E_n^{(T)}}{E_f^{(T)}} \right) - C_K \right) \right) = -\frac{1}{2C_\sigma} \frac{1}{E_n} \quad (9.7)$$

$$\frac{\partial}{\partial E_f^{(T)}} \left(\frac{1}{C_\sigma} \left(\frac{1}{2} \ln \left(\frac{E_f}{E_n} \frac{E_n^{(T)}}{E_f^{(T)}} \right) - C_K \right) \right) = -\frac{1}{2C_\sigma} \frac{1}{E_f^{(T)}} \quad (9.8)$$

$$\frac{\partial}{\partial E_n^{(T)}} \left(\frac{1}{C_\sigma} \left(\frac{1}{2} \ln \left(\frac{E_f}{E_n} \frac{E_n^{(T)}}{E_f^{(T)}} \right) - C_K \right) \right) = \frac{1}{2C_\sigma} \frac{1}{E_n^{(T)}} \quad (9.9)$$

Where we have used the identities

$$\begin{aligned}
\frac{\partial}{\partial x} \ln \left(\eta b \frac{1}{x} \right) &= -\frac{1}{x} \\
\frac{\partial}{\partial x} \ln(\eta x) &= \frac{1}{x}
\end{aligned}$$

Continuing,

$$\begin{aligned}\frac{\partial}{\partial C_\sigma} \left(\frac{1}{C_\sigma} \left(\frac{1}{2} \ln \left(\frac{E_f}{E_n} \frac{E_n^{(T)}}{E_f^{(T)}} \right) - C_K \right) \right) &= -\frac{1}{C_\sigma^2} \left(\frac{1}{2} \ln \left(\frac{E_f}{E_n} \frac{E_n^{(T)}}{E_f^{(T)}} \right) - C_K \right) \quad (9.10) \\ &\quad - \frac{1}{C_\sigma} \left(\frac{1}{C_\sigma} \left(\frac{1}{2} \ln \left(\frac{E_f}{E_n} \frac{E_n^{(T)}}{E_f^{(T)}} \right) - C_K \right) \right) \\ &= -\frac{1}{C_\sigma} L_C [\text{ppm} \cdot \text{m}]\end{aligned}$$

$$\frac{\partial}{\partial C_K} \left(\frac{1}{C_\sigma} \left(\frac{1}{2} \ln \left(\frac{E_f}{E_n} \frac{E_n^{(T)}}{E_f^{(T)}} \right) - C_K \right) \right) = -\frac{1}{C_\sigma} \quad (9.11)$$

Substituting these partials into the equation for σ_L^2 yields

$$\begin{aligned}\sigma_L^2 &= \left(\frac{1}{2C_\sigma} \right)^2 \left(\left(\frac{\sigma_{E_f}}{E_f} \right)^2 + \left(\frac{\sigma_{E_n}}{E_n} \right)^2 + \left(\frac{\sigma_{E_f^{(T)}}}{E_f^{(T)}} \right)^2 + \left(\frac{\sigma_{E_n^{(T)}}}{E_n^{(T)}} \right)^2 \right. \\ &\quad \left. + (2L_C [\text{ppm} \cdot \text{m}])^2 \left(\frac{\sigma_{C_\sigma}}{C_\sigma} \right)^2 + 4\sigma_{C_K}^2 \right) \\ &\quad + \left(\frac{1}{2C_\sigma} \right)^2 \left(2\text{cov}(E_n, E_f^{(T)}) \frac{1}{E_n} \frac{1}{E_f^{(T)}} - 2\text{cov}(E_n, E_f)^2 \frac{1}{E_n} \frac{1}{E_f} - 2\text{cov}(E_f^{(T)}, E_n^{(T)}) \frac{1}{E_f^{(T)}} \frac{1}{E_n^{(T)}} \right. \\ &\quad \left. + \left(\frac{1}{2C_\sigma} \right)^2 \left(2\text{cov}(E_f, E_n^{(T)}) \frac{1}{E_n^{(T)}} \frac{1}{E_f} - 2\text{cov}(E_n, E_n^{(T)}) \frac{1}{E_n^{(T)}} \frac{1}{E_n} - 2\text{cov}(E_f, E_f^{(T)}) \frac{1}{E_f^{(T)}} \frac{1}{E_f} \right. \right. \\ &\quad \left. \left. - \left(\frac{1}{C_\sigma} \right)^2 L_C [\text{ppm} \cdot \text{m}] \left(\text{cov}(C_\sigma, E_f) \frac{1}{E_f} - \text{cov}(E_n, C_\sigma) \frac{1}{E_n} + \text{cov}(E_n^{(T)}, C_\sigma) \frac{1}{E_n^{(T)}} - \text{cov}(C_\sigma, E_n^{(T)}) \frac{1}{E_n^{(T)}} \right) \right. \right. \\ &\quad \left. \left. + \left(\frac{1}{C_\sigma} \right)^2 \left(+\text{cov}(E_n, C_K) \frac{1}{E_n} - \text{cov}(C_K, E_f) \frac{1}{E_f} \right) \right)\right)\end{aligned}$$

This is the basic equation we will use for this analysis. The first five terms

are proportional to $\frac{1}{SNR_i}$ for each quantity i

$$\begin{aligned}\sigma_L^2 &= \left(\frac{1}{2C_\sigma}\right)^2 \left(\left(\frac{1}{SNR_{E_f}}\right)^2 + \left(\frac{1}{SNR_{E_N}}\right)^2 + \left(\frac{1}{SNR_{E_f^{(T)}}}\right)^2 + \left(\frac{1}{SNR_{E_n^{(T)}}}\right)^2 + (2L_C[\text{ppm} \cdot \text{m}])^2 \left(\frac{1}{SNR_{C_\sigma}}\right) \right. \\ &\quad + \left(\frac{1}{2C_\sigma}\right)^2 \left(2\text{cov}(E_n, E_f^{(T)}) \frac{1}{E_n} \frac{1}{E_f^{(T)}} - 2\text{cov}(E_n, E_f) \frac{1}{E_n} \frac{1}{E_f} - 2\text{cov}(E_f^{(T)}, E_n^{(T)}) \frac{1}{E_f^{(T)}} \frac{1}{E_n^{(T)}} \right) \\ &\quad + \left(\frac{1}{2C_\sigma}\right)^2 \left(2\text{cov}(E_f, E_n^{(T)}) \frac{1}{E_n^{(T)}} \frac{1}{E_f} - 2\text{cov}(E_n, E_n^{(T)}) \frac{1}{E_n^{(T)}} \frac{1}{E_n} - 2\text{cov}(E_f, E_f^{(T)}) \frac{1}{E_f^{(T)}} \frac{1}{E_f} \right) \\ &\quad - \left(\frac{1}{C_\sigma}\right)^2 L_C[\text{ppm} \cdot \text{m}] \left(\text{cov}(C_\sigma, E_f) \frac{1}{E_f} - \text{cov}(E_n, C_\sigma) \frac{1}{E_n} + \text{cov}(E_n^{(T)}, C_\sigma) \frac{1}{E_n^{(T)}} - \text{cov}(C_\sigma, E_f^{(T)}) \frac{1}{E_f^{(T)}} \right) \\ &\quad \left. + \left(\frac{1}{C_\sigma}\right)^2 \left(+\text{cov}(E_n, C_K) \frac{1}{E_n} - \text{cov}(C_K, E_f) \frac{1}{E_f} \right) \right)\end{aligned}$$

An upper bound on the covariances is given by the inequality

$$|\text{cov}(x, y)| \leq \sigma_x \sigma_y$$

so one way to proceed is to take

$$\begin{aligned}\sigma_L^2 &\leq \left(\frac{1}{2C_\sigma}\right)^2 \left(\left(\frac{1}{SNR_{E_f}}\right)^2 + \left(\frac{1}{SNR_{E_N}}\right)^2 + \left(\frac{1}{SNR_{E_f^{(T)}}}\right)^2 \right. \\ &\quad + \left(\frac{1}{SNR_{E_n^{(T)}}}\right)^2 + (2L_C[\text{ppm} \cdot \text{m}])^2 \left(\frac{1}{SNR_{C_\sigma}}\right)^2 + 4\sigma_{C_K}^2 \Bigg) \\ &\quad + \left(\frac{1}{2C_\sigma}\right)^2 \left(2\frac{\sigma_{E_n}}{E_n} \frac{\sigma_{E_f^{(T)}}}{E_f^{(T)}} - 2\frac{\sigma_{E_n}}{E_n} \frac{\sigma_{E_f}}{E_f} - 2\frac{\sigma_{E_f^{(T)}}}{E_f^{(T)}} \frac{\sigma_{E_n^{(T)}}}{E_n^{(T)}} \right) \\ &\quad + \left(\frac{1}{2C_\sigma}\right)^2 \left(2\frac{\sigma_{E_n^{(T)}}}{E_n^{(T)}} \frac{\sigma_{E_f}}{E_f} - 2\frac{\sigma_{E_n^{(T)}}}{E_n^{(T)}} \frac{\sigma_{E_n}}{E_n} - 2\frac{\sigma_{E_f^{(T)}}}{E_f^{(T)}} \frac{\sigma_{E_f}}{E_f} \right) \\ &\quad - \left(\frac{1}{C_\sigma}\right) L_C[\text{ppm} \cdot \text{m}] \left(\frac{\sigma_{E_f}}{E_f} \frac{\sigma_{C_\sigma}}{C_\sigma} - \frac{\sigma_{E_n}}{E_n} \frac{\sigma_{C_\sigma}}{C_\sigma} + \frac{\sigma_{E_n^{(T)}}}{E_n^{(T)}} \frac{\sigma_{C_\sigma}}{C_\sigma} - \frac{\sigma_{E_f^{(T)}}}{E_f^{(T)}} \frac{\sigma_{C_\sigma}}{C_\sigma} \right) \\ &\quad \left. + \left(\frac{1}{C_\sigma}\right)^2 \left(+\frac{\sigma_{E_n}}{E_n} \sigma_K - \frac{\sigma_{E_f}}{E_f} \sigma_K \right) \right)\end{aligned}\tag{9.14}$$

Again identifying SNR for each parameter

$$\begin{aligned}
 \sigma_L^2 &\leq \left(\frac{1}{2C_\sigma}\right)^2 \left(\left(\frac{1}{SNR_{E_f}}\right)^2 + \left(\frac{1}{SNR_{E_N}}\right)^2 + \left(\frac{1}{SNR_{E_f^{(T)}}}\right)^2 + \left(\frac{1}{SNR_{E_n^{(T)}}}\right)^2 \right. \\
 &\quad \left. + (2L_C[\text{ppm} \cdot \text{m}])^2 \left(\frac{1}{SNR_{C_\sigma}}\right)^2 + 4\sigma_{C_K}^2 \right) \\
 &\quad + 2 \left(\frac{1}{2C_\sigma} \right)^2 \frac{1}{SNR_{E_N}} \frac{1}{SNR_{E_f^{(T)}}} - \frac{1}{SNR_{E_N}} \frac{1}{SNR_{E_f}} - \frac{1}{SNR_{E_f^{(T)}}} \frac{1}{SNR_{E_n^{(T)}}} \\
 &\quad \left. + \frac{1}{SNR_{E_n^{(T)}}} \frac{1}{SNR_{E_f}} - \frac{1}{SNR_{E_n^{(T)}}} \frac{1}{SNR_{E_N}} - \frac{1}{SNR_{E_f^{(T)}}} \frac{1}{SNR_{E_f}} \right) \\
 &\quad - \left(\frac{1}{C_\sigma} \right) L_C[\text{ppm} \cdot \text{m}] \frac{1}{SNR_{C_\sigma}} \left(\frac{1}{SNR_{E_f}} - \frac{1}{SNR_{E_N}} + \frac{1}{SNR_{E_n^{(T)}}} - \frac{1}{SNR_{E_f^{(T)}}} \right) \\
 &\quad + \left(\frac{1}{C_\sigma} \right)^2 \sigma_K \left(+\frac{1}{SNR_{E_N}} - \frac{1}{SNR_{E_f}} \right)
 \end{aligned} \tag{9.15}$$

Chapter 10

Pulse Detection

Not done yet

Chapter 11

Background, Clutter, and Noise

In the previous chapter we assumed that all the photons collected by the receiver were generated by the interaction of the transmitter beam and the target material. This is clearly not true in practice. In this chapter we will discuss receiver techniques and the natural and sensor related causes of noise photons. Here noise is defined as any unwanted part of the signal. Noise can have electrical, optical, or environmental origins. The nature of noise depends on the desired measurement. For example, the atmospheric water vapor can be directly sensed by a lidar instrument, however, for a tomographic lidar measurement, the atmospheric water vapor signal can be considered noise. We will first treat types of environmental noise (Background, Clutter) and then treat other optical and electrical noise sources.

11.1 Detection Techniques

Lidar systems utilize some unusual detectors. The details of these detections systems and their noise properties will be discussed in section 11.5. In this section we will introduce the major concepts

11.1.1 Direct Detection

Not done yet

11.1.2 Coherent Detection

Coherent detection utilizes the concept of a heterodyne receiver that is familiar to the RADAR or RF receiver fields. The heterodyne mixes the return signal of the lidar with a “local oscillator” that is a copy of the original emitted pulse.

Mathematically, we can use the simple form

$$E_s = \operatorname{Re}(\mathcal{E}_s e^{-i\omega_s t}) = \mathcal{E}_s \cos(\omega_s t)$$

to represent the electric field of the signal and

$$E_{lo} = \operatorname{Re}(\mathcal{E}_{lo} e^{-i\omega_{lo} t}) = \mathcal{E}_{lo} \cos(\omega_{lo} t)$$

to represent the local oscillator signal. It is customary to drop the “Re” from the notation but remember that the real part is understood. By combining the two (superposition), we have an electric field at the detector

$$E_d = \mathcal{E}_s e^{-i\omega_s t} + \mathcal{E}_{lo} e^{-i\omega_{lo} t}$$

Few detectors measure the electric field, however. Solid-state detectors, and photomultipliers produce current as a function of the power delivered by the field. The power detected can be represented as

$$P = |E_d|^2 = |\mathcal{E}_s e^{-i\omega_s t} + \mathcal{E}_{lo} e^{-i\omega_{lo} t}|^2 \quad (11.1)$$

By writing out the left hand side of equation (11.1), and remembering that use the real parts of E_s and E_{lo} we obtain

$$\begin{aligned} P &= |\mathcal{E}_s e^{-i\omega_s t} + \mathcal{E}_{lo} e^{-i\omega_{lo} t}|^2 \\ &= (\operatorname{Re}(\mathcal{E}_s e^{-i\omega_s t}) + \operatorname{Re}(\mathcal{E}_{lo} e^{-i\omega_{lo} t})) ((\operatorname{Re} \mathcal{E}_s^* e^{i\omega_s t}) + (\operatorname{Re} \mathcal{E}_{lo}^* e^{i\omega_{lo} t})) \\ &= \mathcal{E}_s^2 \cos^2(\omega_s t) + \mathcal{E}_{lo}^2 \cos^2(\omega_{lo} t) + 2\mathcal{E}_s \mathcal{E}_{lo} \cos(\omega_s t) \cos(\omega_{lo} t) \\ &= \mathcal{E}_s^2 \cos^2(\omega_s t) + \mathcal{E}_{lo}^2 \cos^2(\omega_{lo} t) \\ &\quad + \mathcal{E}_s \mathcal{E}_{lo} \cos((\omega_s - \omega_{lo}) t) + \mathcal{E}_s \mathcal{E}_{lo} \cos((\omega_s + \omega_{lo}) t) \\ &= \mathcal{E}_s^2 \frac{1}{2} (1 + \cos(2\omega_s t)) + \mathcal{E}_{lo}^2 \frac{1}{2} (1 + \cos(2\omega_{lo} t)) \\ &\quad + \mathcal{E}_s \mathcal{E}_{lo} \cos((\omega_s - \omega_{lo}) t) + \mathcal{E}_s \mathcal{E}_{lo} \cos((\omega_s + \omega_{lo}) t) \end{aligned}$$

Thus we have terms with high frequency ($2\omega_s, \omega_{lo}, \omega_s + \omega_{lo}$) and one low frequency term with frequency $\omega_s - \omega_{lo}$. It is easier to build low frequency detectors or A/D converters, so one reason for employing a heterodyne is to take advantage of cheaper, lower noise technology. This is a principal reason for using coherent detectors in radios, RADAR, and Lidar. But the reasons for using a heterodyne go beyond this.

The difference frequency is usually very different than the signal or oscillator frequency. Thus the detection can happen after a notch filter is applied to the mixed signal with no contamination from the original signal or local oscillator. This ability to isolate the signal from surrounding noise sources is a great benefit

Not done yet

11.2 Background

By observing equation (3.19), we observe that the detector will be exposed to any incident radiation over the period τ_d . Thus we could write equation (3.19) as

$$E(\lambda, R) = \int_{\frac{2R}{c} - \tau_d}^{\frac{2R}{c} + \tau_d} [P(\lambda, t) + P_b(\lambda, t)] dt \quad (11.2)$$

where $P_b(\lambda, t)$ represents the background radiation. The next two sections will discuss different origins for this background radiation.

11.2.1 Solar Illumination

The Sun will illuminate the atmosphere and surface of the Earth. We will write this solar spectral radiance as $L_{sol}(\lambda)$ with units ($\text{W}^{-2} \text{cm}^{-2} \mu\text{m}^{-1} \text{sr}^{-1}$). To find the total power received by the receiver, we must integrate over the receiver solid angle, effective aperture, and band pass. We can treat the solar radiance as uniform over the acceptance angle and detector area for diffuse sources. We will make this assumption here, but we must realize that a specular reflection from a highly reflective surface may increase the background many orders of magnitude. Because the receiver is usually matched to the narrow laser line, we may often assume that the slowly varying solar spectrum is constant across the band pass as well. For Raman scattering and Fluorescence lidar this is not the case, so we will retain in our expression for the background

$$P_{b_{sol}}(\lambda, t) = \int_{\Delta\lambda_o} L_{sol}(\lambda') \xi(\lambda') \Omega_o A_o d\lambda' \quad (11.3)$$

For common detector integration times the solar radiance can be considered constant in time, therefore the radiance received by the detector will be simply $P_b(\lambda, t) \tau_d$ or

$$E_{b_{sol}}(\lambda, t) = \int_{\Delta\lambda_o} L_{sol}(\lambda') \xi(\lambda') \Omega_o A_o \tau_d d\lambda' \quad (11.4)$$

11.2.2 Thermal Background

A parcel of air or a surface will emit radiation following Planck's law modified by the emissivity of the air or surface. For the surface we can express the emitted radiance as

$$L_{therm}(\lambda) = \varepsilon(\lambda) B(T, \lambda) T(R_T, \lambda) \quad (11.5)$$

The radiance from the atmosphere can be approximated by assuming the atmosphere is made of many plane parallel layers, each with a constant temperature.[5][38] Then the contribution to the downwelled radiation due to the i th layer is given

by

$$\begin{aligned}\Delta L(\theta, \phi) &= L_{T_i} (1 - \Delta T_i) \prod_{j=1}^{i-1} \Delta T_j \\ &\simeq L_{T_i} (T_i - T_{i+1})\end{aligned}\quad (11.6)$$

The term $(1 - \Delta T_i)$ can be thought of like an emissivity. From conservation of energy we know

$$\Delta T_i + \Delta R_i + \Delta \alpha_i = 1 \quad (11.7)$$

where T is the transitivity, R is the reflectivity, and α is the absorptivity and the subscript i indicates layer number i . The reflection from a parcel of air will be negligible, thus

$$\Delta T_i + \Delta \alpha_i = 1 \quad (11.8)$$

which can be compared to Kirchhoff's rule

$$\Delta T_i + \Delta \varepsilon_i = 1 \quad (11.9)$$

Thus, we can consider

$$\Delta \varepsilon_i = (1 - \Delta T_i) \quad (11.10)$$

as the emissivity of the parcel of air.

The approximation in equation (11.6)¹ is taken in radiative transfer codes like LOTTRAN and MODTRAN.[38] The total radiance from the atmosphere is given by

$$L_{down}(\theta, \phi) = \sum_{i=1}^N L_{T_i} (T_i - T_{i+1}) \quad (11.11)$$

where N is the total number of layers and the angles (θ, ϕ) give the direction from which the radiation comes .Likewise the upwelled radiance is

$$L_{up}(\theta, \phi) = \sum_{i=N}^1 L_{T_i} (T_i - T_{i+1}) \quad (11.12)$$

Because we have assumed a semi-infinite plane parallel atmosphere we can easily calculate the total downwelled radiation.

$$L_{down} = \frac{1}{\pi} \int_{2\pi} L_{down}(\theta, \phi) \cos \theta d\Omega \quad (11.13)$$

Likewise, for the upwelled radiation

$$L_{up} = \frac{1}{\pi} \int_{2\pi} L_{up}(\theta, \phi) \cos \theta d\Omega \quad (11.14)$$

¹See derivation in [38] page 108

The downwelling radiation must be scattered back towards the detector to be important, therefore the detected radiation from emissive sources is

$$L_{therm}(\lambda) = \varepsilon(\lambda) B(T, \lambda) T(R_T, \lambda) + \rho L_{down} T(R_T, \lambda) + L_{up} \quad (11.15)$$

These terms are usually computed with a plane parallel atmospheric radiative transfer model like MODTRAN or FASCODE.[39][38] The resulting radiance must still be integrated over the detector band pass, solid angle, aperture area, and integration time

$$E_{b_{therm}}(\lambda, t) = \int_{\Delta\lambda_o} L_{therm}(\lambda') \xi(\lambda') \Omega_o A_o \tau_d d\lambda' \quad (11.16)$$

11.2.3 Scattered Laser Radiation

Not done yet

11.3 Clutter

Not done yet

11.4 Speckle

Not done yet

11.5 Optical and Electrical Noise

Not very good, see Vincent's book instead

Measures recognizes four types of noise.[3] The first three types (see table below) he calls types of *shot noise*. We have already dealt with fluctuations of the signal due to speckle and the background. In this section we will study electrical sources of noise and compare them to the optical sources. Finally we will derive expressions for the signal to noise ration (SNR).

Noise Origin	Common Name	Physical Mechanism
Optical	-	Statistical Fluctuations of the Desired Signal
Optical	Background/Clutter	Statistical Fluctuations of the Background Signal
Electrical	Dark Current	Thermally generated current (in the absence of optical signal)
Electrical	Johnson (Thermal) Noise	Thermal agitation of current carriers

Many noise sources are frequency dependent. For example, wall current in the United States of America is an alternating current wth a frequency of 60 Hz. A poor power supply may not remove all the 60 Hz oscillation in the DC output. This 60 Hz ripple in the DC voltage supplied to the detector circuit would be a

source of noise at 60 Hz. If we know the frequency of the desired signal is, say, 400 Hz, then we could use a filter to remove any signals below about 350 Hz and above 450 Hz and our 60 Hz noise would be eliminated.

Some noise sources do not occur at just one frequency. Thermal based noise, for example, may contain many frequencies. When a noise source causes noise uniformly across all frequencies, it is called “white noise” (think of mixing a uniform amount of all visible frequencies of light—the resulting color would be white). In these cases, using our filter would reduce the total amount of noise. We will describe the range of frequencies that can participate in our detection as the *bandwidth* (Δf) of our system. In our filter case above $\Delta f = 100$ Hz.[9]

11.5.1 Dark Current

Dark current is that current that flows in a photodetector in the absence of an optical signal (desired signal and background). Dark current is usually described by its DC value i_d [40]. This noise source is entirely due to the characteristics of the detector.

11.5.2 Johnson Noise

Johnson noise is generated by all resistors and is a function of the thermal environment of the electronics.

$$i_J^2 = \frac{4kT}{R} \Delta f$$

where k is Boltzmann’s constant (1.38×10^{-23} J/K), T is the temperature of the resistor (or equivalent resistance) and is in Kelvin, R is the resistance (Ohms), and Δf is the noise bandwidth in hertz[9]. To combine the noise due to two resistive elements in parallel we *rss* the two currents

$$i_{R_1+R_2}^2 = i_{R_1}^2 + i_{R_2}^2$$

If the resistances represent a detector and a load resistance, the load resistance should be as large as possible to minimize the Johnson noise on the detector resistance.

The voltage due to the Johnson noise of our parallel resistances is given by

$$v_J^2 = (i_{R_1}^2 + i_{R_2}^2) \frac{R_1 R_2}{R_1 + R_2}$$

For resistors in series the voltages are *rss’ed*

$$v_{R_1+R_2}^2 = v_{R_1}^2 + v_{R_2}^2$$

and the current is given by

$$v_J^2 = \frac{(v_{R_1}^2 + v_{R_2}^2)}{R_1 + R_2}$$

Johnson noise is also known as *thermal noise* or *Nyquist noise*.

11.5.3 Photovoltaic Sensors

Shot Noise

Ideally there is no Johnson noise in a photovoltaic detector because there is no resistance. The detector does generate noise, however, due to the random arrival rate of carriers at the photovoltaic junction[9]. It is only at the atomic or electron level that shot noise is seen. The average rate of carriers is predictable, but at the atomic level carriers arrive in “bundles.” We will state without proof that the shot noise current is given by

$$i_{\text{shot}} = \delta \dot{N} e = e \sqrt{2 \dot{N} \Delta f}$$

where $\delta \dot{N}$ is the variation in arrival rate of carriers, and e is the electron charge. Again Δf is the noise band width. If we define $I = \dot{N} e$ then

$$i_{\text{shot}}^2 = 2 I e \Delta f$$

There is a subtlety in applying this equation pointed out by Vincent.[9] The formula is valid whether the carriers are generated thermally or by photons. If the current is due to two or more independent phenomena, the noise from each must be calculated using the absolute value of the current.

Shot Noise Photon Limit Suppose we can cool the detector to the point where the only source of carriers is the arrival of photons. Then the variation in the carrier rate is due to the variation in the arrival of the photons

$$I = \eta Q A_d e$$

where η is the quantum efficiency, Q is the photon incidence, and A_d is the detector area. Then the shot noise is given by

$$i_{\text{shot}}^2 = 2 \eta Q A_d e \Delta f$$

(seems to be a factor of e that has gone missing?). Now this treatment has been to simple. In reality the photons obey Bose-Einstein statistics which have a larger fluctuation rate than was assumed here. We will fix this by multiplying the spectral photon incidence by the Bose Factor before integrating over wavelength.

$$Q(\lambda) \rightarrow Q(\lambda) \frac{e^{\frac{hc}{\lambda kT}}}{e^{\frac{hc}{\lambda kT}} - 1}$$

where h is Planck’s constant and c is the speed of light. For an ideal detector viewing under room-temperature conditions, the Bose factor is only slightly larger than one, thus this correction is often ignored and is normally not considered in noise and D^* predictions. However, because of the wavelength dependence, this factor can be larger for longwave IR detectors.

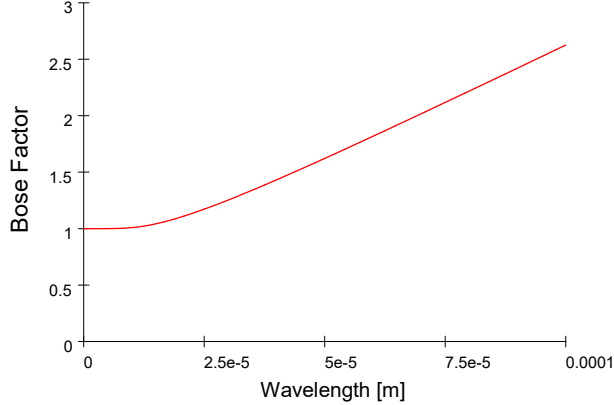


Figure 11.1:

Shot Noise Thermal Limit Now let's apply the shot noise formula to the thermally induced current.

$$I = I_s \left(\exp \left(\frac{eV}{kT} \right) - 1 \right)$$

where I_s is the saturation current

$$I_s = \frac{kT}{eR_o}$$

where R_o is the dynamic impedance or the slope of a voltage versus current plot measured at V equals zero.

$$R_o = \left(\frac{dI}{dV} \right)_{V=0}^{-1} \quad (11.17)$$

where V is the voltage and I is, of course, the current.

Here we must use the subtlety mentioned in section 11.5.3. The current is really a sum of two currents ($I_s \exp(\frac{eV}{kT})$ and $-I_s$). Thus we must use the absolute value of the current and apply the noise formula to each current separately and rss the result. This yields

$$i_{\text{shot}}^2 = 2I_s \left(\exp \left(\frac{eV}{kT} \right) + 1 \right) e\Delta f$$

Thus even though there is zero net current at zero bias voltage, the noise is not zero (and is is certainly not negative!). Using equation (11.17) we can write

$$i_{\text{shot}}^2 = \frac{4kT}{R_o} \Delta f$$

Total Photovoltaic Noise In real photovoltaic detectors there is a leakage current associated with the diode. Thus, dV/dI is lower than would be expected from the thermal current equation. The leakage current will contribute Johnson noise. We will find the total dynamic impedance

$$\frac{1}{R_{\text{total}}} = \frac{1}{R_{\text{thermal}}} + \frac{1}{R_{\text{leakage}}}$$

and

$$\begin{aligned} i_{\text{total}}^2 &= \frac{4kT}{R_{\text{thermal}}} + \frac{4kT}{R_{\text{leakage}}} = \frac{4kT}{R_{\text{total}}} \\ &= \left(2\eta Q A_d e + \frac{4kT}{R_o}\right) \Delta f \end{aligned}$$

where here R_o is the observed value of dV/dI . This equation does not include amplifier noise nor does it include $1/f$ noise. Prediction of $1/f$ noise is generally empirical.

11.5.4 Photoconductor Sensors

Generation Recombination Noise There is one more noise type that we will deal with here. In photoconductors, there is noise due to carrier generation and recombination. The randomness in this noise source comes from two different mechanisms. The carriers are generated at a random rate, and the carriers have a random lifetime. The fluctuation in carrier concentration due to generation and recombination is given by

$$d\dot{N} = \sqrt{4\dot{N}\Delta f}$$

As in the case of the photoconductor current, we derive the noise current

$$\dot{i}_{gr}^2 = 4IeG\Delta f \quad (11.18)$$

where G is the photoconductive gain term and we have a factor of (4 instead of 2)

GR Noise in the Photon Limited Limit The photoconductor current is calculated from the carrier concentration, n , the mean drift velocity, v , the electron charge, e , and the cross-sectional area, a .

$$I = nvea$$

For the photoconductor, the carrier generation rate is still

$$\dot{N} = \eta Q A_d$$

The total number of free carriers at any given time is $\dot{N}\tau$ where τ is the mean lifetime of the carriers. The quantity n is the total number of carriers divided by the volume of the material sample that makes the photoconductor.

$$n = \frac{(\eta Q A_d) \tau}{as}$$

where s is the spacing between electrodes. The drift velocity is the product of the mobility, μ , and the electric field E (the voltage across the detector divided by the interelectrode spacing s).

$$v = \mu E$$

Thus

$$I = (\eta Q A_d e) \frac{\mu \tau E}{s}$$

The photoconductive gain is expressed as

$$G = \frac{\mu \tau E}{s}$$

so we can write

$$I = (\eta Q A_d e) G$$

Using this expression we can find the photon limit noise for combination/recombination

$$i_{gr}^2 = 4\eta Q A_d e^2 G^2 \Delta f$$

again we must apply the Bose factor to the photon incidence associated with generation noise for long wavelengths, however, we must not apply the factor to recombination noise. Thus

$$4Q(\lambda) \rightarrow 2Q(\lambda) \frac{e^{\frac{hc}{\lambda kT}}}{e^{\frac{hc}{\lambda kT}} - 1} + 2Q(\lambda)$$

GR Noise in the Thermal Limit To find the GR noise in the thermal limit we would insert the equations for thermally generated currents into the noise equation for GR noise. The result is cumbersome and therefore a more empirical approach is often used. We note that the current is dominated by the number of carriers and that the noise varies as the square root of the number of carriers.[9] Carrier production increases rapidly as temperature increased beyond the background limited value. Thus, the procedure is to reduce the temperature so that thermally generated noise is negligible. Then the measured current can be inserted into equation (11.18). This procedure is valid no matter whether the current is photon generated or thermally generated.

Total Photoconductive noise The total photoconductive noise is due to GR and Johnson noise.

$$i_{\text{total}}^2 = \left(4IeG + \frac{4kT}{R} \right) \Delta f$$

In the limit of negligible thermal noise this is

$$i_{\text{total}}^2 = \left(4\eta q A_d e^2 G^2 + \frac{4kT}{R} \right) \Delta f$$

11.6 Quantization error

Not done yet

Formula for propagation of errors

$$\sigma_u^2 = \left(\frac{\partial f}{\partial x} \right)^2 \sigma_x^2 + \left(\frac{\partial f}{\partial y} \right)^2 \sigma_y^2 + 2\text{cov}(x, y) \frac{\partial f}{\partial x} \frac{\partial f}{\partial y}$$

Suppose the maximum power in each channel is the same $P = P_{\max_o} = P_{\max_w}$. The A/D is the same for both wavelengths, so this is likely true. The power in each channel is by definition some fraction of the total power range.

Our algorithm equations

$$L_C = \frac{1}{2C_\sigma} \left(\ln \frac{P_w}{P_o} \right) - C_K$$

Where:

$P_w = P(\lambda_{off}, t) = wP$ which is w times the maximum where 100 w would be the percent of P

$P_{on} = P(\lambda_{on}, t) = pP$ which is p times the maximum where 100 p would be the percent of P (p for peak, I don't want to use o as a variable). The units are inverse area. We have

$$\sigma_u^2 = \left(\frac{\partial L_C}{\partial P_w} \right)^2 \sigma_{P_w}^2 + \left(\frac{\partial L_C}{\partial P_o} \right)^2 \sigma_{P_o}^2 + 2\text{cov}(P_o, P_w) \frac{\partial L_C}{\partial P_w} \frac{\partial L_C}{\partial P_o}$$

Units of σ_u^2 are inverse area squared. The partials are

$$\begin{aligned} \frac{\partial}{\partial P_w} \left(\frac{1}{2C_\sigma} \left(\ln \frac{P_w}{P_o} \right) - C_K \right) &= \frac{1}{C_\sigma P_w} \\ \frac{\partial}{\partial P_o} \left(\frac{1}{2C_\sigma} \left(\ln \frac{P_w}{P_o} \right) - C_K \right) &= -\frac{1}{C_\sigma P_o} \end{aligned}$$

Then we have

$$\sigma_u^2 = \left(\frac{1}{C_\sigma P_w} \right)^2 \sigma_{P_w}^2 + \left(-\frac{1}{C_\sigma P_o} \right)^2 \sigma_{P_o}^2 - 2 \text{cov}(P_o, P_w) \frac{1}{C_\sigma P_w} \frac{1}{C_\sigma P_o}$$

We give the least significant bit as

$$LSB = \frac{P}{2^b}$$

and the error due to quantization as

$$\sigma_P = \frac{P}{2^b \sqrt{12}}$$

which is the LSB divided by the square root of 12

Our variance is

$$\sigma_u^2 = \left(\frac{1}{C_\sigma P_w} \right)^2 \left(\frac{P}{2^b \sqrt{12}} \right)^2 + \left(-\frac{1}{C_\sigma P_o} \right)^2 \left(\frac{P}{2^b \sqrt{12}} \right)^2 - 2 \text{cov}(P_o, P_w) \frac{1}{C_\sigma P_w} \frac{1}{C_\sigma P_o}$$

or

$$\sigma_u^2 = \left(\frac{1}{C_\sigma w P} \right)^2 \left(\frac{P}{2^b \sqrt{12}} \right)^2 + \left(-\frac{1}{C_\sigma p P} \right)^2 \left(\frac{P}{2^b \sqrt{12}} \right)^2 - 2 \text{cov}(P_o, P_w) \frac{1}{C_\sigma w P} \frac{1}{C_\sigma p P}$$

Ignore the covariance terms

$$\begin{aligned} \sigma_u^2 &= \left(\frac{1}{C_\sigma w P} \right)^2 \left(\frac{P}{2^b \sqrt{12}} \right)^2 + \left(-\frac{1}{C_\sigma p P} \right)^2 \left(\frac{P}{2^b \sqrt{12}} \right)^2 \\ &= \frac{p^2 + w^2}{12 C_\sigma^2 p^2 w^2 2^{2b}} \end{aligned}$$

11.6.1 Compare to concentration signal

Our signal is

$$L_C = \frac{1}{2C_\sigma} \left(\ln \frac{w}{p} \right) - C_K$$

For now ignore C_K .

$$L_C \sim \frac{1}{2C_\sigma} \left(\ln \frac{w}{p} \right)$$

The attenuation is mostly due to the presence of the plume, we can approximate w/p . Assume that

$$P_o \approx P_w * T_T^2.$$

where T_T^2 is the two-way target (plume) transmission. To make the numbers simple, we assume a 1 m plume and write the transmission as

$$T_T^2 = e^{-2\sigma_T \rho_a z_T C}$$

where σ_T is the target gas cross section, ρ_a is the air density, $z_T = 1$ is the plume thickness, and C is the (assumed constant) target gas concentration in *ppm*.

We have the following values

$$\begin{aligned}\sigma_T &= 6.0 \times 10^{-23} \text{ m}^2 \text{ for methane} \\ z_T &= 1 \text{ m} \\ c &= \frac{C}{1 \times 10^6} = \frac{400}{1 \times 10^6} \\ N_a &= 2.686 \cdot 10^{25} \frac{1}{\text{m}^3} \text{ (air density)}\end{aligned}$$

$$\begin{aligned}T_T^2 &= e^{-2\sigma_T N_a z_T c} \\ &= 0.30703\end{aligned}$$

and we can approximate w/p by assuming all other factors in the atmosphere are the same for both wavelengths

$$\begin{aligned}\frac{w}{p} &\approx \frac{1}{T_T^2} \\ &= e^{2\sigma_T N_a z_T c} \\ &= 1.3434\end{aligned}$$

Thus, from our model, the plume attenuates the laser power by a factor of 1.3434 for a 1 m plume of 400 ppm methane at our wavelength. If we assume that $\sigma_w = 0$, then $C_\sigma = \sigma_T = 6.0 \times 10^{-23} \text{ m}^2$ and the signal equation gives

$$\begin{aligned}L_{400ppmm} &\sim \frac{1}{2C_\sigma} (\ln(e^{2\sigma_T N_a z_T c})) \\ &= 9.84 \times 10^{21} \text{ m}^{-2} \\ &= 400.0 \text{ m} \cdot \text{ppm}\end{aligned}$$

as expected.

The error for the 400ppm-m plume

Suppose from experience we find that the wing return power is 63 percent of the maximum return power that our A/D system is able to handle.

$$w = 0.63$$

We will approximate p so we can vary the concentration

$$\begin{aligned} p &= w \exp \left(-2\sigma_T \rho_a z_T \frac{400}{1 \times 10^6} \right) \\ &= 0.19343 \end{aligned}$$

then we may write

$$\begin{aligned} \sigma_u^2 &= \frac{p^2 + w^2}{12C_\sigma^2 p^2 w^2 2^{2b}} \\ &= \frac{6.7701 \times 10^{44}}{\text{m}^4 (2^{2b})} \end{aligned}$$

Our percent error would be

$$\begin{aligned} \frac{100\sigma_u}{L_{400ppmm}} &= 100 \frac{\sqrt{\frac{6.7701 \times 10^{44}}{\text{m}^4 (2^{2b})}}}{9.8444 \times 10^{23} \text{ m}^{-2}} \\ &= \frac{3.0337 \times 10^8}{4^{\frac{1}{2}b}} \end{aligned}$$

The error for the 400ppm-m plume

suppose we have a 400ppm, 1m plume. Our model gives the following values we still have $w = 0.63$.

$$p = w \exp \left(-2\sigma_T N_a z_T \frac{400}{1 \times 10^6} \right)$$

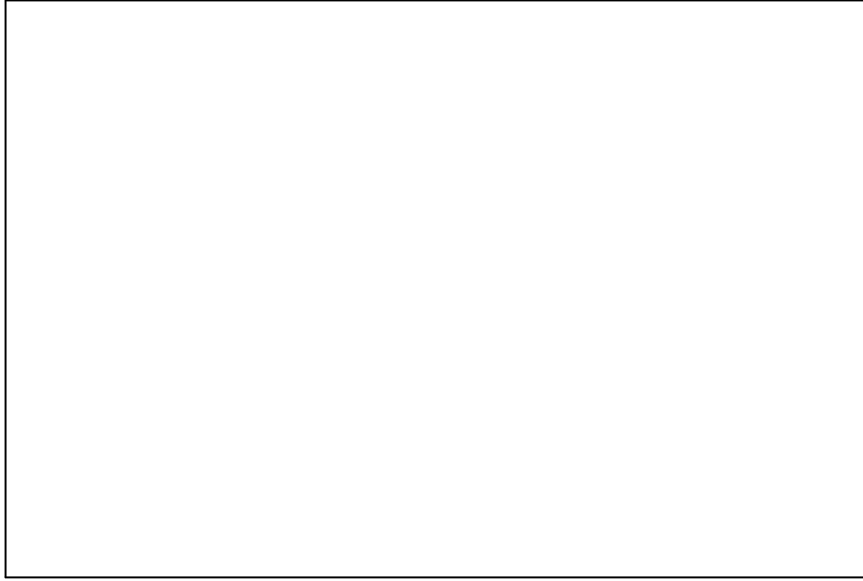
then

$$\sigma_u^2 = \frac{p^2 + w^2}{12C_\sigma^2 p^2 w^2 2^{2b}} = \frac{6.1757 \times 10^{45}}{\text{m}^4 4^b}$$

Our percent error would be

$$\frac{100\sigma_u}{L_{400ppmm}} = \frac{\sqrt{\frac{6.1757 \times 10^{45}}{\text{m}^4 4^b}}}{9.84 \times 10^{21} \text{ m}^{-2}} = \frac{7.9823}{4^{\frac{1}{2}b}}$$

Comparison, percent error



We need to find a place where for a desired bit depth we can achieve a desired error level. Lets say we want to know what size plume gives a 10% error for a 7 bit digitizer We define

$$p = w \exp \left(-2\sigma_T \rho_a z_T \frac{C}{1 \times 10^6} \right)$$

We use the form

$$\sigma_u^2 = \frac{p^2 + w^2}{12C_\sigma^2 p^2 w^2 2^{2b}}$$

and define $b = 7$

$$\begin{aligned} \sigma_u^2 &= \frac{p^2 + w^2}{12C_\sigma^2 p^2 w^2 2^{2b}} \\ &= 3.5597 \times 10^{39} (\exp(-5.904 \times 10^{-3}C) + 1.0) \frac{\exp(5.904 \times 10^{-3}C)}{m^4} \end{aligned}$$

The signal is

$$\begin{aligned} L &= \frac{1}{2C_\sigma} \left(\ln \left(\exp \left(2\sigma_T N_a z_T \frac{C}{1 \times 10^6} \right) \right) \right) \\ &= \frac{1}{2C_\sigma} \left(\left(2\sigma_T N_a z_T \frac{C}{1 \times 10^6} \right) \right) \\ &= \frac{2.4611 \times 10^{19}}{m^2} C \end{aligned}$$

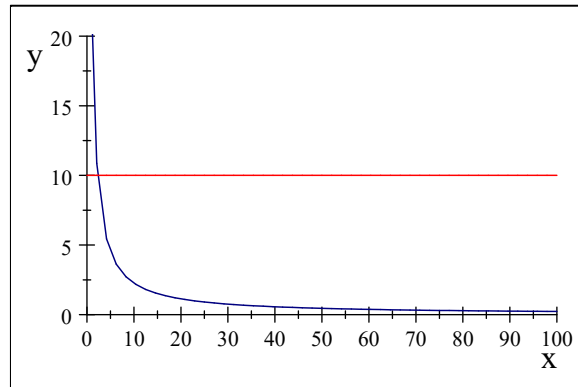
Percent error is then

$$\begin{aligned}\frac{100\sigma_u}{L} &= 100 \frac{\sqrt{3.5597 \times 10^{39} (\exp(-5.904 \times 10^{-3}C) + 1.0) \frac{\exp(5.904 \times 10^{-3}C)}{m^4}}}{\frac{2.4611 \times 10^{19}}{m^2} C} \\ &= \sqrt{58771 (\exp(-5.904 \times 10^{-3}C) + 1) \exp(5.904 \times 10^{-3}C)} \frac{1}{C}\end{aligned}$$

Now we require the percent error to be 10.

$$10 = \sqrt{58771 (\exp(-5.904 \times 10^{-3}C) + 1) \exp(5.904 \times 10^{-3}C)} \frac{1}{C}$$

This looks hard to solve in closed form, but graphically it is easy.



We see that around 10 ppm we exceed the 10% line.

Start working here, changed cross section in text above

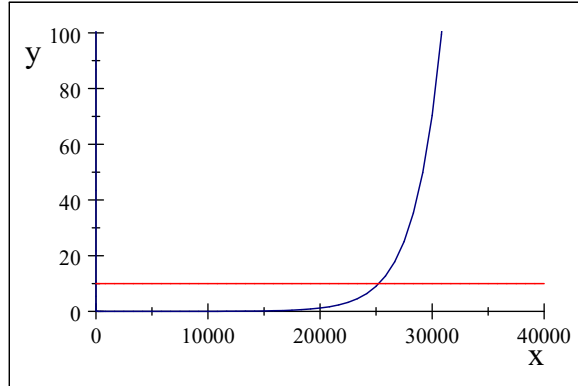
We can write out the percent error for any bit depth and concentration

$$\frac{100\sigma_u}{L} = 100 \frac{\sqrt{\frac{p^2 + w^2}{12C_\sigma^2 p^2 w^2 2^{2b}}}}{\frac{2.4611 \times 10^{19}}{m^2} C}$$

and try other bit depths, say $b = 16$

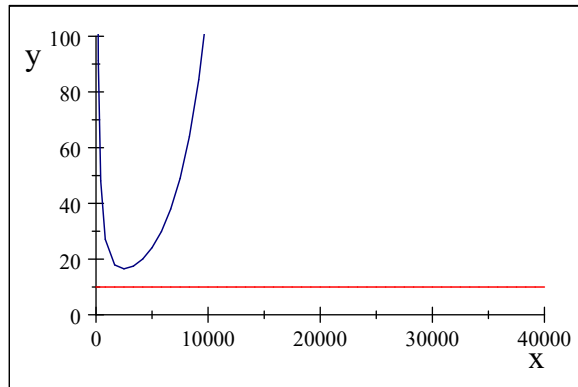
$$\frac{100\sigma_u}{L} = 3.1253 \sqrt{\exp(-8.9486 \times 10^{-4}C) + 1.0} \frac{\exp(4.4743 \times 10^{-4}C)}{C}$$

and we can again solve for a 10% error graphically



We see that 16 bits gives us over 25000 ppm but does not achieve 40000 ppm

One more example is instructive. If we have only $b = 4$ we never meet the 10% error criteria

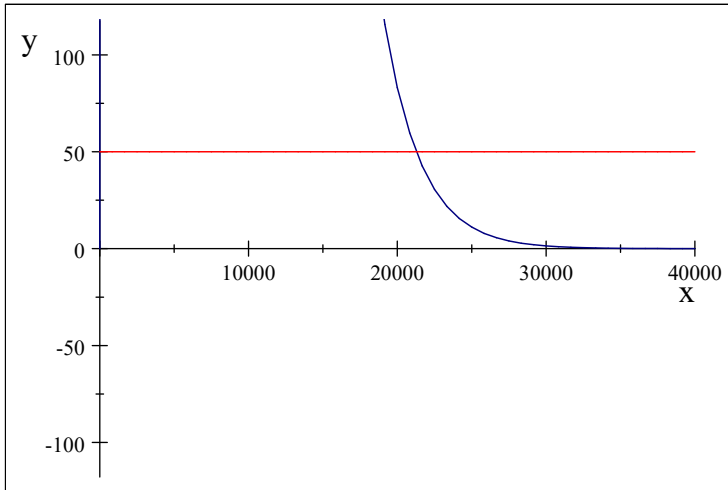


SNR calculation

We can also calculate a signal to noise ration (but remember, this if for quantization noise only!)

$$\begin{aligned} SNR &= \frac{L}{\sigma_u} = \frac{\frac{2.4611 \times 10^{19}}{m^2} C}{\sqrt{\frac{p^2 + w^2}{12C_\sigma^2 p^2 w^2 2^{2b}}}} \\ &= 31.997 \frac{C}{\sqrt{\exp(-8.9486 \times 10^{-4}C) + 1.0}} \exp(-4.4743 \times 10^{-4}C) \end{aligned}$$

we would like a SNR of, say 50



For our $b = 16$ scenario we have a SNR of 50 at about 22000 ppm-m

11.6.2 SNR

Not done yet

11.7 False Alarm Rate Calculation

It is often useful to translate the result of the error propagation to a false alarm or probability of detection. These quantities are recognized and intuitive ways to express the performance of a sensor system. This section will first develop the theory behind calculating these probabilities, and will then give an example for a systems dominated by Gaussian errors. Finally we will connect this analysis to our error analysis for Methane detection.

11.7.1 Probability of Detection Theory

We will assume a signal of the form[41][42][43]

$$y(t) = s(t) + n(t)$$

where $s(t)$ is the true signal and is deterministic and $n(t)$ is the noise which we will assume to be a zero mean random variable. Our application is detection of some target. We define two outcomes or hypothesis: H_1 that the desired target is present, and H_0 that the target is not present. We wish to find the probability of a correct decision $\mathcal{P}(C)$. The problem can be structured in terms of a null

hypothesis and a compound alternative. We write the probability of a correct decision as

$$\mathcal{P}(C) = \int \mathcal{P}(C|y) \mathcal{P}(y) dy$$

where

$$\mathcal{P}(C|y) = \frac{\mathcal{P}(C,y)}{\mathcal{P}(y)}$$

is the conditional probability distribution of C given y . The quantity $\mathcal{P}(C,y)$ is the joint distribution of C and y . Thus,

$$\begin{aligned} \mathcal{P}(C) &= \int \frac{\mathcal{P}(C,y)}{\mathcal{P}(y)} \mathcal{P}(y) dy \\ &= \int \mathcal{P}(C,y) dy \end{aligned}$$

We wish to maximize $\mathcal{P}(C)$. Since $\mathcal{P}(y) \geq 0$ the probability of a correct decision $\mathcal{P}(C)$ can be maximized by making the decision that maximizes $\mathcal{P}(C|y)$. Then an ideal decision scheme is that a target shall be determined as detected if and only if the conditional probability of a target being present given y ($\mathcal{P}(H_1|y)$) is greater than the conditional probability of no target being present given y .

$$\mathcal{P}(H_1|y) > \mathcal{P}(H_o|y)$$

In other words, given a measurement $y(t)$ the probability $\mathcal{P}(C)$ is maximized by choosing H_1 or H_o depending on whether $\mathcal{P}(H_1|y)$ or $\mathcal{P}(H_o|y)$ is larger. These conditional probabilities ($\mathcal{P}(H_1|y)$ and $\mathcal{P}(H_o|y)$) are called the *a posteriori* probabilities. They can be calculated from truth data after the measurement. We would prefer to use the *a priori* probabilities $\mathcal{P}(y|H_1)$ and $\mathcal{P}(y|H_o)$ which can be calculated from knowledge of the noise characteristics of the system before the measurement is performed. To do this we employ an theorem due to Bayes

$$\mathcal{P}(y|x) = \frac{\mathcal{P}(y)\mathcal{P}(x|y)}{\mathcal{P}(x)}$$

which, when applied, yields

$$\frac{\mathcal{P}(H_1)\mathcal{P}(y|H_1)}{\mathcal{P}(y)} > \frac{\mathcal{P}(H_o)\mathcal{P}(y|H_o)}{\mathcal{P}(y)}$$

The meaning of $\mathcal{P}(y|H_1)$ is the probability distribution of y given that we have H_1 . This is the probability distribution of the signal containing the target response. Likewise $\mathcal{P}(y|H_o)$ is the probability distribution of the signal with no target response and therefore is equal to the probability distribution of the noise alone.

We can rewrite our condition as

$$\frac{\mathcal{P}(y|H_1)}{\mathcal{P}(y|H_o)} > \frac{\mathcal{P}(H_o)}{\mathcal{P}(H_1)}$$

and define

$$\mathcal{T} = \frac{\mathcal{P}(H_o)}{\mathcal{P}(H_1)}$$

where we will find \mathcal{T} is a threshold value.[41][43]

Probability detection, false alarm, miss

We define R_1 as the region of values, $y(t)$, over which the target signal is declared to be present (that is, for which H_1 is chosen). Likewise, we define R_o as the region of values over which the target signal is declared to be absent (H_o is chosen). For any choice of the threshold \mathcal{T} , there will be a finite probability that H_o was really true, but H_1 is chosen. This gives a true value of H_o for a value of y is in R_1 . There is also a finite probability that H_1 was really true, but that H_o is chosen giving a placing y within R_o . These errors are given the names type 1 and type 2 and can be expressed as follows[41][42][43]:

Type 1 Error: The probability α that H_1 is selected but H_o is true

$$\alpha = \int_{R_1} \mathcal{P}(y|H_o) dy$$

Type 2 Error: The probability β that H_o is selected but H_1 is true

$$\beta = \int_{R_o} \mathcal{P}(y|H_1) dy$$

It is important to notice the region of integration. We identify the type 1 error as the probability of a false alarm and the type 2 error as the probability of a miss

$$\begin{aligned} \alpha & \text{ probability of false alarm, } \mathcal{P}_{fa} \\ \beta & \text{ Probability of a miss, } \mathcal{P}_{miss} \end{aligned}$$

It is customary do define the probability of detection \mathcal{P}_d , the probability of correctly declaring a target to be present

$$\mathcal{P}_d = \int_{R_1} \mathcal{P}(y|H_1) dy$$

We can write this in terms of β as

$$\begin{aligned} \mathcal{P}_d &= 1 - \int_{R_o} \mathcal{P}(y|H_1) dy \\ &= 1 - \beta \end{aligned}$$

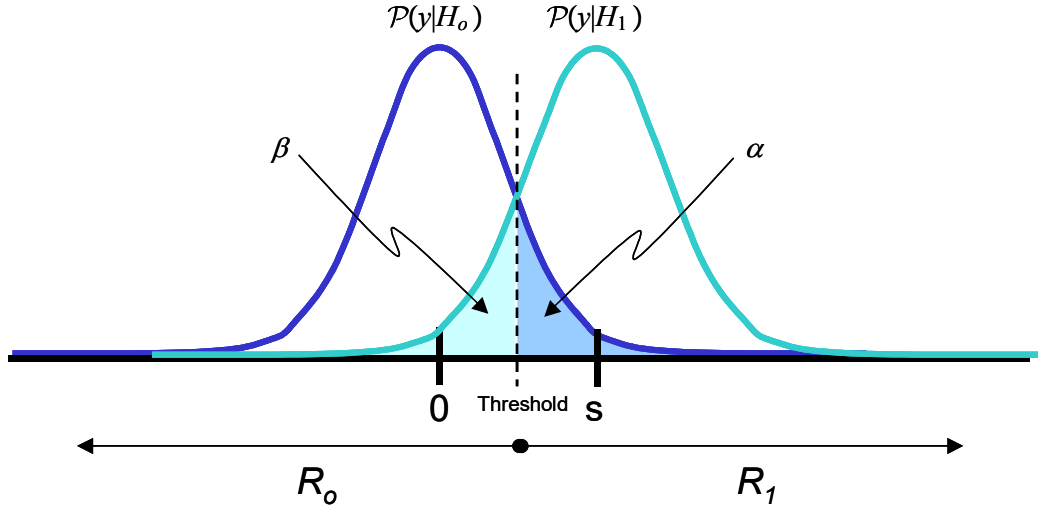


Figure 11.2: Depiction of the *a priori* probabilities and the definitions of α and β for the false alarm probability and the miss probability (see text for more detail and section 11.7.2 for the Gaussian case specifically)

Determination of threshold

There are three common systems of determining the decision criteria

1. *Bayes Criterion:* This is the optimum choice for the point of view of maximizing the probability of a correct decision. We let

$$\mathcal{T} = \frac{\mathcal{P}(H_o)}{\mathcal{P}(H_1)}$$

as we said earlier. Although this is optimum in one sense, it is not always the best choice depending on the application and the cost of a false alarms or miss. It also suffers from the need to know $\mathcal{P}(H_o)$ and $\mathcal{P}(H_1)$.

2. *Maximum Likelihood:* Choose H_1 if $\mathcal{P}(y|H_1)$ is larger than $\mathcal{P}(y|H_o)$ otherwise choose H_o . In this case the threshold value is unity.

$$\mathcal{T} = 1$$

This is equivalent to the Bayes criteria when $\mathcal{P}(H_o) = \mathcal{P}(H_1) = 1/2$. This scheme is sometimes used in communication systems where only two values are possible (1 and 0) and both are equally probable.

3 *Neyman-Pearson:* This selection scheme is more complicated, but based on quantitative evaluation. We will derive this criteria by starting with the probability of detection, \mathcal{P}_d , and use a Lagrange multiplier, η , to find a maximum[41][43].

$$\mathcal{D} = \mathcal{P}_d + \eta(\alpha - \mathcal{P}_{fa})$$

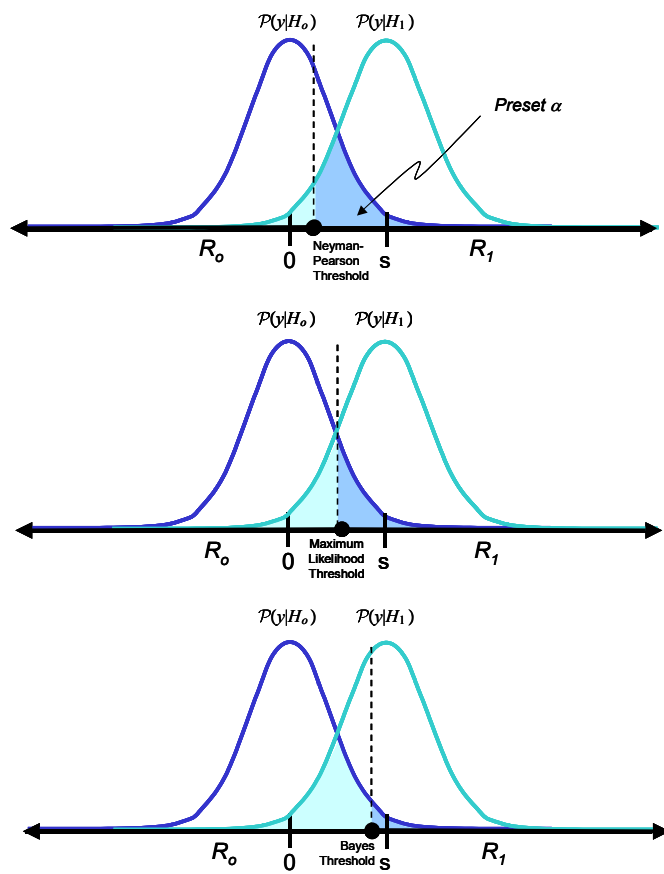


Figure 11.3: Schematics of the Three Threshold Types

where of course,

$$(\alpha - \mathcal{P}_{fa}) = 0$$

We will assume a value for α that is desired and solve for the Lagrange multiplier

$$\begin{aligned} \mathcal{D} &= \int_{R_1} \mathcal{P}(y|H_1) dy + \eta \left(\alpha - \int_{R_1} \mathcal{P}(y|H_o) dy \right) \\ &= \eta\alpha + \int_{R_1} \mathcal{P}(y|H_1) dy - \eta \int_{R_1} \mathcal{P}(y|H_o) dy \\ &= \eta\alpha + \int_{R_1} (\mathcal{P}(y|H_1) - \eta\mathcal{P}(y|H_o)) dy \end{aligned}$$

We will attempt to maximize \mathcal{D} by choosing the region R_1 . We select the range, R_1 , such that the integrand $(\mathcal{P}(y|H_1) - \eta\mathcal{P}(y|H_o))$ is positive. This gives the criteria

$$(\mathcal{P}(y|H_1) - \eta\mathcal{P}(y|H_o)) > 0$$

or rearranging we see

$$\frac{\mathcal{P}(y|H_1)}{\mathcal{P}(y|H_o)} < \eta$$

and we can identify the Lagrange multiplier as the threshold we are looking for!

$$\mathcal{T} = \eta$$

To evaluate η we define[41] $\mathcal{P}(y|H_1) \mathcal{P}(y|H_o)$

$$\Lambda(y) = \frac{\mathcal{P}(y|H_1)}{\mathcal{P}(y|H_o)}$$

$$\begin{aligned} \alpha &= \int_{\eta}^{\infty} \mathcal{P}(\Lambda(y)|H_o) dy \\ &= \int_{\eta}^{\infty} \frac{\mathcal{P}(\Lambda(y), y)}{\mathcal{P}(H_o)} dy \end{aligned}$$

Or we can just say[41][42][43]

$$\alpha = \int_{\eta}^{\infty} \mathcal{P}(y|H_o) dy$$

and solve for η .

11.7.2 Example, Gaussian noise

Here we will pause in the theoretical development to give a concrete example of these probabilities. Suppose our noise $n(t)$ is governed by Gaussian statistics, then it follows the distribution[41][42][43]

$$\mathcal{P}_n(x) = \frac{1}{\sigma\sqrt{2\pi}} \exp\left(-\frac{x^2}{2\sigma^2}\right)$$

We can use this form to write

$$\begin{aligned}\mathcal{P}(y|H_o) &= \mathcal{P}_n(y|H_o) \\ &= \frac{1}{\sigma\sqrt{2\pi}} \exp\left(-\frac{y^2}{2\sigma^2}\right)\end{aligned}$$

and

$$\begin{aligned}\mathcal{P}(y|H_1) &= \mathcal{P}_n(y|H_1) \\ &= \frac{1}{\sigma\sqrt{2\pi}} \exp\left(-\frac{(y-s)^2}{2\sigma^2}\right)\end{aligned}$$

This last equation can has the same noise statistics but has been a different mean due to the presence of the signal $s(t)$. Thus in computing $\mathcal{P}_n(y|H_1)$ we have subtracted s from y to again make $\mathcal{P}_n(y|H_1)$ a zero mean distribution.

Let's pick a value for the desired false alarm rate[41]

$$\alpha = 10^{-6}$$

For the Gaussian case we have

$$\begin{aligned}\alpha &= \int_{\eta}^{\infty} \mathcal{P}_n(y|H_o) dy \\ &= \int_{\eta}^{\infty} \frac{1}{\sigma\sqrt{2\pi}} \exp\left(-\frac{y^2}{2\sigma^2}\right) dy\end{aligned}$$

This is hard to solve analytically, we get

$$\begin{aligned}\alpha &= \frac{1}{2} - \int_0^{\eta} \frac{1}{\sigma\sqrt{2\pi}} \exp\left(-\frac{y^2}{2\sigma^2}\right) dy \\ &= \frac{1}{2} \left(1 - \text{erf}\left(\frac{\eta}{\sigma\sqrt{2}}\right)\right)\end{aligned}$$

where

$$\text{erf}(x) = \frac{2}{\sqrt{\pi}} \int_0^x e^{-t^2} dt$$

Values for the error function ($\text{erf}(x)$) are tabulated or can be found numerically. We rearrange to find

$$\text{erf}\left(\frac{\eta}{\sigma\sqrt{2}}\right) = 1 - 2\alpha$$

where in our case we have erf

$$\text{erf}\left(\frac{\eta}{\sigma\sqrt{2}}\right) = 0.999998$$

$\operatorname{erf}(x) = 0.999998$, Solution is: $\{[x = 3.361178563]\}$
which gives

$$\frac{\eta}{\sigma\sqrt{2}} = 3.361178563$$

and therefore

$$T = \eta = (3.361)\sigma\sqrt{2}$$

In this example we can write out forms for \mathcal{P}_d and \mathcal{P}_{fa} in terms of the error function

$$\begin{aligned}\mathcal{P}_d &= 1 - \int_{R_o} \mathcal{P}(y|H_1) dy \\ &= 1 - \beta\end{aligned}$$

Recall that

$$\mathcal{P}_d = \int_{R_1} \mathcal{P}(y|H_1) dy$$

and

$$\mathcal{P}(y|H_1) = \frac{1}{\sigma\sqrt{2\pi}} \exp\left(-\frac{(y-s)^2}{2\sigma^2}\right)$$

We now know that R_1 is the region from η to ∞ so we may write

$$\begin{aligned}\mathcal{P}_d &= \int_{\eta}^{\infty} \frac{1}{\sigma\sqrt{2\pi}} \exp\left(-\frac{(y-s)^2}{2\sigma^2}\right) dy \\ &= 1 - \int_0^{\eta} \frac{1}{\sigma\sqrt{2\pi}} \exp\left(-\frac{(y-s)^2}{2\sigma^2}\right) dy\end{aligned}$$

now let

$$\begin{aligned}t &= \sqrt{\frac{(y-s)^2}{2\sigma^2}} \\ t^2 &= \frac{(y-s)^2}{2\sigma^2} \\ t &= \frac{y-s}{\sigma\sqrt{2}} \\ dt\sigma\sqrt{2} &= dy\end{aligned}$$

$$\begin{aligned}
\mathcal{P}_d &= \frac{1}{2} - \int_0^{(\eta-s)/\sigma\sqrt{2}} \frac{1}{\sqrt{\pi}} \exp(-t^2) dt \\
&= \frac{1}{2} - \frac{2}{2\sqrt{\pi}} \int_0^{(\eta-s)/\sigma\sqrt{2}} \exp(-t^2) dt \\
&= \frac{1}{2} \left(1 - \operatorname{erf}\left(\frac{\eta-s}{\sigma\sqrt{2}}\right) \right) \\
&= \frac{1}{2} \left(1 + \operatorname{erf}\left(\frac{s-\eta}{\sigma\sqrt{2}}\right) \right)
\end{aligned}$$

For the false alarm rate, we have

$$\begin{aligned}
\mathcal{P}_{\text{fa}} &= \int_{\eta}^{\infty} \mathcal{P}(y|H_o) dy \\
&= \int_{\eta}^{\infty} \frac{1}{\sigma\sqrt{2\pi}} \exp\left(-\frac{y^2}{2\sigma^2}\right) dy \\
&= \frac{1}{2} - \int_0^{\eta} \frac{1}{\sigma\sqrt{2\pi}} \exp\left(-\frac{y^2}{2\sigma^2}\right) dy \\
&= \frac{1}{2} - \frac{2}{2\sqrt{\pi}} \int_0^{(\eta)/\sigma\sqrt{2}} \exp(-t^2) dt \\
&= \frac{1}{2} \left(1 - \frac{2}{\sqrt{\pi}} \int_0^{(\eta)/\sigma\sqrt{2}} \exp(-t^2) dt \right) \\
&= \frac{1}{2} \left(1 - \operatorname{erf}\left(\frac{\eta}{\sigma\sqrt{2}}\right) \right)
\end{aligned}$$

To summarize

$$\mathcal{T} = \eta = (3.361\,178\,563) \sigma\sqrt{2}$$

$$\mathcal{P}_d = \frac{1}{2} \left(1 - \operatorname{erf}\left(\frac{\eta-s}{\sigma\sqrt{2}}\right) \right)$$

$$\mathcal{P}_{\text{fa}} = \frac{1}{2} \left(1 - \operatorname{erf}\left(\frac{\eta}{\sigma\sqrt{2}}\right) \right)$$

for the assumption that $\alpha = 10^{-6}$

Equation for the range

We may revisit the question of the range of values of $y(t)$ for which we shall choose H_1 . We use the criteria derived above

$$\frac{\mathcal{P}(y|H_1)}{\mathcal{P}(y|H_o)} > \mathcal{T}$$

or

$$\frac{\mathcal{P}(y|H_1)}{\mathcal{P}(y|H_o)} > \eta$$

For the Gaussian case we have

$$\begin{aligned} \frac{\frac{1}{\sigma\sqrt{2\pi}} \exp\left(-\frac{(y-s)^2}{2\sigma^2}\right)}{\frac{1}{\sigma\sqrt{2\pi}} \exp\left(-\frac{y^2}{2\sigma^2}\right)} &> \eta \\ \exp\left(-\frac{(y-s)^2}{2\sigma^2} + \frac{y^2}{2\sigma^2}\right) &> \eta \\ \exp\left(-\frac{s^2 - 2sy + y^2}{2\sigma^2} + \frac{y^2}{2\sigma^2}\right) &> \eta \\ \exp\left(-\frac{s^2 - 2sy}{2\sigma^2}\right) &> \eta \end{aligned}$$

It is convenient to take the natural logarithm of both sides and solve for y

$$\begin{aligned} \frac{2sy - s^2}{2\sigma^2} &> \ln(\eta) \\ 2sy - s^2 &> 2\sigma^2 \ln(\eta) \\ y &> \frac{1}{2s} 2\sigma^2 \ln(\eta) + \frac{1}{2}s \end{aligned}$$

We recall that for the maximum likelihood method we had $\eta = 1$ which gives

$$y_{ml} > \frac{1}{2}s$$

For the Bayes case, we need to know $\eta = \mathcal{P}(H_1)/\mathcal{P}(H_o)$

$$y > \frac{1}{2s} 2\sigma^2 \ln\left(\frac{\mathcal{P}(H_1)}{\mathcal{P}(H_o)}\right) + \frac{1}{2}s$$

we could choose a value for and for for η , say $\mathcal{P}(H_1)/\mathcal{P}(H_o) = 2$. Then the Bayes case becomes

$$y > \frac{2\sigma^2 \ln(2)}{2s} + \frac{1}{2}s$$

In the Neyman-Pearson case $\eta = (3.361\,178\,563)\sigma\sqrt{2}$ (for our Gaussian example with $\alpha = 10^{-3}$) which yields

$$y > \frac{1}{2s} 2\sigma^2 \ln\left((3.361\,178\,563)\sigma\sqrt{2}\right) + \frac{1}{2}s$$

Example summary

For the Gaussian case, the error function $\text{erf}(x) \rightarrow 1/2$ as $x \rightarrow \infty$. Thus the value of \mathcal{P}_d can be made arbitrarily close to unity for large enough signal to noise ratio (the factor $s/(\sigma\sqrt{2})$ in the form for \mathcal{P}_d being proportional to the signal to noise ratio). This makes the Neyman-Pearson method attractive for some applications. It also allows \mathcal{P}_d to be optimized for a particular \mathcal{P}_{fa} . The maximum likelihood method has the advantage that $\mathcal{P}_d = 1 - \mathcal{P}_{fa}$ which is not true for the Neyman-Pearson or Bayes methods. The Bayes solution maximizes the probability of a correct decision, but it does this at the expense of the false alarm probability.

11.8 Connection to error analysis

Our error analysis assumes Gaussian statistics, so the connection of our calculated false alarm probability and our error analysis is simple. The following formulae apply

$$\begin{aligned}\text{erf}\left(\frac{\eta}{\sigma\sqrt{2}}\right) &= 1 - 2\alpha \\ \mathcal{P}_d &= \frac{1}{2} \left(1 - \text{erf}\left(\frac{\eta - s}{\sigma\sqrt{2}}\right) \right) \\ \mathcal{P}_{fa} &= \frac{1}{2} \left(1 - \text{erf}\left(\frac{\eta}{\sigma\sqrt{2}}\right) \right)\end{aligned}$$

where we identify

$$s = L$$

the concentration length, and

$$\sigma = \sigma_L$$

is the standard deviation of the concentration length. Note that both quantities vary with concentration and other parameters, so we won't have one false alarm probability, but rather a probability that is a function of concentration length. For methane we found

$$\sigma_L^2 = 1.5509 \times 10^{41} (\exp(-8.9486 \times 10^{-4}C) + 1.0) \frac{\exp(8.9486 \times 10^{-4}C)}{m^4}$$

$$\sigma_L = \sqrt{1.5509 \times 10^{41} (\exp(-8.9486 \times 10^{-4}C) + 1.0) \frac{\exp(8.9486 \times 10^{-4}C)}{m^4}}$$

and the signal was

$$L = \frac{2.4611 \times 10^{19}}{m^2} C$$

Then

$$\mathcal{P}_d = \frac{1}{2} \left(1 - \text{erf}\left(\frac{\eta - L}{\sigma_L\sqrt{2}}\right) \right)$$

$$\mathcal{P}_{\text{fa}} = \frac{1}{2} \left(1 - \operatorname{erf} \left(\frac{\eta}{\sigma_L \sqrt{2}} \right) \right)$$

$$\operatorname{erf} \left(\frac{\eta}{\sigma_L \sqrt{2}} \right) = 1 - 2\alpha$$

If we stick with $\alpha = 10^{-6}$ we have

$$\begin{aligned} \eta &= (3.361\,178\,563) \sigma_L \sqrt{2} \\ &= (3.361\,178\,563) \sqrt{2 \left(1.550\,9 \times 10^{41} (\exp(-8.948\,6 \times 10^{-4}C) + 1.0) \frac{\exp(8.948\,6 \times 10^{-4}C)}{m^4} \right)} \end{aligned}$$

To see how this relates to \mathcal{P}_d and \mathcal{P}_{fa} we will pick a few values of C

C	L [m $^{-2}$]	σ_L [m $^{-2}$]	η [m $^{-2}$]	\mathcal{P}_d	\mathcal{P}_{fa}
4	$9.844\,4 \times 10^{19}$	$5.574\,4 \times 10^{20}$	$2.649\,735\,103 \times 10^{21}$	$2.360\,450\,321 \times 10^{-6}$	$9.999\,999\,942 \times 10^{-7}$
40	$9.844\,4 \times 10^{20}$	$5.619\,9 \times 10^{20}$	$2.671\,373\,304 \times 10^{21}$	$9.999\,999\,942 \times 10^{-7}$	$9.999\,999\,942 \times 10^{-7}$
400	$9.844\,4 \times 10^{21}$	$6.139\,5 \times 10^{20}$	$2.918\,341\,191 \times 10^{21}$	1.0	$9.999\,999\,942 \times 10^{-7}$
4000	$9.844\,4 \times 10^{22}$	$2.390\,7 \times 10^{21}$	$1.136\,416\,678 \times 10^{22}$	1.0	$9.999\,999\,942 \times 10^{-7}$
40000	$9.844\,4 \times 10^{23}$	$2.333\,2 \times 10^{28}$	$1.109\,056\,528 \times 10^{29}$	$1.000\,208\,805 \times 10^{-6}$	$9.999\,999\,942 \times 10^{-7}$

This tells us that the false alarm rate stays low, but the probability of detection is only good for the 400 and 4000 cases. This makes sense, because the signal to noise ratio is poor for the other cases. It appears that the Neyman-Pearson criteria delivered the requested false alarm rate and may be the selection rule to use in this scenario. It is interesting to compare this to values calculated with $\alpha = 10^{-3}$

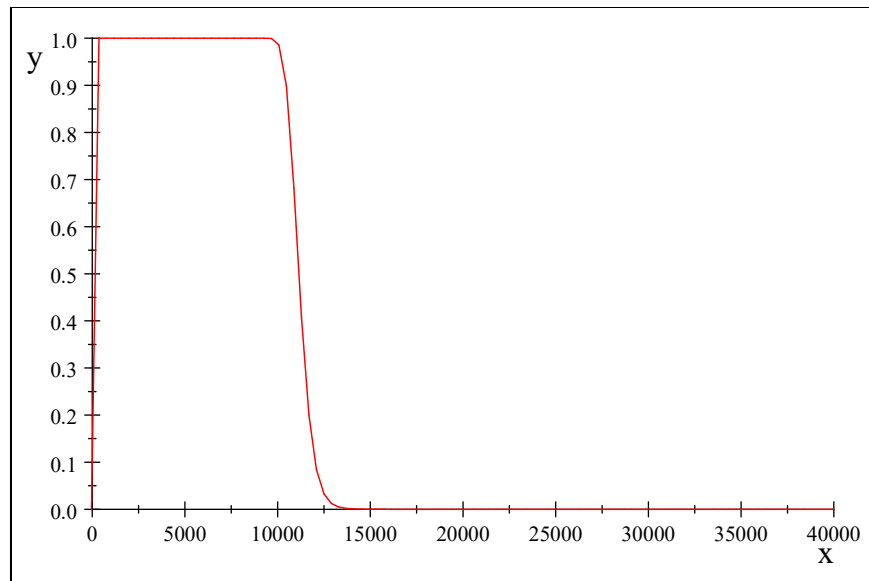
C	L [m $^{-2}$]	σ_L [m $^{-2}$]	η [m $^{-2}$]	\mathcal{P}_d	\mathcal{P}_{fa}
4	$9.844\,4 \times 10^{19}$	$5.574\,4 \times 10^{20}$	$1.722\,6 \times 10^{21}$	$1.646\,9 \times 10^{-3}$	$9.181\,4 \times 10^{-4}$
40	$9.844\,4 \times 10^{20}$	$5.619\,9 \times 10^{20}$	$1.736\,7 \times 10^{21}$	$9.035\,6 \times 10^{-2}$	$9.998\,6 \times 10^{-4}$
400	$9.844\,4 \times 10^{21}$	$6.139\,5 \times 10^{20}$	$1.897\,2 \times 10^{21}$	1.0	$1.000\,2 \times 10^{-3}$
4000	$9.844\,4 \times 10^{22}$	$2.390\,7 \times 10^{21}$	$7.387\,9 \times 10^{21}$	1.0	0.001
40000	$9.844\,4 \times 10^{23}$	$2.333\,2 \times 10^{28}$	7.21×10^{28}	$1.000\,2 \times 10^{-3}$	$1.000\,1 \times 10^{-3}$

The pattern is the same. The range of concentration values over which \mathcal{P}_d is significant is shrinking, however.

To graph \mathcal{P}_d as a function of concentration length, we will resolve all variables except C . This yields

$$\mathcal{P}_d = \frac{1}{2} - \frac{1}{2} \operatorname{erf} \left(\sqrt{2} \frac{1.680\,589\,282 \sqrt{(3.101\,8 \times 10^{41} \exp(-0.000\,894\,86C) + 3.101\,8 \times 10^{41}) e^{0.000\,894\,86C}} - 1.230\,55 \times 10^{-6}}{\sqrt{(1.550\,9 \times 10^{41} \exp(-0.000\,894\,86C) e^{0.000\,894\,86C} + 1.550\,9 \times 10^{41} e^{0.000\,894\,86C})}} \right)$$

and the plot follows.

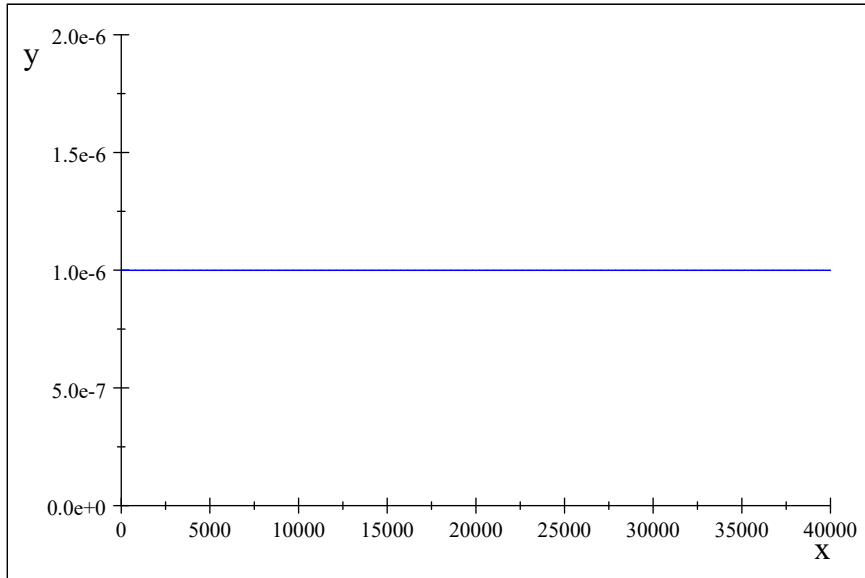


We see there is a region above about 200 ppm-m and below about 10000 ppm-m where the detection probability is 100%.

Likewise for \mathcal{P}_{fa}

$$\mathcal{P}_{fa} = \frac{1}{2} - \frac{1}{2} \operatorname{erf} \left(\frac{1.680589282}{\sqrt{(1.5509 \times 10^{41} \exp(-0.00089486C) e^{0.00089486C} + 1.5509 \times 10^{41} e^{0.00089486C})}} \right) \sqrt{2} (3)$$

and the plot follows



As we required, the probability of false alarm is uniformly 1×10^{-6} .

11.9 Geometric Form Factor

In the previous calculations, it was assumed that the geometric form factor or geometric probability factor $\xi(R, \mathbf{r}) = 1$ where the field of view of the receiver optics overlapped the laser beam and $\xi(R, \mathbf{r}) = 0$ otherwise. We also assumed the distribution of laser irradiance across the target was uniform over the area of illumination, $A_L(R)$. Often these assumptions are reasonable, and much work is done with these assumptions as stated. However, there are times when these approximations do not hold, e.g. for short range time resolved work. In this section we will look at the effects of $\xi(R, \mathbf{r})$.

We may write the laser irradiance at \mathbf{r} in the target plane located at range R from the lidar system as

$$I(R, r, \psi) = \frac{P_L T(\lambda_L, R)}{\pi W^2(R)} F(R, r, \psi) \quad (11.19)$$

where to start out, we assume azimuthal symmetry. This allows us to describe \mathbf{r} in polar coordinates (r, ψ) with the coordinate system origin at the intersection of the target plane with the axis of the receiver optics. The factor $W(R)$ represents the radius of the laser pulse in the target plane and thus $\pi W^2(R)$ is the area illuminated at range R . The factor P_L is the laser power and $T(\lambda_L, R)$ is the transmission function at the laser wavelength at range R which, for now, we assume to be independent of \mathbf{r} . The factor $F(R, r, \psi)$ represents the distribution of the laser power over the target plane at range R . Two common forms used for $F(R, r, \psi)$ are the Gaussian beam and the flat beam. The Gaussian beam

is of the form

$$F(R, r, \psi) = \exp\left(-\left(\frac{r_L}{W(R)}\right)^2\right) \quad (11.20)$$

where

$$r_L = \sqrt{r^2 + d^2 - 2rd \cos \psi} \quad (11.21)$$

and d is the separation between the laser beam axis and the receiver axis. This distribution is common for lasers operating in the TEM₀₀ mode. We shall limit our discussion to this case for Gaussian beams???. Then for this case the laser beam radius is given by

$$W(R) = \sqrt{W_o^2 + \theta^2 R^2} \quad (11.22)$$

where W_o is the laser output aperture radius and θ is the laser's half divergence angle.

The flat distribution is given by

$$F(R, r, \psi) = \mathbb{H}(R, r, \psi) \begin{cases} 1 & \text{where the receiver FOV and} \\ & \text{the laser beam overlap} \\ 0 & \text{elsewhere} \end{cases}$$

This simple form is useful for calculations for higher order mode structures but is not strictly physically realizable.

Need Picture

We assume the receiver optics are circular and describe a circular field of view in the target plane with radius

$$r_T(R) = r_0 + \phi R$$

where ϕ is the receiver have divergence angle and r_0 represents the effective radius of the telescope aperture.

If we invoke assumption 3.1.2-2, then we can use equation (3.9) and equation (11.19) to find the power received by the detector at time $t = 2R/c$.

$$\begin{aligned} P(\lambda, t) &= r_o^2 \xi(\lambda) \int_0^{R=ct/2} \frac{1}{R^2} \beta(\lambda_L, \lambda, R) T(\lambda, R) \\ &\quad \int_{r=0}^{r_T} \int_{\psi=0}^{2\pi} \xi(R, r, \psi) \frac{P_L T(\lambda_L, R)}{W^2(R)} F(R, r, \psi) r dr d\psi dR \end{aligned} \quad (11.23)$$

where we have used

$$A(R, \mathbf{r}) = \pi r_T^2$$

and thus,

$$dA(R, \mathbf{r}) = r_T dr_t d\psi$$

we have also used the fact that $A_o = \pi r_o^2$. Because we have assumed a rectangular laser pulse, P_L represents the average laser output power.

Making assumption 3.1.2-4 we can simplify this expression.

$$\begin{aligned} P(\lambda, t) &= P_L \frac{c\tau_L}{2} \frac{r_o^2}{R^2} \xi(\lambda) \beta(\lambda_L, \lambda, R) \frac{T(\lambda, R) T(\lambda_L, R)}{W^2(R)} \\ &\quad \int_{r=0}^{r_T} \int_{\psi=0}^{2\pi} \xi(R, r, \psi) F(R, r, \psi) r dr d\psi dR \end{aligned} \quad (11.24)$$

To develop this equation further we must know the details of the transmission and detection systems. Often the *effective receiver aperture* is defined to place all these details into one neat term

$$A_e(R) = \frac{A_o}{\pi W^2(R)} \int_{r=0}^{r_T} \int_{\psi=0}^{2\pi} \xi(R, r, \psi) F(R, r, \psi) r dr d\psi dR \quad (11.25)$$

which yields the form

$$P(\lambda, t) = P_L \frac{c\tau_L}{2} \frac{A_e(R)}{R^2} \xi(\lambda) \beta(\lambda_L, \lambda, R) T(\lambda, R) T(\lambda_L, R) \quad (11.26)$$

which is identical to equation (3.20), the basic scattering lidar equation, except that $A_e(R)$ has replaced the product $A_o \xi(R)$. We therefore define the geometric form factor as

$$\xi(R) = \frac{1}{A_o} A_e(R) \quad (11.27)$$

11.9.1 Simple Cases

The simplest of all cases is a coaxial lidar system with no obstructions and which has a laser beam divergence angle that is less than the opening angle of the telescope. In this case $\xi(R)$ is truly equal to one. Such a system is difficult (perhaps impossible) to achieve in practice. Common telescope designs involve secondary mirrors and supports that obstruct the primary mirror.

Another simple case is a biaxial system where the limiting aperture of the receiver is the objective mirror (or lens). We will make three critical assumptions:

- Assumption 11.9.1-1: Obstructions of the aperture are negligible
- Assumption 11.9.1-2: Laser illumination distribution is flat (uniform)
- Assumption 11.9.1-3: The target area is described by a plane
- Assumption 11.9.1-4: All apertures are circular

The first two assumptions combined cause $\xi(R, r, \psi)$ to be equal to 1 in the overlap region between the laser illumination and the field of view and zero everywhere else. Then, equation (11.27) becomes

$$\begin{aligned} \xi(R) &= \frac{1}{\pi W^2(R)} \int_{r=0}^{r_T} \int_{\psi=0}^{2\pi} \mathbb{H}(R, r, \psi) r dr d\psi dR \\ &= \frac{1}{\pi W^2(R)} \mathbb{A}(W, r_T, d) \end{aligned} \quad (11.28)$$

where $\mathbb{A}(W, r_T, d)$ is the simple *area overlap function*. The last assumption (11.9.1-3) allows us to focus on the geometry of the transmitter and receiver. For remote sensing of the atmosphere the target can usually be described by an imaginary plane at range R . For tomographic remote sensing or surface enhanced DIAL measurements, the approximation 11.9.1-3 will at some point break down.

For what follows, we will assume that the radius of the laser illumination spot is given by equation (11.22).

$$W(R) = \sqrt{W_o^2 + \theta^2 R^2} \quad (11.29)$$

From equation(11.21) we recall the laser spot illumination radius as defined in the receiver spot coordinate system is given by

$$r_L = \sqrt{r^2 + d^2 - 2rd \cos \psi} \quad (11.30)$$

The separation distance grows as a function of range and can be expressed as

$$d = d_o - R\delta \quad (11.31)$$

Need Picture

where d_o is the initial separation (at the lidar) and δ is the angle of inclination between the laser and telescope axes. Using the separation as a parameter, we will examine three cases:

1. d is so large that there is no overlap.
2. d is small enough so that either the area of the laser spot lies totally within the area of the receiver FOV or the receiver FOV lies totally within the laser spot.
3. d lies somewhere in between case one and case two

Case 1 No Overlap

In case 1 $d(R) > r_T(R) + W(R)$ and $\mathbb{A}(W, r_T, d) = 0$.

Case 2 Complete Overlap

We can summarize this case by saying $d(R) < |r_T(R) - W(R)|$. The area overlap function $\mathbb{A}(W, r_T, d) = \pi r_i^2$ where i is the smaller of $r_T(R)$ and $W(R)$.

Case 3 Partial Overlap

This case is defined by stating $|r_T(R) - W(R)| < d < r_T(R) + W(R)$. The area overlap function is given as the intersection of two circles. Measures gives this as

$$\mathbb{A}(W, r_T, d) = W^2 \psi_W + r_T^2 \psi_r - r_T d \sin \psi_r$$

where

$$\psi_W = \cos^{-1} \left(\frac{d^2 + W^2 - r_T^2}{2Wd} \right)$$

and

$$\psi_r = \cos^{-1} \left(\frac{d^2 + r_T^2 - W^2}{2r_T d} \right)$$

It should be noted that for a bistatic lidar system, all three cases described apply at some point along the lidar path.

Case 4 Simple Physical Obstructions

For a final simple case, we readdress the physical obstruction of the apertures.

11.10 Surface Reflectivity

11.11 Lambertian Surfaces

A Lambertian surface is an idealization that is useful in performing calculations, but is almost never achieved in practice. The definition of a Lambertian reflecting surface is one in which the radiant intensity follows the following form

$$I_\zeta = I_o \rho \cos \zeta \quad (11.32)$$

$$\cos \theta$$

where ζ is the angle from the normal and I_o is the intensity normal to the surface. The radiance leaving a surface is given by the standard definition

$$L_\zeta = \frac{dI_\zeta}{dA \cos \zeta} \quad (11.33)$$

where at normal incidence we would have just

$$L_o = \rho \frac{dI_o}{dA} \quad (11.34)$$

If the surface is Lambertian, then we use equation (11.32) to give

$$dI_\zeta = \rho dI_o \cos \zeta$$

and therefore

$$L_\zeta = \rho \frac{dI_o \cos \zeta}{dA \cos \zeta} = \rho \frac{dI_o}{dA} = L_o \quad (11.35)$$

Thus for a Lambertian reflector the radiance leaving a surface is constant in every direction. The reason is clear from equation (11.35). The surface area

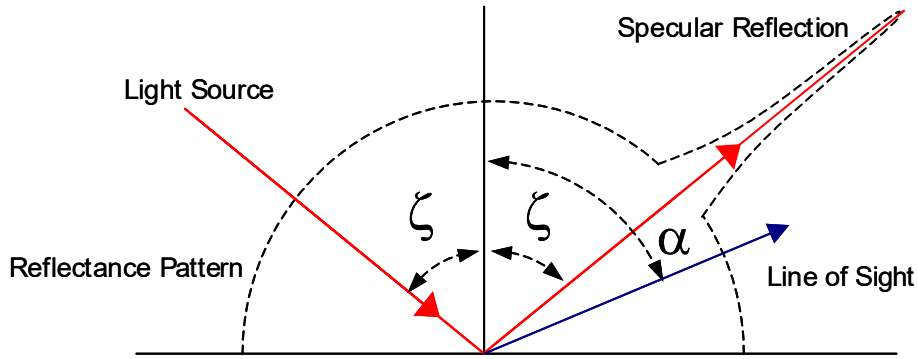


Figure 11.4:

contributing to the radiance (the area of the surface "seen") decreases as a function of the angle ζ just as the radiant intensity decreases with ζ . Thus the ratio will be constant.

As stated before, Lambertian surfaces are rarely found in practice. Man made approximations to Lambertian surface are possible by taking a smooth target surface and making it rough. Sand blasted Aluminum is a good approximation to a Lambertian reflector at visible to UV wavelengths. The Lambertian approximation is not very good for most natural surfaces. Most surfaces have a peak in the reflectance pattern due to specular reflection.

11.11.1 Non-Lambertian Surfaces

The topic of non-Lambertian covers a vast amount of research. In this treatment we will address the simplest of models and simply point to more complex treatments for the interested reader. We will start with a model due to Phong

Phong Model

The Phong model adds a specular point to the surface scattering pattern. The equation for the radiance is as follows

$$I_\zeta = I_a \rho_a + I_o (\rho_d (\cos \zeta) + \rho_s \cos^n \alpha)$$

The first term, $I_a k_a$ is the ambient contribution where I_a is the ambient incident radiant intensity and ρ_a is the ambient reflectivity. The term $I_o \rho_d (\cos \zeta)$ is the Lambertian case that we previously studied but with (smaller) reflectivity ρ_d . The last term, $I_o \rho_s \cos^n \alpha$ is the specular reflection where ρ_s is the specular reflectivity and α is the view angle specular hot point (peak of the specular reflection pattern) and the look direction.

Note that the reflectivity ρ_d must be smaller than the value we used in the Lambertian case because some of the energy that was previously evenly

distributed is now in the specular peak. We will assume that the ambient case can be ignored because it is a constant and not important for our analysis, then

$$dI_\zeta = dI_o (\rho_d (\cos \zeta) + \rho_s \cos^n (\alpha - \zeta))$$

and we can write the radiance as

$$\begin{aligned} L_\zeta &= \frac{dI_\zeta}{dA \cos \zeta} \\ &= \frac{dI_o (\rho_d (\cos \zeta) + \rho_s \cos^n (\alpha - \zeta))}{dA \cos \zeta} \\ &= \frac{dI_o \rho_d (\cos \zeta)}{dA \cos \zeta} + \frac{dI_o \rho_s \cos^n (\alpha - \zeta)}{dA \cos \zeta} \\ &= \rho_d \frac{\rho_o}{\rho_o} \frac{dI_o}{dA} + \rho_s \frac{\rho_o}{\rho_o} \frac{dI_o \cos^n (\alpha - \zeta)}{dA \cos \zeta} \\ &= \frac{\rho_d}{\rho_o} L_o + \frac{\rho_s}{\rho_o} L_o \frac{\cos^n (\alpha - \zeta)}{\cos \zeta} \\ L_\zeta &= \frac{L_o}{\rho_o} \left(\rho_d + \rho_s \frac{\cos^n (\alpha - \zeta)}{\cos \zeta} \right) \end{aligned} \quad (11.36)$$

Thus the Phong model differs from the Lambertian model by a factor of

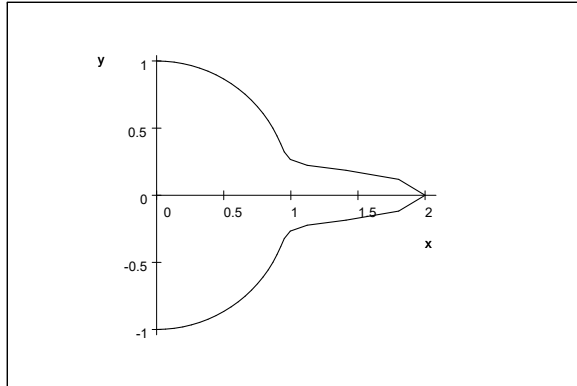
$$\frac{1}{\rho_o} \left(\rho_d + \rho_s \frac{\cos^n (\alpha - \zeta)}{\cos \zeta} \right)$$

In the simple case where $\rho_o = \rho_d = \rho_s$ then the factor is

$$\left(1 + \frac{\cos^n (\alpha - \zeta)}{\cos \zeta} \right)$$

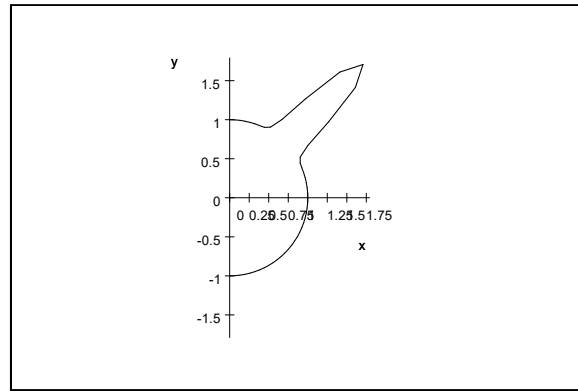
Clearly we have a maximum value for $\alpha = \zeta$. when $\zeta = 0$, we have a maximum at $\alpha = 0$ and the form of the reflectance looks like the following graph where $n = 100$.

$$\left(1 + \frac{\cos^{100} (\alpha - 0)}{\cos 0} \right)$$



For $\zeta = \pi/4$ we have

$$\left(1 + \frac{\cos^{100}(\alpha - \frac{\pi}{4})}{\cos \frac{\pi}{4}} \right)$$

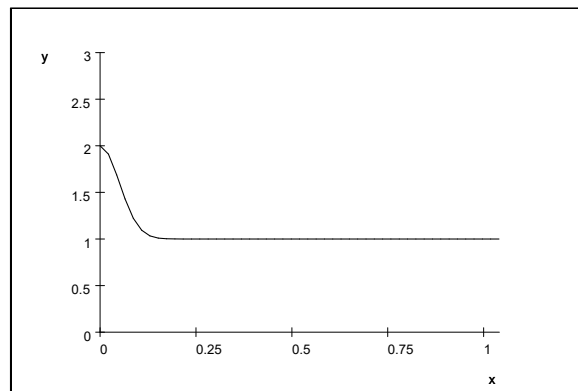


$$\int_0^\pi \frac{\cos^{100}(\alpha - \frac{\pi}{4})}{\cos \frac{\pi}{4}} d\alpha = 0.35360566$$

$$\int_0^\pi 1 da = \pi$$

Now for our case of interest, we wish to vary ζ and look at the backscatter. In a more realistic scenario, ρ_s will be much smaller than ρ_d .

$$\begin{aligned} & \left(1 + \frac{\cos^n(-2\zeta)}{\cos \zeta} \right) \\ & \left(1 + \frac{\cos^{100}(-2x)}{\cos x} \right) \end{aligned}$$



$$\frac{\pi}{3} = 1.0471976$$

$\frac{\pi}{3}$ rad = y° , Solution is: $19.098593\pi = 59.99999$

$$\lim_{x \rightarrow \frac{\pi}{2}} \left(\frac{\cos^{100}(-2x)}{\cos x} \right)$$

Not done yet

11.11.2 Cross section of a circular extended target

Related to the area of illumination from a circular aperture (see Appendix 12) is the cross section of an extended target (a hard surface, like the surface of the Earth) illuminated by the laser beam. The cross section may be written as[7]

$$d\sigma = \frac{4\pi}{\Omega} \rho dA$$

where ρ is the surface reflectivity, Ω is the scattering solid angle of the surface, and dA is the area illuminanated. The factor of 4π is the total solid angle available into which light may be scattered, and has units of sr, so the units of $d\sigma$ are length squared. The cross section of the entire illumination spot on and extend target will be

$$\sigma = \int_{A_L} \frac{4\pi}{\Omega} \rho dA$$

If we assume a Lambertian target, we can say the surface has a large solid angle of π and the total solid angle must be reduced by a factor of 2. This is because only the hemisphere above the surface is available for scattering (the light is not scattered into the ground). Thus

$$\begin{aligned} \sigma &= \int_{A_L} 2\rho dA \\ &= 2\rho A_L \end{aligned}$$

From Appendix 12 we have and equation for A_L for a circular aperture, (equation 12.2). Using this expression yields

$$\sigma = 2\pi\rho R^2\phi^2$$

For non-nadir viewing we use equating (12.16) to obtain

$$\sigma = \frac{1}{\cos\zeta} 2\pi\rho R^2\phi^2$$

11.11.3 Scattering

Not done yet

11.11.4 Light Sources

Not done yet

Chapter 12

Area of Illumination for a Circular Aperture

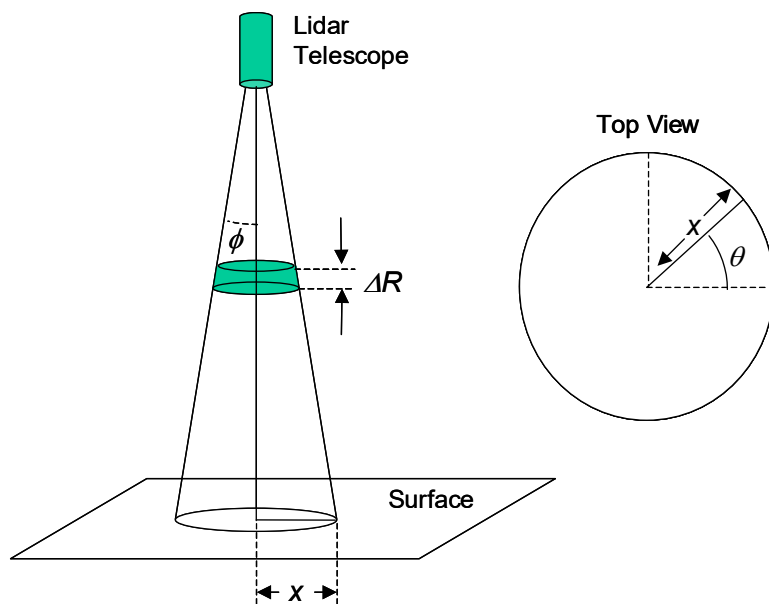


Figure 12.1: Geometry for Calculation of the Area of Illumination

Suppose the aperture is circular and the range R is large compared to the diameter of the aperture D . The laser system will illuminate a disk on a plane perpendicular to the look direction of area $A_L = \pi x^2$ where x is the radius of

the disk. Using the beam width (half angle) ϕ , we can write

$$\begin{aligned} x &= R \tan \phi \\ &\approx R\phi \end{aligned} \quad (12.1)$$

where in the last expression the fact that $\tan \phi \approx \phi$ for small values of ϕ has been used. Thus in this case

$$A_L = \pi R^2 \phi^2 \quad (12.2)$$

This is the expression that is assumed in writing the basic lidar equation in many texts

The element of area, $A_L(R, \mathbf{r})$ can be viewed as a circular ring of circumference $2\pi x$ and width dx , thus

$$\begin{aligned} dA_L(R, \mathbf{r}) &= 2\pi x dx \\ &= 2\pi R^2 \phi d\phi \end{aligned} \quad (12.3)$$

or conversely it can be written as a differential element in polar coordinates

$$\begin{aligned} dA_L(R, \mathbf{r}) &= x dx d\theta \\ &= R^2 \phi d\phi d\theta \end{aligned} \quad (12.4)$$

where (x, θ) are the polar radius and angle respectively.

12.1 Effects of the Earth's Curvature.

The fact that the Earth is curved will effect the range of a measurement. Near the earth's surface, the Earth incidence angle, ζ , is nearly equal to the sensor look angle, β , as it would be for a flat Earth. Farther from the Earth's surface, ζ becomes larger than β and the effect of curvature must be taken into account. Let us assume a spherical Earth for simplicity. Let us start by assuming β , H , and R are known (see figure 12.2). Recall that for any triangle with angles A , B , C and opposite sides a , b , c the law of sines states

$$\frac{a}{\sin A} = \frac{b}{\sin B} = \frac{c}{\sin C} \quad (12.5)$$

Then in our case,

$$\frac{R}{\sin \beta} = \frac{R+H}{\sin \delta} \quad (12.6)$$

or, by rearranging,

$$\sin \delta = \frac{R+H}{R} \sin \beta \quad (12.7)$$

But

$$\delta = \pi - \zeta \quad (12.8)$$

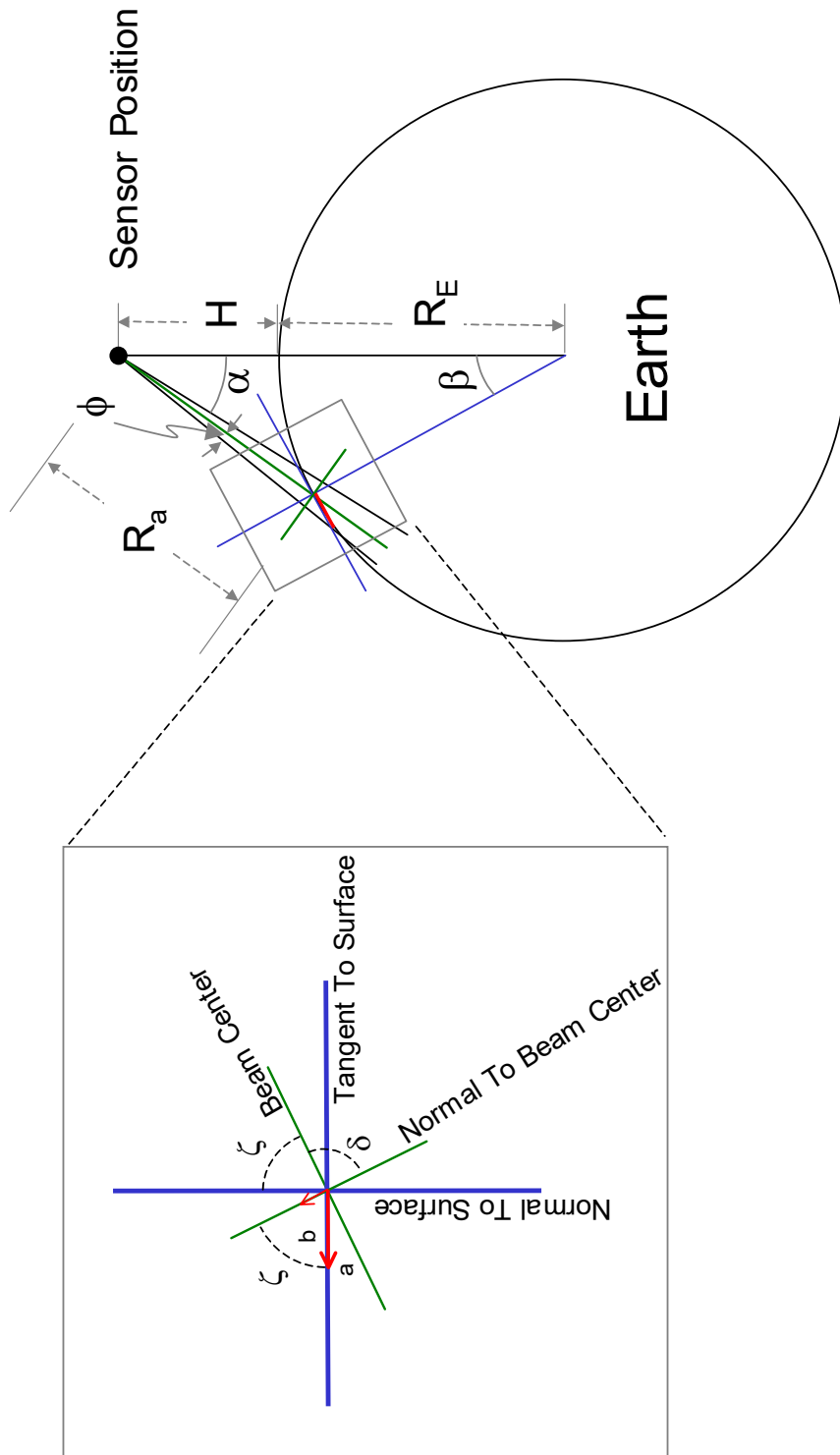


Figure 12.2:

and we recall that

$$\sin(\pi - \zeta) = \sin \zeta \quad (12.9)$$

thus,

$$\sin \zeta = \frac{R + H}{R} \sin \beta \quad (12.10)$$

So the incidence angle is given by

$$\zeta = \arcsin\left(\frac{R + H}{R} \sin \beta\right) \quad (12.11)$$

Because we know ζ and $\delta = \pi - \zeta$, we can find the angle α

$$\pi = \alpha + \beta + \delta \quad (12.12)$$

$$\alpha = \zeta - \beta \quad (12.13)$$

The range is found again using the law of sines.

$$\frac{R}{\sin \beta} = \frac{R_{arm}}{\sin \alpha} \quad (12.14)$$

12.2 Spherical Earth Sensor footprint

We now take the expression for the foot print size, equation (12.1), and apply the spherical earth model. Looking at figure 12.2, the foot print will be described by the intersection of the receiver cone (or transmitter cone, depending on design) and the Earth's surface. We can obtain an approximate expression for the area by intersecting the sensor cone with a plane tangent to the Earth's surface at the intersection of the surface and the boresight line (we pretend the Earth is locally flat). In this plane, the foot print is described by an ellipse where the semiminor axis, b , is the same length as in equation (12.1), but the semimajor axis, a , is increased by a factor of $\cos^{-1} \zeta$ or

$$a = b \frac{1}{\cos \zeta} \quad (12.15)$$

(see figure 12.2). We can describe the ellipse by its axes, a and b . The area of the ellipse will be

$$\begin{aligned} A_L &= \pi ab \\ &= \frac{\pi}{\cos \zeta} b^2 \\ &= \frac{\pi}{\cos \zeta} R^2 \tan^2 \phi \\ &\approx \frac{\pi}{\cos \zeta} R^2 \phi^2 \end{aligned} \quad (12.16)$$

thus we can write

$$\begin{aligned} dA_L &= \left(\frac{1}{\cos \zeta} \right) d\theta b db \\ &= \left(\frac{1}{\cos \zeta} \right) R^2 \phi d\phi d\theta \end{aligned}$$

As we expect, for small values of ζ , the area is close to that of a circle.

This approximation fails completely as the telescope boresight reaches the horizon, and is not applicable for sensor at extreme heights (e.g. a geosynchronous satellite). In these cases, the Earth's curvature makes the footprint more egg-shaped. At aircraft heights, this is rarely a problem for $\zeta \leq 60^\circ$ and for low flying aircraft or tower mounted equipment the approximation may be good for larger values.

The actual area of illumination will depend on the local surface roughness. This calculation has assumed the Earth's surface is flat. Such an approximation is not good in western Colorado, for example. Actual illumination, therefore, can only be calculated using detailed terrain information. The AFRL IRMA LENDER module is designed to perform such calculations.[44] The code assumes a faceted surface and calculates the illumination based on basic sensor parameters.

Chapter 13

Discussion of Solid Angle

Not done yet

Chapter 14

Using Spectral Libraries

In Progress

Spectral libraries are collections of measurement spectra representing single substances. The data is usually taken in a laboratory where the environment can be controlled. The most widely known spectral library is probably the HITRAN database produced by

14.1 Library Units

Libraries use different units to express spectral content.

Pacific Northwest National Laboratory (PNNL) gives spectra in units of absorptance.

$$\begin{aligned}\text{Absorbance} &= -\log_{10} \left(\frac{I(\nu)}{I_o(\nu)} \right) \\ &= -\log_{10} (\text{Transmission})\end{aligned}$$

Generally, it is assumed that the ideal gas law holds

$$PV = nRT$$

so that pressure can be converted to moles.

NIST uses the units $(\mu\text{mole}/\text{mole})^{-1}$. The PNNL units can be converted to NIST units through the ideal gas law.

The HITRAN[2] data base gives spectral line intensities in units of $(\text{cm}^{-1}/(\text{molecule} \cdot \text{cm}^{-2}))$ along with self and air broadened halfwidths in units of $(\text{cm}^{-1}/\text{atm})$. The spectral line intensity can be related to the absorbance through the absorption coefficient, κ . We begin with the spectral optical depth, $\tau(\nu)$.

$$\frac{I(\nu)}{I_o(\nu)} = \exp(-\tau(\nu)) = 10^{-A}$$

therefore

$$\tau(\nu) = -\ln(10^{-A(\nu)})$$

By definition

$$\tau(\nu) = \int_0^l N(z) \sigma(\nu) dz \quad (14.1)$$

where $\mathcal{L}(\nu - \nu_o)$ is the molecular line shape, and $S(z)$ is the line strength. $N(z)$ is the number density of the species at a position, z . Kyle calls this quantity the "combined absorption coefficient" [39].

We will call integrand of equation (14.1), $\kappa(\nu, z)$, the spectral absorption coefficient as a function of path length. For a single gas species, we can write

$$\begin{aligned} \kappa(\nu, z) &= \mathcal{L}(\nu - \nu_o) S(z) N(z) \\ \kappa(\nu, z) &= N(z) \sigma(\nu) \end{aligned}$$

where $N(z)$ is the number density of the gas molecules and $\sigma(\nu)$ is the cross section of a molecule. $\kappa(\nu, z)$ should have units of inverse length, and thus the cross section will have units of area. The line strength is the integration of the absorption line over wave number

$$S(z) = \int \kappa(\nu, z) d\nu$$

In principal this integration should be taken from $-\infty$ to ∞ , but in practice this is impractical because of surrounding absorption lines. The integration must be take to include as much of the line shape as is practice, however. The line strength is useful because it is relatively invariant to measurement techniques. Because it is the area under the line shape curve, the distortions due to spectrometer line shapes are integrated out of the calculation.

The lineshape function is not usually known, so a model based on physics is used in making calculations. A common model is due to Lorentz[39].

$$\mathcal{L}(\nu) = \frac{1}{\pi} \frac{\alpha}{\alpha^2 + (\nu - \nu_o)^2}$$

The parameter α is the line half width and ν_o is the line center wavenumber. This model is not sufficient to describe all broadening that will happen in a real atmosphere. At high pressure, the Doppler line shape is more accurate. The Voigt line shape combines the Lorentzian and Doppler shapes in to a more realistic model.[39] The HITRAN data base gives line widths and pressure coefficients that extend the basic Lorentzian line shape.[2]

Classically the temperature and pressure dependence of the absorption coefficient is given through the broadening of the lineshape half width.

$$\alpha(T, p) = a_o \left(\frac{p}{p_o} \right) \left(\frac{T_o}{T} \right)^{\frac{1}{2}} \quad (14.2)$$

where p_o and T_o are the reference pressure and temperature at which the half width measurement, a_o , is taken[45].

Most libraries use a standardized temperature of 296 K. If the spectra were not collected at this temperature, they are scaled or normalized to that temperature to make all data bases immediately comparable.

Source	frequency /wavelength units	spectral unit	$\Delta\nu$
PNNL	cm^{-1}	Absorbance	
HITRAN[2]	cm^{-1}	Line Intensity, Line Width, etc.	-
NIST		$(\mu\text{mole}/\text{mole})^{-1}$	

14.2 Calculation of Cross Sections

14.2.1 HITRAN[2] Cross Section Calculation

HTRAN Parameter	Units	Comments	Notation Used Here
$S_{\eta\eta'}$	$\frac{\text{cm}^{-1}}{\text{mol cm}^{-2}}$	Line Intensity	S
$\nu_{\eta\eta'}$	cm^{-1}	Line Transition Frequency	ν_o
$f(\nu, \nu_{\eta\eta'}, T, p)$	cm	Line Shape	$\mathcal{L}(\nu - \nu_o)$
u	$\frac{\text{mol}}{\text{cm}^2}$	number density per length	Nz
γ_{air}	$\frac{\text{cm}^{-1}}{\text{atm}}$	Air broadened half width	γ_a
γ_{self}	$\frac{\text{cm}^{-1}}{\text{atm}}$	Self broadened half width	γ_s
E_η	cm^{-1}	Lower state energy	E_η
n	-	temp coeffient	n
δ	$\frac{\text{cm}^{-1}}{\text{atm}}$	Air broadened pressure shift	δ
$k_{\eta\eta'}$	$\frac{\text{cm}^2}{\text{mol}}$	Monochromatic absorption coefficient	$\sigma(\nu)$
$\tau_{\eta\eta'}$	-	Optical Depth	$\tau(\nu)$
u	$\frac{\text{mol}}{\text{cm}^{-2}}$	# density per unit length	-
-	cm	length	l
-	$\frac{\text{mol}}{\text{cm}^3}$	density	N

Rothman gives the following equation (in his notation) for the optical depth.

$$\begin{aligned}\tau_{\eta\eta'}(\nu, T, p) &= uk_{\eta\eta'}(\nu, T, p) \\ &= uS_{\eta\eta'}(T)f(\nu, \nu_{\eta\eta'}, T, p)\end{aligned}$$

We may write this in our notation as

$$\tau(\nu) = (Nz)S\mathcal{L}(\nu - \nu_o)$$

or more generally,

$$\tau(\nu) = \int_0^l \mathcal{L}(\nu - \nu_o) S(z) N(z) dz$$

We know that the optical depth is given by

$$\tau(\nu) = N\sigma(\nu)l$$

$$N\sigma(\nu)l = \mathcal{L}(\nu - \nu_o)SNl$$

or

$$\sigma(\nu) = \mathcal{L}(\nu - \nu_o)S$$

which is identified as the monochromatic absorption coefficient by Rothman.

HITRAN Temperature Dependence

The HITRAN data base uses a quantum mechanical model for the temperature and pressure dependence[2] e.

Rothman *et. al.* also give a temperature dependence for the line strength, $S(z)$.

$$S = S_o \frac{Q(T_o)}{Q(T)} \frac{\exp\left(\frac{-c_2 E_\eta}{T}\right)}{\exp\left(\frac{-c_2 E_\eta}{T_o}\right)} \frac{(1 - \exp\left(\frac{-c_2 \nu}{T}\right))}{(1 - \exp\left(\frac{-c_2 \nu}{T_o}\right))}$$

where $Q(T)$ is the total internal partition sum

$$Q(T) = \sum_{\eta} g_{\eta} \exp\left(\frac{-c_2 E_{\eta}}{T}\right)$$

and where g_m is the degeneracy of state m . The factor $c_2 = hc/k$ and E_{η} is the lower state energy of the transition[2].

At temperatures that are neither extremely high nor extremely low, this simplifies to[19][46]

$$S = S_o \left(\frac{T_o}{T}\right)^j \frac{\exp\left(\frac{-c_2 E_\eta}{T}\right)}{\exp\left(\frac{-c_2 E_\eta}{T_o}\right)} \frac{(1 - \exp\left(\frac{-c_2 \nu}{T}\right))}{(1 - \exp\left(\frac{-c_2 \nu}{T_o}\right))}$$

14.3 Temperature and Pressure dependence of the Halfwidth

The functional dependence of the half width is simpler.[19][46] [2]

HITRAN also adds a pressure dependent shift parameter, δ . Thus the line shape takes the form

$$\mathcal{L}(\nu) = \frac{1}{\pi} \frac{\alpha}{\alpha^2 + (\nu - (\nu_o + p\delta))^2}$$

and where P_o and P are the gas pressure at which the halfwidth, α_o , was measured and the pressure of the plume. Likewise T_o and T are the temperature at which the halfwidth, α_o , was measured and the temperature of the plume

The HITRAN data set uses a combined air and self broadened halfwidth. In these terms the dependence is[2]

$$\alpha = \left(\frac{T_o}{T} \right)^n (\gamma_a (p - p_s) + \gamma_s p_s)$$

where γ_a is the air broadened half width, γ_s is the self broadened half width, p is the atmospheric pressure, and p_s is the target partial pressure. The value n is the *coefficient of temperature dependence*. The value of n is tabulated in the data base for each species. The classical value of n is 1/2 (see equation 14.2).

14.4 Combined Temperature Dependence

The line shape temperature and pressure dependence can be separated by substituting in our expression for the half width

$$\mathcal{L}(\nu - \nu_o) = \frac{1}{\pi} \frac{\left(\frac{T_o}{T} \right)^n (\gamma_a (p - p_s) + \gamma_s p_s)}{\left(\left(\frac{T_o}{T} \right)^n (\gamma_a (p - p_s) + \gamma_s p_s) \right)^2 + (\nu - (\nu_o - \delta p))^2}$$

Combining with the expression for S yields

$$\begin{aligned} \sigma(\nu) &= \frac{S_o}{\pi} \frac{\left(\frac{T_o}{T} \right)^n (\gamma_a (p - p_s) + \gamma_s p_s)}{\left(\left(\frac{T_o}{T} \right)^n (\gamma_a (p - p_s) + \gamma_s p_s) \right)^2 + (\nu - (\nu_o - \delta p))^2} \left(\frac{T_o}{T} \right)^j \\ &\times \frac{\exp\left(\frac{-c_2 E_\eta}{T}\right)}{\exp\left(\frac{-c_2 E_\eta}{T_o}\right)} \frac{(1 - \exp\left(\frac{-c_2 \nu_o}{T}\right))}{(1 - \exp\left(\frac{-c_2 \nu_o}{T_o}\right))} \end{aligned}$$

If we assume we are locked on the line peak, we may simplify this expression

$$\sigma_{peak} = \frac{S_o}{\pi} \frac{1}{(\gamma_a (p - p_s) + \gamma_s p_s)} \left(\frac{T_o}{T} \right)^{j-n} \frac{\exp\left(\frac{-c_2 E_\eta}{T}\right)}{\exp\left(\frac{-c_2 E_\eta}{T_o}\right)} \frac{(1 - \exp\left(\frac{-c_2 \nu_o}{T}\right))}{(1 - \exp\left(\frac{-c_2 \nu_o}{T_o}\right))}$$

Thus the temperature and pressure dependence becomes separable. We can define the multiplier for temperature using

$$M(T) = \left(\frac{T_o}{T} \right)^{j-n} \frac{\exp\left(\frac{-c_2 E_\eta}{T}\right)}{\exp\left(\frac{-c_2 E_\eta}{T_o}\right)} \frac{(1 - \exp\left(\frac{-c_2 \nu_o}{T}\right))}{(1 - \exp\left(\frac{-c_2 \nu_o}{T_o}\right))}$$

Then

$$\begin{aligned} C_{peak} &= S_o \frac{1}{\pi} \frac{1}{(\gamma_a(p - p_s) + \gamma_s p_s)} M(T) \\ &= S_o \mathcal{L}(\nu_{peak}, p) M(t) \end{aligned}$$

where the pressure dependent line peak function is defined by

$$\mathcal{L}_{peak}(p) = \frac{1}{\pi} \frac{1}{(\gamma_a(p - p_s) + \gamma_s p_s)}$$

Non reactive molecules may be less susceptible to temperature and pressure variations, but more reactive molecules (e.g. H₂O) may have larger variations. Thus we must be careful to account for the proper temperature and pressure of the gas.

14.4.1 Pressure factor $\mathcal{L}_{peak}(p)$

The concentration of methane is often given in parts per million (ppm). Let us start by considering the fraction

$$\frac{\text{number of molecules of methane}}{\text{molecules of air}}$$

This is equivalent to the mole fraction

$$\frac{\text{number of moles of methane}}{\text{number of moles of air}}$$

since a mole is just Avogadro's number of something. The concentration in ppm is given by

$$\frac{\text{number of molecules of methane}}{\text{molecules of air}} 10^6$$

The partial pressure is the mole fraction multiplied the atmospheric pressure

$$\begin{aligned} p_s &= \text{pressure} \times \text{mole fraction} \\ &= \text{pressure} \times \frac{\text{number of moles of methane}}{\text{number of moles of air}} \\ &= \text{pressure} \times C \times 10^{-6} \end{aligned}$$

where C is the concentration. Then in calculating $\mathcal{L}_{peak}(p)$ we can assume a pressure and a partial pressure by choosing the concentration in ppm

$$\begin{aligned} \mathcal{L}_{peak}(p) &= \frac{1}{\pi} \frac{1}{(\gamma_a(p - pC(10^{-6})) + \gamma_s pC(10^{-6}))} \\ &= \frac{1}{\pi p} \frac{1}{(\gamma_a(1 - C10^{-6}) + \gamma_s C10^{-6})} \\ &= \frac{1}{\pi p} \frac{1}{(\gamma_a + 10^{-6}C(\gamma_s - \gamma_a))} \end{aligned}$$

Thus the peak line width value is inverse proportional to the pressure. The dependence on concentration is not as strong and can often be ignored.

14.5 Example: Methane Cross Section

14.5.1 Input Data

We will use the HITRAN[2] data base. We will assume a plume with a pressure of 1 atm and a temperature of 296 K. We will treat the air/methane mixture as a mixture of just two species, with air defined by some "average molecule" that represents the average molecular weight of the atmospheric constituent gases weighted by their relative abundance. The temperature dependence of the cross section drops out because of our use of $T = 296$ K, the standard temperature for most spectral data bases, but other temperatures can be used by running HAWKS[2] software. The data used are as follows

$C = \frac{100}{1 \times 10^6}$	Concentration in ppm
$P = 1$ atm	Reference pressure
$T = 296$ K	Reference temperature
$t = 296$ K	Actual temperature
$p = 1$ atm	Actual pressure
$p_s = CP$	Partial pressure of Methane
ν	Wavenumber of interest
$\nu_o = \frac{1}{\lambda} = \frac{2916.302\,129}{\text{cm}}$	Line Peak
$\lambda = 3.429 \times 10^{-4}$ cm	Line Peak in wavelength units
$\delta = -0.0044 \frac{\text{cm}^{-1}}{\text{atm}}$	Air broadened pressure shift
$\nu_p = \nu_o + \delta p$	Air broadened peak shift
$S = 1.22 \times 10^{-20} \frac{\text{cm}^{-1}}{\text{mol cm}^{-2}}$	from Hawks (must account for temperature dependence)
$\gamma_a = 0.0427 \frac{\text{cm}^{-1}}{\text{atm}}$	Air broadened half-width
$\gamma_s = 0.063 \frac{\text{cm}^{-1}}{\text{atm}}$	Self broadened halfwidth
$n = 0.75$	Coefficient of temperature dependence of the air broadened half width

14.5.2 Halfwidth

The halfwidth is given by[2]

$$\alpha = \left(\frac{T}{t} \right)^n (\gamma_a (p - Cp) + \gamma_s Cp) = \frac{4.2702 \times 10^{-2}}{\text{cm}}$$

and the linewidth shape is given by[2]

$$\mathcal{L} = \frac{1}{\pi} \frac{\alpha}{\alpha^2 + (\nu - \nu_o - \delta p)^2}$$

14.5.3 Cross Section

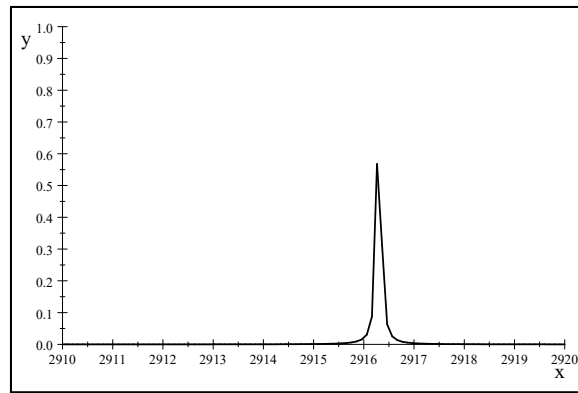
This yields a cross section of

$$\begin{aligned}
 \sigma &= S \frac{1}{\pi} \frac{\alpha}{\alpha^2 + (\nu - \nu_o - \delta p)^2} \\
 &= \frac{5.2096 \times 10^{-22}}{\pi \left(\frac{1.8235 \times 10^{-3}}{\text{cm}^2} + (\nu - \frac{2916.3}{\text{cm}})^2 \right)} \\
 &= \frac{5.2096 \times 10^{-22}}{\pi \left(1.8235 \times 10^{-3} + (\nu [\text{cm}^{-1}] - 2916.3)^2 \right)} \text{ cm}^{-2}
 \end{aligned}$$

14.5.4 Max at ν_p

$$\sigma_o = S \frac{1}{\pi} \frac{\alpha}{\alpha^2 + (\nu_p - \nu_o - \delta p)^2} = 9.0683 \times 10^{-20} \text{ cm}^2$$

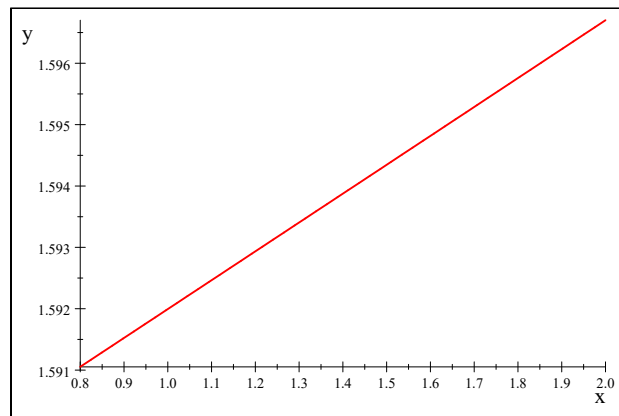
Normalized Plot



14.5.5 Pressure variation at ν_o

$$S \frac{1}{\pi} \frac{\alpha}{\alpha^2 + (\nu_o - \nu_o - \delta p)^2} = \frac{8.9986 \times 10^{-20}}{p}$$

Normalized pressure variation



14.5.6 PMNNL Cross Section Calculation

The PNNL cross section has the following temperature dependence

$$\sigma = 4.033 \times 10^{-16} \text{ cm}^2 A \left[\frac{1}{\text{ppm} \cdot m} \right] \frac{T [\text{K}]}{296.14 \text{ K}}$$

The Set Counter Was Here

Appendix A: Conversion from concentration in ppm to molecules/Vol

Lets say that the air has an "average" molecular weight. Then we can say that

$$n = \frac{m}{\bar{M}}$$

where m is the total mass and \bar{M} is the average molecular weight. We also know that n is the number of moles of the gas we have so it is also given by

$$n = \frac{\text{molecules}}{N_A}$$

From the ideal gas law we know that

$$n = P \frac{V}{RT}$$

we can rewrite this as

$$\frac{\text{molecules}}{N_A} = P \frac{V}{RT}$$

and then rearrange to get molecules per unit volume

$$\frac{\text{molecules}}{V} = \frac{N_A P}{RT}$$

A.1 DATA

$$R = 8.2057 \times 10^{-2} \frac{\text{latm K}^{-1}}{\text{m}}$$

The parameter N_a varies with temperature and pressure. If we approximate this variation with the ideal gas law we obtain.

$$pV = NkT$$

we find

$$\begin{aligned} N_a &= \frac{N}{V} = \frac{p}{kT} = \frac{(1 \text{ atm})}{(1.381 \times 10^{-23} \frac{\text{J}}{\text{K}})(273.15 \text{ K})} \\ &= 2.6861 \times 10^{25} \frac{1}{\text{m}^3} \\ \frac{(1 \text{ atm})}{(1.381 \times 10^{-23} \frac{\text{J}}{\text{K}})(296 \text{ K})} &= \frac{2.4787 \times 10^{25}}{\text{m}^3} \end{aligned}$$

A.2 Calculations

I have a published value at STP for air density so let's try to duplicate it.

$$T = 273.15 \text{ K}$$

$$P = 1 \text{ atm}$$

$$\begin{aligned} \frac{\text{molecules}}{V} &= \frac{N_A P}{RT} \\ &= 2.6858 \times 10^{22} \frac{\text{m}}{\text{l}} \frac{1}{1000 \text{ ml}} \\ &= 2.6858 \times 10^{19} \frac{\text{m}}{\text{ml}} \end{aligned}$$

The published value is (http://pas.ce.wsu.edu/CE341/air_comp.htm)

$$2.69 \times 10^{19} \frac{\text{m}}{\text{cm}^3} @ \text{STP}$$

The same publication has a value at $T = 298 \text{ K}$ so lets try to get that one.

$$T = 298 \text{ K}$$

$$P = 1 \text{ atm}$$

$$\begin{aligned} \frac{\text{molecules}}{V} &= \frac{N_A P}{RT} = \\ &= 2.4619 \times 10^{22} \frac{\text{m}}{\text{l}} \frac{1}{1000 \text{ ml}} \\ &= 2.4619 \times 10^{19} \frac{\text{m}}{\text{ml}} \end{aligned}$$

$$2.46 \times 10^{19} \frac{\text{m}}{\text{cm}^3} @ 298 \text{ K and } 1 \text{ atm}$$

The HITRAN data are all at 296 K so once again

$$T = 296 \text{ K}$$

$$P = 1 \text{ atm}$$

$$\begin{aligned} \frac{\text{molecules}}{V} &= \frac{N_A P}{RT} \\ &= 2.4785 \times 10^{22} \frac{m}{l} \frac{l}{1000 \text{ ml}} \\ &= 2.4785 \times 10^{19} \frac{m}{\text{ml}} \\ 2.4785 \times 10^{19} \frac{1}{\text{ml}} \frac{1 \text{ ml}}{1 \text{ cm}^3} &= \frac{2.4785 \times 10^{19}}{\text{cm}^3} = \frac{2.4785 \times 10^{19}}{\text{cm}^3} = \frac{2.4785 \times 10^{25}}{\text{m}^3} \end{aligned}$$

I think this is the value we should use.

A.3 Conversion from ppm to #mol/V

To get the concentration of methane, we multiply the air concentration by the relative concentration in ppm

$$C [\#/V] = \frac{C [\text{ppm}]}{1 \times 10^6} \frac{\text{molecules}}{V}$$

Appendix B: Poisson Statistics

The Poisson distribution is given by

$$P(x, \lambda) = \frac{e^{-\lambda} \lambda^x}{x!} \quad (\text{A.3})$$

where in this case λ is the mean of the distribution. The cumulative distribution is given by

$$C(x, \lambda) = \sum_{k=0}^x \frac{e^{-\lambda} \lambda^k}{k!} \quad (\text{A.4})$$

This distribution is the probability that the variable takes a value less than or equal to x .

For many applications it is desired to know if a detector will receive more than one photon. To calculate this it is best to first calculate the probability that there will be no photons detected

$$P(0, \lambda) = e^{-\lambda} \quad (\text{A.5})$$

Then the probability that there will be one or more photon is

$$1 - P(0, \lambda) = 1 - e^{-\lambda} \quad (\text{A.6})$$

Now suppose we have an array of photons. If the beam of incident photons is uniform across its cross section, we can say that each pixel will have the same mean number of photons incident (the same value of λ). Then if we have N pixels the mean number of pixels that have more than one photon is given by

$$(1 - e^{-\lambda}) N \quad (\text{A.7})$$

In the more difficult case of a Gaussian beam, the probability of an individual detector receiving one or more photons is dependent on the location of that detector within the cross section of the beam. The mean, λ , would change for each detector in the array.

Note: we could use the cumulative distribution to calculate the probability of having one or more photons incident on the detector, but there is a danger that as λ gets large, $\exp(-\lambda)$ gets small as λ^x gets big and round-off error can cause error in the calculation.

Appendix C: Glossary

B.1 Basic Suffixes in Radiometry

The suffix *-ion* signifies a process. E.g. emission, transmission.

The suffix *-ance* signifies a property of a particular material sample. E.g absorptance, emittance.

The suffix *-ivity* indicates a material property of an idealized generic substance. E.g. emissivity, reflectivity. Note that reflectance and reflectivity are often used interchangeable, but do have subtle difference in meaning.

An example will help show the distinctions. Absorptance is the percentage of the incident energy which is absorbed due to the process of absorption.

B.2 General Glossary

Bibliography

- [1] P. W. Milonni and J. H. Eberly, *Lasers*. NY: John Wiley & Sons, 1988.
- [2] L. S. Rothman, C. P. Rinsland, A. Goldman, S. T. Massie, D. P. Edwards, J. Flaud, A. Perrin, C. Camy-Peyret, V. Dana, J. Mandin, J. Schroeder, A. McCann, R. R. G. nad R. B Wattson nad K. Yoshino, K. V. Chance, K. W. Jucks, L. R. Brown, V. Nemtchinov, and P. Varanasi, “The HITRAN molecular spectroscopic database and HAWKS (HITRAN atmospheric workstation): 1996 edition,” *Journal of Quantitative Spectroscopy and Radiative Transfer*, vol. 60, pp. 665–710, 1998.
- [3] R. M. Measures, *Laser Remote Sensing: Fundamentals and Applications*. NY: John Wiley & Sons, 1984.
- [4] J. D. Jackson, *Classical Electrodynamics*. New York: John Wiley & Sons, 2nd ed., 1975.
- [5] K.-N. Liou, *An Introduction to Atmospheric Radiation*. NY: Academic Press, 1980.
- [6] R. T. Lines and G. H. Goedecke, “Scattering by irregular homogeneous particles using a variational Green function algorithm,” *Applied Optics*, Submitted 1999.
- [7] A. V. Jelalian, *Laser Radar Systems*. Norwood, MA: Artech House, 1992.
- [8] G. W. Kamerman, *Advanced Coherent Laser Radars: Short Course Notes SPIE's 14th Annual Internation Symposium on Aerospace Defense Sensing, Simulation and Controls, 24-28 April*. Orlando, Florida: SPIE, 2000.
- [9] J. D. Vincent, *Fundamentals of Infrared Detector Operation & Testing*. NY: John Wiley & Sons, 1990.
- [10] W. C. Priedhorsky, R. C. Smith, and C. Ho, “Laser ranging and mapping with a photon-counting detector,” *Applied Optics*, vol. 35, pp. 441–452, January 1996.
- [11] C. Ho, K. L. Albright, A. W. Bird, J. Bradley, D. E. Casperson, M. Hindman, W. C. Priedhorsky, W. R. Scarlett, R. C. Smith, J. Theiler, and S. K.

- Wilson, "Demonstration of literal three-dimensional imaging," *Applied Optics*, vol. 35, pp. 1833–1840, March 1999.
- [12] M.-C. Amann, T. Bosch, M. Lescure, R. Myllyliä, and M. Rioux, "Laser ranging: A critical review of unusual techniques for distance measurement," *Optical Engineering*, vol. 40, pp. 10–19, January 2001.
- [13] B. R. Foy, B. D. McVey, R. R. Petrin, J. J. Tiee, and C. W. Wilson, "Remote mapping of vegetation and geological features by lidar in the 9-11 μm region," *Applied Optics*, vol. 40, pp. 4244–4352, August 2001.
- [14] E. E. Remsberg and L. L. Gordley, "Analysis of differential absorption lidar from the space shuttle," *Applied Optics*, vol. 17, pp. 624–630, February 1978.
- [15] G. Megie and R. T. Menzies, "Complementarity of UV and IR differential absorption lidar for global measurements of atmospheric species," *Applied Optics*, vol. 19, pp. 1173–1183, April 1980.
- [16] G. J. Megie, G. Ancellet, and J. Pelon, "Lidar measurements of ozone vertical profiles," *Applied Optics*, vol. 24, pp. 3454–3463, November 1985.
- [17] E. V. Browell, A. F. Carter, S. T. Shipley, R. J. Allen, C. F. Butler, M. N. Mayo, J. H. Siviter Jr., and W. M. Hall, "NASA multipurpose airborne DIAL system and measurements of ozone and aerosol profiles," *Applied Optics*, vol. 22, pp. 522–534, October 1983.
- [18] G. Ehret, K. P. Hoinka, J. Stein, A. Fix, C. Kiemle, and G. Poberaj, "Low stratospheric water vapor measured by and airborne DIAL," *Journal of Geophysical Research*, vol. 104, pp. 31351–31359, December 1999.
- [19] S. Ismail and E. V. Browell, "Airborne and spaceborne lidar measurements of water vapor profiles: A sensitivity analysis," *Applied Optics*, vol. 28, pp. 3603–3606, September 1989.
- [20] T. Fukuchi, T. Fujii, N. Goto, K. Nemotoi, and N. Takeuchi, "Evaluation of differential absorption lidar (DIAL) measurement error by simultaneous DIAL and null profiling," *Optical Engineering*, vol. 40, pp. 141–145, March 2001.
- [21] E. E. Uthe, J. M. Livingston, and N. B. Nielsen, "Airborne lidar mapping of ozone concentrations during the lake michigan ozone study," *Journal of the Air Waste Management Association*, vol. 42, pp. 1313–1318, 1992.
- [22] C. Kiemle, G. Ehret, and A. Giez, "Estimation of boundary layer humidity fluxes and statistics from airborne differential absorption lidar (DIAL)," *Journal of Geophysical Research*, vol. 104, pp. 29189–29203, December 1999.

- [23] R. M. Schotland, "Errors in the lidar measurement of atmospheric gases by differential absorption," *Journal of Applied Meteorology*, vol. 13, pp. 71–77, February 1974.
- [24] G. Megie, "Mesure de la pression et de la temperature atmospheriques par absorption differentielle lidar: Influence de la largeur demission laser," *Applied Optics*, vol. 19, pp. 34–43, January 1980.
- [25] W. B. Grant, "Effect of differential spectral reflectance on DIAL measurements using topographic targets," *Applied Optics*, vol. 21, pp. 2390–2394, July 1982.
- [26] E. V. Browell, S. Ismail, and B. E. Grossmann, "Temperature sensitivity of differential absorption lidar measurements of water vapor in the 720-nm region," *Applied Optics*, vol. 30, pp. 1517–1524, April 1991.
- [27] P. F. Ambrico, A. Amodeo, P. D. Girolamo, and N. Spinelli, "Sensitivity analysis of differential absorption lidar measurements in the mid-infrared region," *Applied Optics*, vol. 39, pp. 6847–6865, December 2000.
- [28] V. Wulfmeyer and J. Bosenberg, "Ground-based differential absorption lidar for water-vapor profiling: Assessment of accuracy, resolution, and meteorological applications," *Applied Optics*, vol. 37, pp. 3825–3844, June 1998.
- [29] T. Fukuchi, N. Gogo, T. Fujii, and K. Nemoto, "Error analysis of SO₂ measurement by multiwavelength differential absorption lidar," *Optical Engineering*, vol. 38, pp. 141–145, January 1999.
- [30] T. Fukuchi, T. Nayuki, N. Cao, T. Fujii, K. Nemoto, H. Mori, and N. Takuchi, "Differential absorption lidar system for simultaneous measurement of O₃ and NO₂ system development and measurement error estimation," *Optical Engineering*, vol. 42, pp. 98–104, January 2003.
- [31] C. Cahen and G. Megie, "A spectral limitation of the range resolved differential absorption lidar technique," *Journal of Quantitative Spectroscopy and Radiative Transfer*, vol. 25, pp. 151–157, 1981.
- [32] N. Cao, T. Fujii, T. Fukuchi, N. Gogo, K. Nemoto, and N. Takuchi, "Estimation of differential absorption lidar measurement error for NO₂ profiling in the lower troposphere," *Optical Engineering*, vol. 41, pp. 98–104, January 2002.
- [33] R. L. Byer and M. Garbuny, "Pollutant detection by absorption using Mie scattering and topographic targets as retroreflectors," *Applied Optics*, vol. 12, pp. 1496–1505, July 1973.
- [34] E. V. Browell, S. Ismail, and W. B. Grant, "Differential absorption lidar (DIAL) measurements from air and space," *Applied Physics B*, vol. 67, no. 4, pp. 399–410, 1988.

- [35] A. Ben-David, S. L. Emery, S. W. Gotoff, and F. M. D'Amico, "High pulse repetition frequency, multiple wavelength, pulsed CO₂ lidar system for atmospheric transmission and target reflectance measurements," *Applied Optics*, vol. 31, pp. 4224–4232, July 1992.
- [36] P. V. Cvijin, D. Ignatijevic, I. Mendas, M. Sreckovic, L. Pantani, and I. Pippi, "Reflectance spectra of terrestrial surface materials at CO₂ laser wavelengths: Effects on DIAL and geological remote sensing," *Applied Optics*, vol. 26, pp. 4323–4329, October 1987.
- [37] N. S. Prasad and A. R. Geiger, "Remote sensing of propane and methane by means of a differential absorption lidar by topographic reflection," *Optical Engineering*, vol. 35, pp. 1105–1111, April 1996.
- [38] J. R. Schott, *Remote Sensing: The image Chain Approach*. NY: Oxford University Press, 1997.
- [39] T. G. Kyle, *Atmospheric Transmission, Emission and Scattering*. NY: Pergamon Press, 1991.
- [40] RCA, *Electro-Optics Handbook*. Harrison, NJ: RCA Commercial Engineering, 1974.
- [41] N. Mahanty, *Signal Processing: Signals, Filtering, and Detection*. NY: van Nostrand Reinhold Co., 1987.
- [42] J. Minkoff, *Signals, Noise, and Active Sensors*. NY: John Wiley & Sons, 1992.
- [43] S. M. Kay, *Fundamentals of Statistical Signal Processing Volume II Detection Theory*. Upper Saddle River, New Jersey: Prentice Hall PTR, 1998.
- [44] N. Research, *IRMA 4.1 Users Manual*. Eglin AFB, FL: US Air Force Research Laboratory, 1998.
- [45] Stanley Q. Kidder and T. H. V. Haar, *Satellite Meteorology: An Introduction*. NY: Academic Press, 1995.
- [46] H. I. Heaton, "Temperature scaling of absorption coefficients," *Journal of Quantitative Spectroscopy and Radiative Transfer*, vol. 16, pp. 801–804, 1976.

Index

- Absorptance, 131
- Aerosol Backscatter, 8
- Background
 - Raman Scattering, 40
- Background concentration, 46
- backscatter, 8
- Backscatter coefficient, 25
- Cross section, 36
- Dark Current, 90
- DIAL, 43, 45
- DIAL clutter reduction, 50
- Differential absorption lidar, 9
- Differential absorption spectroscopy, 9, 11
- Digital elevation map, 5
- Dirac delta function, 25, 27
- Elastic Scattering, 28
- Elastic scattering, 26
- Filter function, 37
- Fluorescence, 34
- Fluorescence cross section, 38
- Fluorescence lifetime, 36
- Fluorescence lifetime correction factor, 38
- Geometric form factor, 24
- Gometric form factor, 114
- HCl, 11
- HITRAN, 131
- Ideal gas law, 131
- Illumination factor, 32
- Ladar, 5
- Lidar eqation, scattering form, 25
- Line shape, 132
- Line strength, 132
- Line width
 - Laser, 7
- Minimum detectable concentration, 54
- Niquest Noise, 90
- NIST, 131
- Nitrogen, 40
- Number density, 25, 35, 132
- Optical depth, 131
- Overlap factor, 24
- Plume, 32
- Pollution monitoring, 32
- Probability, 23
- Pulse, 5
- Pulse Shape, 30
- Pulse shape, 5, 30
- Radiation scattered fraction, 25
- Raman cross section, 40
- Raman Scattering, 39
- Range, 4, 23
- Range resolution, 6, 28
- Reflectance, 50
- Scattering cross section, 25
- Shot Noise, 89
- Solid angle, 23
- Spectral transmission factor, 24
- Speed of light, 4
- Surface Reflectance DIAL, 11
- Surface reflectivity, 32, 45, 49

Surface type, 33

Target

Raman scattering, 39

Thermal Noise, 90

Tomographic lidar equation, 34, 53

Transmission, 23, 28